UNIVERSITETET I AGDER

Voltage Regulation Assessment in the Distributed Network with Wind Turbines and Photovoltaics Implemented

Viljar Danielsen

SUPERVISOR

Prof. Mohan Lal Kolhe

University of Agder, 2019

Faculty of Engineering and Science

Department of Engineering

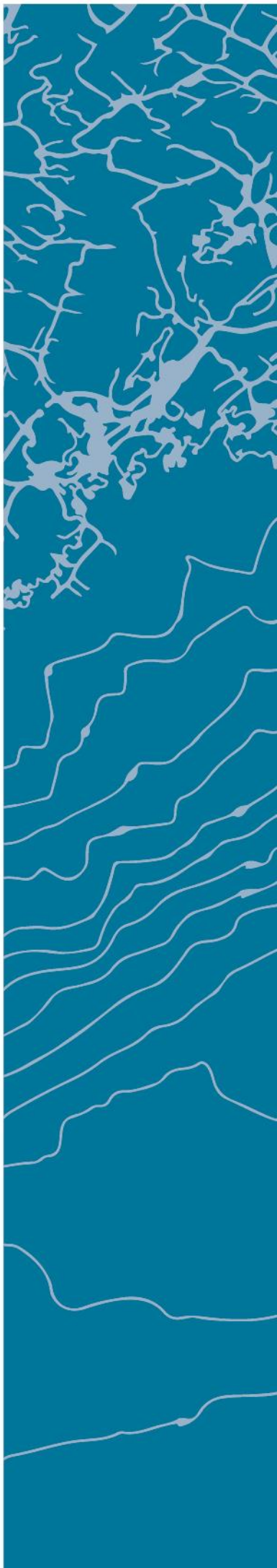

Abstract

High penetration of Distributed Generators (DGs) in the Distributed Network (DN) could cause undesirable operating conditions. The DN is by conventional means planned, and operated in a *passive* manner, i.e., the level of monitoring is low, and the power flow is predicted in order to provide satisfactory power quality at the customer's Point of Common Coupling (PCC). However, the implementation of DGs based on intermittent renewable energy sources, such as Photovoltaics (PV) or Wind Turbines (WT) stress the existing voltage regulation scheme in the DN. One of the objectives of the Distribution System Operators (DSO) is to provide voltage levels within admissible limits at all PCCs, and thus, the impact of DGs in the DN, and strategies for mitigating problems, if present, is of interest.

The main aim of this paper is to inspect the impact of DG integration in the DN, with respect to voltage levels. In particular, the steady-state conditions through the course of a day are studied, in balanced system. The assessed types of DGs are considered to be PV in the Low Voltage (LV) grid, and WT (one Wind Farm) in the MV network. Firstly, some basic load-flow simulations were performed on a radial MV network with three feeders, illustrating the impact of DG in a generic manner. Simulations were conducted by applying load curves and PV generation curves in a LV network. No novel approach of voltage regulation has been introduced in this paper, however, the strategy of applying On-Load Tap Changer (OLTC) technology on the MV/LV Transformer (TF), by using apparent power measurement for determining the desired voltage setpoint, was briefly introduced. Furthermore, evaluating reactive power control by operating the PVs in a cabled LV network at constant Power Factors (PF) was performed. The Fully rated converter WTs ability to provide reactive power support and its impact on network voltage was briefly assessed.

The main findings of the work conducted; was the serious voltage rises recorded in all systems, when DG was introduced. In a MV network; a maximum voltage of 1.04 p.u. was recorded in the Low Load High Production (LLHP) scenario, thus it was close to the limit considered admissible in this work. The high voltage was recorded to be the result of DG injecting power into the grid. A Wind Farm implemented in the MV network was found to have a major impact on voltage level on the respective feeder. This yielded voltage levels in a connected LV grid to be pushed out of permissible limits, thus breaking regulations in steady-state. Fairly low penetration of PV (19.25 %) was reported to have negative effects on voltage and mitigating further penetration growth when clustered to the LV feeder end. However, if clustered near the TF, a high hosting capacity was observed. The high R/X ratio in the LV grid was recorded to suppress the impact of constant PF control, as the maximum voltage profile improvement was 0.03 p.u. when penetration was 52.25 %. However, the maximum reactive power flow seen by the TF was in such a case increased by 115 %, provoking considerations towards TF overloading necessary if integrating const. PF control of PVs in LV networks.

Preface

This Master Thesis is the concluding work of my five year-long period as a student on the Renewable Energy Master's programme at the University of Agder. I would like to thank my fellow students and the University for a great time, indeed. Gratitude is directed towards my supervisor Prof. Mohan Lal Kolhe, and in addition to PhD Candidate Arvind Sharma for valuable inputs and help with the DIgSILENT PowerFactory® simulation tool used in the thesis. Nevertheless, I hope you enjoy reading this paper!

_____

May 24th, 2019

Viljar Danielsen

Individual/group Mandatory Declaration

The individual student or group of students is responsible for the use of legal tools, guidelines for using these and rules on source usage. The statement will make the students aware of their responsibilities and the consequences of cheating. Missing statement does not release students from their responsibility.

1.	I/We hereby declare that my/our thesis is my/our own work and that I/We have not used any other sources or have received any other help than mentioned in the thesis.	☒
2.	I/we further declare that this thesis: i. has not been used for another exam at another department/university/university college in Norway or abroad; ii. does not refer to the work of others without it being stated; iii. does not refer to own previous work without it being stated; iv. have all the references given in the literature list; v. is not a copy, duplicate or copy of another's work or manuscript.	☒
3.	I/we am/are aware that violation of the above is regarded as cheating and may result in cancellation of exams and exclusion from universities and colleges in Norway, see Universitets- og høgskoleloven §§4-7 og 4-8 og Forskrift om eksamen §§ 31.	☒
4.	I/we am/are aware that all submitted theses may be checked for plagiarism.	☒
5.	I/we am/are aware that the University of Agder will deal with all cases where there is suspicion of cheating according to the university's guidelines for dealing with cases of cheating.	☒
6.	I/we have incorporated the rules and guidelines in the use of sources and references on the library's web pages.	☒

Publishing Agreement

Authorization for electronic publishing of the thesis.

Author(s) have copyrights of the thesis. This means, among other things, the exclusive right to make the work available to the general public (Åndsverkloven. §2).

All theses that fulfill the criteria will be registered and published in Brage Aura and on UiA's web pages with author's approval.

Theses that are not public or are confidential will not be published.

I hereby give the University of Agder a free right to

make the task available for electronic publishing: ☒JA ☐NEI

Is the thesis confidential? ☐JA ☒NEI

(confidential agreement must be completed)

- If yes:

Can the thesis be published when the confidentiality period is over? ☐JA ☐NEI

Is the task except for public disclosure? ☐JA ☒NEI

(contains confidential information. see Offl. §13/Fvl. §13)

Table of Contents

List of Figures

List of Tables

Notation

X_k	The reactance of the component *k*
R_k	The resistance of component *k*
PF	Power Factor
$\cos\varphi$	The second notation used for Power Factor.
φ	The phase difference between voltage and current []
ΔU	Voltage drop [V]
U	Voltage magnitude [V]
I	Current magnitude [A]
S	Apparent power [VA]
P	Active power [W]
Q	Reactive power [var]
U_N	Nominal voltage (the system voltage) [V]
U_i	The recorded voltage at any node i
P_i	Refers to the actual or nominal active power of element i
Q_i	Refers to the actual or nominal reactive power of element i
n_ϕ	Refers to a network or element within a network with n phases
δ	Angle (difference) between voltages at two different nodes
t_{k+1}	Indexing of an instant in time, after an instant t_k
ΔT_k	Time interval for a tap change on the OLTC to be commanded
T_d	Time delay setting of OLTC
d	Half of the deadband of OLTC controller
T_f	Fixed intentional time delay of OLTC controller
T_m	Mechanical time delay due to switching of the tap-changer
U_{ref}	Voltage reference setpoint for the OLTC controller
r_k	Current tap position of the OLTC
U_{comp}	Compensated voltage setpoint in LDC operation of OLTC
Δv	Voltage error computed in the voltage regulator of the OLTC
DB	Deadband of the OLTC controller (voltage)
$U_{i,PCC}$	Voltage of phase *i* at the PCC

Y	Admittance
G	Conductance
B	Susceptance
ΔU_{lim}	The maximum voltage deviation considered satisfactory (±)
ΔU_{max}	The maximum voltage deviation which has been recorded in simulation
$PEN_{\%}$	DG penetration ratio [%] in the MV network. Referred to base load and losses
$\sum_{i=1}^{n_{DG}} P_{DG}$	Sum of installed active power capacity of DGs in the MV network
P_L^0	Base case active power load of the MV network
P_{Loss}^0	Base case active power loss within the MV network
$I_{\Delta V}$	Voltage profile flattening index (positive if the voltage profile is flattened)
V_{max}	The maximum recorded network voltage
V_{min}	The minimum recorded network voltage
I_{Loss}	Active power loss index (negative value implies increased losses)
f	Frequency of the network
PEN_{PV}	Penetration ratio [%] of PV in the LV network, referred to the installed apparent load
$\sum S_{PV,installed}$	Total apparent capacity of installed PVs (i.e., inverters) in the LV network
$S_{Load,installed}^{max}$	Maximum allowable apparent demand of the respective LV customers
PEN_{Load}	Penetration ratio [%] as a ratio between installed PVs and customers (PCCs) in LV DN
n_{Loads}	Number of loads (customers or PCCs) in the LV network
n_{PV}	Number of customers having PVs installed in the LV network
Tap_{pos}	Tap position of the NLTC or OLTC which is assessed.
P_{PV}	The maximum active power output of any PV system (W or Wp) in the LV DN
P_{Load}	The maximum active power load demand of any customer in the LV DN
$Q_{max,import}^{LV}$	Maximum recorded reactive power flow into the LV network

Abbreviations

AC	Alternating Current
AMI	Advanced Metering Infrastructure
AVR	Automatic Voltage Regulator
CENELEC	European Committee for Electrotechnical Standardization
CIRED	International Conference on Electricity Distribution
DB	Deadband, On-Load Tap Changer (Transformer)
DC	Direct Current
DFAG	Doubly Fed Asynchronous Generator
DG	Distributed Generator
DMS	Distribution Management System
DN	Distribution Network
DSO	Distribution System Operator
ENTSO-E	European Network of Transmission System Operators for Electricity
ESS	Energy Storage System
EV	Electric vehicle
FCB	Fixed Capacitor Bank
HLNP	High Load No Production
HV	High Voltage
IEC	International Electrotechnical Commission
IEEE	Institute of Electrical and Electronics Engineers
IGBT	Insulated Gate Bipolar Transistor
LDC	Line Drop Compensation
LLHP	Low Load High Production
LV	Low Voltage
MOSFET	Metal Oxide Field Effect Transistor
MV	Medium Voltage
NLTC	No Load Tap-Changer
OLTC	On Load Tap-Changer
p.u.	per unit
PCC	Point of Common Coupling

PE	Protective Earth
PEN	Protective Earth Neutral (Not to be confused with the notation of penetration ratio)
PF	Power Factor
PFC	Power Factor Control
PV	Photovoltaic
PWM	Pulse Width Modulation
RfG	Requirements for Generators
RMS	Root Mean Square
SCADA	Supervisory Control and Data Acquisition
SCB	Switchable Capacitor Bank
SCC	Short Circuit Capacity
STATCOM	Static Synchronous Compensator
SVC	Static Var Compensator
TF	Transformer
TN-C-S	Terra Neutral Combined – Separated
TSC	Thyristor Switched Capacitor
TSO	Transmission System Operator
WT	Wind Turbine
WTG	Wind Turbine Generator

1 Introduction

The Electric Power System provides us all with electricity, and we expect it to be available continuously. Power consumed by us do by conventional means come from centralized production, through the transmission grid and its high voltage (HV) lines, before it is distributed in the regional areas. Lastly, it is supplying customers through the Distributed Network (DN). This scheme is changing, as the penetration of Distributed Generating units (DG) based on renewable energy sources continue to grow at lower voltage levels, e.g. Low Voltage (LV) and Medium Voltage (MV) levels. This fact contributes to new challenges arising, as the DN conventionally was planned in a *passive* manner, i.e., the conditions at various places in the DN could be predicted and taken into consideration when planning and building the DN. The integration of intermittent DGs require a thorough analysis in terms of technical requirements and indeed commercial aspects, as it is implemented in a network it initially was not intended for. The foundation of such a statement lies in the fact that DGs can cause power quality issues, e.g. voltage rise along feeders due to reverse power flow (or simply elimination of the predicted voltage drop), and loss increase. Impacts of DG can be negative and thus initiate challenges, however, they can also contribute to lower losses, improved voltage quality and suppress the power demand seen by the overlying grid [1]. The DN is typically operating in a radial configuration (not meshed, where power can take multiple routes), i.e., the voltage drop along any feeder can be estimated by using the expected loading of the respective feeder. Furthermore, the level of monitoring is generally low, which provokes a minor paradigm change in regard of these networks. The DGs have to be taken into account as protection schemes, voltage regulation and bottleneck issues potentially exist. The inherent reason for this is that all customers should be provided with power quality within admissible limits, which are determined by regulative authorities. The objective of this paper is to examine the impacts DGs could have on steady-state voltages, with emphasize towards residential Photovoltaics (PV) in the LV DN, and Wind Turbines (WT) if it were to be connected to the MV network, and how the highly dynamic nature of customer loads interfere with the DGs output.

Voltage regulation describes the process and equipment to maintain voltage within admissible limits as stated. The primary objective of this process is to provide all connected customers with a voltage that correspond to the limitations of the customer's utilization equipment [2]. Significance of this process in the DN increase when more DGs are connected, and several techniques exist to mitigate eventual problems (e.g., reactive power control, tap-changing transformer etc.) [3]**.** Furthermore, the voltage control approach could be performed in a *centralized* or *decentralized* manner, which justifies investigating the DG integration and rational solutions. It is of great importance that the challenges introduced are addressed, as the "business as usual" operation of the DN could cause the issues to become critical, which further provokes an immature solution.

This paper builds on the previous work performed in the Autumn 2018, *Voltage Regulation in the Distribution Network* [4], which studied the effect on heavy loading (load profile) on a radial LV secondary feeder, and the mitigation of voltage limit violations by implementing OLTC on the MV/LV transformer (TF), and evaluating how using a distant node on the feeder as the controlled variable could improve voltage quality in steady state. The implementation and the possible challenges that arises is of great interest and is therefore further assessed in this thesis. The paper has a power system with a high level of inertia in mind, e.g. the Nordic grid. Contributions of this paper are insight in the impact of DG implementation, with specific aim towards PV implementation in the residential LV

network and WT integration on the MV side of the substation, or some distance from the substation. Voltage quality is assessed with respect to PV penetration and clustering in the LV DN, and the possible consequence of power demand seen by the TF is considered. The concern of TFs supplying LV DN becoming overloaded when integrating Power Factor (PF) control on PVs are investigated. LV DN's characteristics varies significantly across networks, however the ratio of Resistance (R) and Reactance (X) and its impact on voltage regulation is examined.

1.1 Background

The instantaneous voltage at any node is basically a function of the flow of power through it, and it will depend upon neighboring voltages and the characteristics of the line. Hence it is a local property of the power system, and it has, at distribution level, normally been calculated and estimated, so the right dimensioning measures can be executed before installation. This is based on the conventional picture of that the DN in general serves load (i.e., downstream power flow). As the penetration of new smart technology and DG increase, the challenge of instability is expected to grow (eg., Electric Vehicle (EV) charging, heat pumps, smart houses and PV systems). It needs to be taken seriously, that the future is still unclear in regard of market solutions and flexibility-based power flow. Furthermore, the integration of DG could lead to protection schemes needing re-solving and updating, as the short-circuit capacity (SCC) increases [5]**.** The requirement of fault-ride-through (FRT) operation, if present, will induce detailed analysis as the DG contribution to the fault current will depend on the topological place of fault. Due to obvious reasons, the PVs and WTs are typically connected to LV and MV (or higher) voltage levels, respectively.

Wind power installations has increased by large amounts in Europe over the last few years, and may pose a source of challenges regarding power quality [6] [7]. PVs are simple to install, and can typically be placed on rooftops, integrated into building facades, etc. Amongst other reasons as wee, such as technology and cost developments, the penetration of PVs in the DN has increased by large amounts over a period of time and is expected to continue to grow [8]. Note, that DGs could both cause challenges in regard of power system operation such as bottlenecks and voltage issues, but furthermore, it can suppress network losses and improve voltage profiles if installed at preferable points in the network.

The utilities are to hold their operational constraints and quality of delivered energy in the process, therefore the aim of being precautionary should be in place. Bear in mind that the utilities are strictly regulated by the executive authority, as of in Norway is *The Norwegian Water Resources and Energy Directorate* [9], which is operated as a directorate under *The Ministry of Petroleum and Energy* . This is valid for both the Transmission System Operator (TSO) and the Distribution System Operator (DSO).

In terms of regulations and common guidelines, there exists several methods the DSOs perform, to sustain the quality of delivery. When operating as a monopoly, the DSO are strictly overlooked and they must follow the regulations regarding operation, customer contact and the interconnection of other grids and devices. The evolving Smart Grid technologies provides us with an ocean of possibilities but in the same bulk [10] the industry faces several challenges and problems that need attention. As we alter the infrastructure scheme, we move away from the conventional idea that infeed of power is done in large central generating plants, into the transmission grid and distributed downstream to the end-customer. Several large industry organizations which are involved in the development, has

reported their point of view on the possibilities and challenges we face in the time to come, with focus on the DN [10] [11] [12] [13] [6].

The subject of ICT application in the DN is indeed a topic investigated in the literature. The number of components in the DN is very high and the level of monitoring has been minimum in the past years, i.e., it has been operated passively. The more active control of the DN, if found necessary by research, may lead to technical challenges regarding implementation of such infrastructure. The advanced metering infrastructure (AMI) is a step in this direction, and the DSO receives data on the PCC condition (and in some cases also on distribution TFs). If, however, these measurements should be used for "real-time" control of the DN, the resolution of information is considered "too slow". On the other side, the AMI data could be a valuable source in regard of DG and EV integration, as voltage levels can be logged and regulation schemes can be revised before critical levels are reached, for instance.

This interaction between components is also a challenge in the regard of equipment made for conducting and breaking current, furthermore, equipment made to support and regulate network properties. This is in the essence an ICT problem as the control systems is provided a setpoint value at minimum. If other parameters also should be available for modernization from the control room, the control scheme needs to be able to understand and use these signals (e.g., provided by wireless networks, fiber cables, etc.).

The technical challenges considering an increase of DGs present in the DN are varying in form and significance. The most significant is considered to be the design of the DN; as it is normally designed for one-way power flow. Thus, the thermal and short-circuit protection scheme is set with the known short-circuit capacity in the network. The system is in addition mostly consisting of radials and not as much redundancy as in the transmission networks. The impact of reactance and resistance has on voltage drop varies between transmission and distribution grids. On the transmission level or in urban DNs, the reactance has far more significance as the ratio of X/R is high, i.e., $X/R > 5$. In a rural DN for instance, the resistance is often larger than, or similar to the reactance [14]. Thus, the resistance of lines in the DN has typically largest impact on line losses and voltage drop.

1.2 Challenges & Motivation

There are many challenges present in the hunt for the efficient and sustainable smart grid, considering all voltage levels. One of the motivations of the author of this paper is that the technology and cost development of small generator systems based on renewable energy will out-run the process of implementing a well-tested, trusted and sustainable regulation schemes. This reflection emphasizes voltage regulation in detail, and the role of the DSO, who is assumed to be authority in need of evaluating future feed-in into the DN. The challenge consists of course by many decisions within several fields. The technical-economic aspect is maybe one of the most important when assessing a utility which operates with a monopoly in its area and are based on regulated incomes payed by each customer connected to the grid. Their decisions and work-method should be well defended from all perspectives! Furthermore, the technology and world we live in today changes so fast that the solutions we propose today could in theory be "outdated" in the matter of short time.

1.2.1 Several Solutions Plausible

Voltage and power quality in general are topics of interest for several parties who are connected to the power system. Both normal customers and plant operators wish to use the grid as desired, i.e. power quality and capacity for import and export are essentials.

In the literature and within research organizations worldwide, one can find an ocean of formulations of both challenges and possible solutions. The power grid is in contact with many stakeholders, and in the process, one must separate between private and state-run operations. As will be further presented, the implementation of more equipment that the DN conventionally was not planned for, open doors for business models for all stakeholders. This challenge alone, evaluating several thoughts of how this should be solved takes time and effort, as well as challenges regarding "*who is to say what solution is better than the other?"* the author find interesting, and further fear of that this process may lead to *last minute* resort in cases where customers will install DG, or even get declined due to predicted power quality violations.

The author of this paper will stress the view of that a solution for the DN should be easy to implement, as the number of components at this level is very high, and a complex solution for instance, with a high degree of communication and control commands/operations may lead to further problems. Systems like this is assumed to be very expensive, and one must ask oneself *is it worth it, is it techno-economic sustainable?* Let us say that a section of a network at LV level reaches voltage and thermal constraint problems due to heavy loading and DG penetration. If the problem could be solved by upgrading the transformer and lines, is it more feasible than trying to implement a complex solution with a lot of ICT involved, which should operate in all climatic situations (e.g. ESS, Q control, pay customers to curtail power)? It becomes a question of economics and robustness of the system.

As the penetration of DG is increasing in both LV and MV grids, the utilities are facing gradually growing challenges in regard of power flow and the fundamental electrical properties (e.g. voltage and network loading). The stochastic nature of the typical DG power output, typically due to weather conditions, leads to a variable source seen by the grid [15]. This consideration disregards the instalment of an energy storage system (ESS). The majority of the distributed networks is assumed to have been designed and built several decades ago, at a time the network design was mainly aimed to serve loads in the distributed networks. This means the power flow, and hence the voltage drop takes place in the downstream direction, towards the consumer. The main challenge in this aspect is the fact that the nature of customers is changing, in relation to technology evolution. Voltage stability is a local property, and it has to be taken seriously in order to ensure a proper, rational and beneficial for society and utilities (e.g. being easy to implement and cost-effective). The solution of Microgrids may be mitigating technology on the case of what the DN "sees" but involves challenges like protection schemes, cost of energy and the electric operation of the system.

In Norway, the customer who activates the need of reinvestment or upgrading of network components, have to bear a share of the cost [16]. The investment must be techno-economically rational in order for the DSO to go forward with it. As DSOs constantly are operating the grid while thinking ahead, their operative "roadmap" can be thought to be something like the one depicted in Figure 1. It illustrates that the power system is a challenging system to do experimental development on.

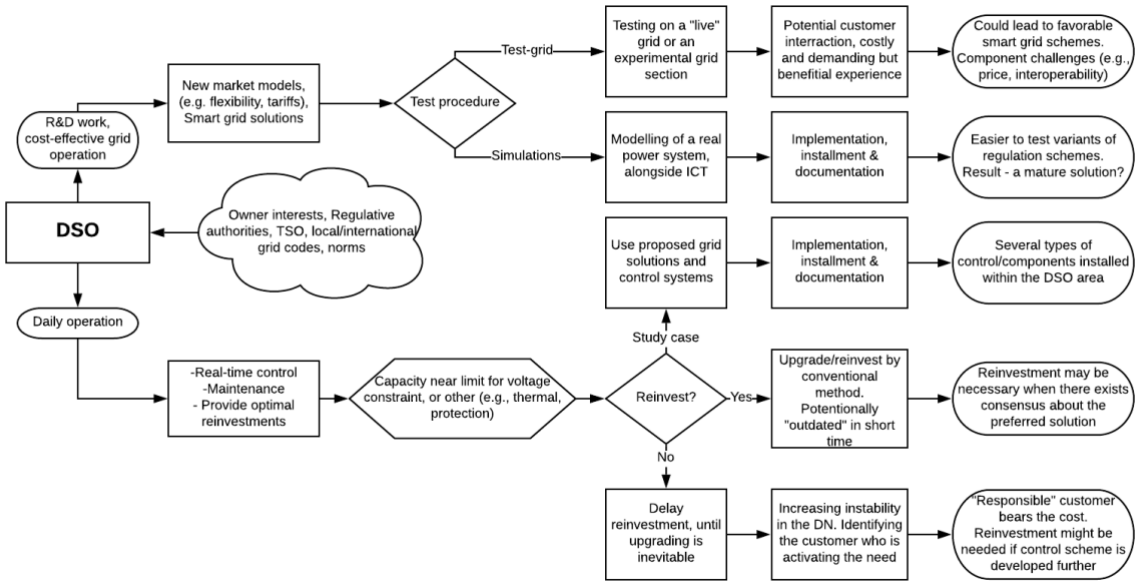

Figure 1 - A "roadmap" example of how one can see the task of DSOs when both operating and developing their system.

1.3 Thesis Objectives

The work conducted in this thesis is based on gaining further insight and understanding of how the integration of DGs impacts voltage and power quality in the DN. The main concern is voltage levels, which are to be kept within statutory limits. Both MV and LV networks is to be put under the scope, with focus on WTs and PVs. In a broad specter, this thesis is set to include;

i. Study of the impact on DG implementation on MV feeders connected to a substation, where the factor of varying DG penetration between the feeders will be examined in addition to voltage and loss considerations.
ii. Illustrate the objective of the on-load tap-changers on transformers and assess if the integration of DGs pose a threat to the conventional scheme of voltage regulation.
iii. Shine light on the R/X ratio in DN, and its impact on voltage regulation if DGs use reactive power as a regulation scheme to provide voltage-support.
iv. Examine the integration challenges of PV and WT, with emphasizes on LV and MV network, respectively.

1.4 Approach of Research

The approach of research includes thorough analysis of reported literature on the topic, establishing an objective for the work, determining the tool(s) appropriate for the thesis and then the execution of the prescribed work. The evaluated systems will to some degree have a high degree of simplifications in them. This is in an effort to reduce the scope of the work. Challenging network conditions will not be pursued in order to achieve "satisfying" results, the work is carried out in an objective manner. One secondary goal of this work is indeed to improve knowledge on the field and become familiar with the work structure. Results reported in this thesis may be viewed as a contribution to the subject of DG integration and possible challenges arising as a result of this.

1.5 Limitations and Validity of Potential Findings

This paper has been compiled with reasonable skill and care. However, the author cannot guarantee the precision and accuracy of information herein. The discussed topics are indeed subjects that is vastly discussed in the literature and the author holds no responsibility associated to the resources used.

The networks and components being modelled have a topology based upon theoretical grounding, common sense and field experience. Methods used and results obtained should be regarded as valid only for this work and its respective distribution network. Software parameters within the modelling aspects is a source of insecurity itself and should be thoroughly examined when analyzing the findings. However, the work of this thesis aims to contribute to the research within impacts of DG at the distributed level, although in a simplified manner. For a more specific research work, the recommendations concluding this report holds some rational guidelines for further studies.

The work conducted, is in majority steady-state scenarios with a large time-step, or at least calculated as such. Due to this fact, the transient and short-time resolution happenings associated with DG integration and DN operation are neglected or disregarded. Furthermore, results obtained are only valid for the simulated models and scenarios applied. No protection scheme considerations are included, as this is a problem for itself. The reader is given sufficient information to test the results and is encouraged to perform studies of the same nature.

1.6 Research Questions

Within in the scope of this work and the topic addressed; the following research questions have been defined;

- Which challenges arises in terms of voltage regulation, when MV feeders obtain high penetration of DG?
- Will the OLTC operation be affected by voltage scenarios taking place due to DG?
- Topologically, where is it rational to implement a large DG plant, say, a Wind Farm?
- If large DG plants were installed on MV feeders supplying residential customers, how would it impact the performance of the LV grids?
- How does penetration of PVs influence voltage levels in LV grids, if no active power curtailment scheme is active?
- How does the characteristics of a LV network affect voltage control by reactive power support?

1.7 Thesis Outline

- **Section 1 – Introduction**
  Overall background and foundation of the problem is briefly presented. The approach of research, research objectives and motivation for the work are given.

- **Section 2 – Voltage Regulation in Distributed Networks**
  This section presents some specifics about the challenge regarding integration of DGs. Some theoretical foundation is presented, essential when assessing voltage drop and voltage regulation within DNs. Furthermore, the section concludes with a literature review of the

relevant state-of-the-art strategies and techniques reported, for mitigating voltage issues, if present, at the distributed level.

- **Section 3 – Voltage Regulation of Transformer by On-Load Tap Changing**
  An introduction to the TF is given, focusing on the OLTC principle and control basics. Some mathematical description is indeed included. The OLTC is an essential object although not assessed in detail in this research, as it usually regulates the voltage which the DN use as the primary source. Understanding its role is important in this thesis.

- **Section 4 – Generator Representation in the Distributed Network**
  Generating units (or DG) are a key element in this research, as the impact of these is to be examined. Hence, it is within reason to briefly present some fundamental grounding on their representation within the DN and how they can operate. The theoretical base is emphasized towards the modern WT and PV types, as they are the types of DG considered in this work.

- **Section 5 – Power Flow Analysis**
  This section provides some basics on power flow analysis and modelling**.** Furthermore, a short introduction to the software chosen for modelling and simulation purposes in this work is given.

- **Section 6 – Assessing the Impact of Distributed Generation**
  The respective network systems considered, and the cases applied to the models within this work is presented in devoted subsections. The methodology and key choices taken for each system is provided.

- **Section 7 – Simulation Results**
  The simulation results obtained are presented as per the description in Section 6. Some discussion takes place, where it is found reasonable to do so. In addition, some comparison of results which are correlated is included, in order to sustain the report structure in a good manner.

- **Section 8 – Discussion of Key Results and their Significance**
  Discussion is continued on a higher level in Section 8, where uncertainties, special considerations towards the simulations performed and so on are briefly discussed.

- **Section 9 – Sources of Error and Challenges**
  Section 9 presents some quick remarks on sources of error, and challenges in regard of “smart” control of the DN. Some electrical challenges in regard of DGs are also briefly given.

- **Section 10 – Conclusion and Recommendations**
  The concluding remarks for this work, and recommendations for further work is presented.

2 Voltage Regulation in Distributed Networks

In this Section, the literature is reviewed in terms of the topic *DG integration into the DN.* It consists of an overview on how the situations is today and the trends growing, as well as some theoretical grounding. As discussed, the industry faces "endlessly" of possibilities. As both national and regional interests, regulations and grid codes have an effect on the development in some degree, the number of processes running simultaneously are considerable. Furthermore, new market and business models being developed increase the complexity of the challenge ahead. This paper takes the reported research into account but have a greater focus towards primarily the Norwegian and secondly European grids, as per the author origin.

2.1 Penetration of Distributed Generation – Possibilities and Challenges

The DGs vary significantly in rating and power output, in addition to the voltage level of connection. It seems that the literature is not consistent in terms of DG definitions. However, in this thesis the smaller types of PVs in the LV (e.g. less than 10 kW) and a Wind Farm with a capacity of some megawatts (10-20 MW). In [14], a definition of DG is given, and it is stressed that every distribution system is unique – which imply the DG should be defined as to which role it plays in the respective DN. This is due to the fact that different voltage levels and hosting capacity exists in the networks.

As it is emphasized mainly on small DGs in this paper, PV is mostly considered to be the type of source. However, WT is assessed as a single wind farm coupled to the MV grid. Small hydro-generators could also be considered, but they do not have the same potential to such high penetration as that of a DG which "only" requires sun and area to deliver power. The PV and WT are connected to the grid via an interface of power electronics, i.e., an inverter converting DC to AC with the required frequency. These inverters have the capability of delivering active and reactive current, hence they could be used for voltage regulation on the distributed level [17]. This fact introduces both possibilities and issues in the regard of control schemes in the DN [18]. In fact, the integration of such devices in the voltage control sense, and not controlled via centralized manners, they could be a source of further issues by interacting and possibly working against each other or existing regulative equipment, causing oscillating power within the grid [14].

The evolving ICT solutions existing today and beyond provide both the market and utilities many possible scenarios regarding grid operation, control and protection as well as market models. The DN could to a higher degree become smart, in the manner of using real-time measurements in optimizing the voltage – and frequency support by taking into account OLTC operation and available Q-supportive devices within the DN [19]. Maintenance and operation could be optimized with such data available. The increasing penetration of DG could reduce the investment in distribution capacity, in addition they could be the source of energy during loss of the feeder. In such a case, the cost and control issues will be more severe [18].

The Active Distribution Network of tomorrow should be robust, have quick signal responses and a good interface between the digital and components performing topology – or system changes, assuring steady operation without random fall-outs.

A critical topic is the ICT protocols and communication flow security, i.e., ensuring the right secrecy levels and protection against possible attacks on the system. In addition, the handling of the large data feed is considered a challenge itself, e.g. from advanced metering infrastructure (AMI) and decentralized phasor measurements. Some of the real-time technology and architectures for smart grid are provided in [20]. The information gap between the generation and consumption is severe and a good cooperation of several industries are necessary in order to develop a proper solution. In [10] a good rundown of what the different stakeholders' interests could be, policy implications and the most known smart grid concepts (e.g. self-healing networks, virtual power plants and demand side management) on the basis of ICT.

To summarize; in theory we could see a DN with close to real-time measurements and communication on every part of interest, i.e. critical nodes, DG terminals and voltage-supporting devices, implemented into the SCADA or DMS. However, the practical and technical aspects could withhold the "smartness" of our system on the distributed level.

2.2 Theoretical Foundation of Voltage Control

2.2.1 The Reason for Voltage Drop: How Can we Predict and Control it?

The implementation of more DG and power demanding loads, e.g. PV, Wind turbines, EV chargers and controlled household loads, may represent a regulation paradigm change. The power flows and voltage levels could fluctuate more than previously and cause the regulation to be in need of quicker responses and a wide regulation reserve. In Figure 2, the situation of varying power flows in the radial MV and LV grid is considered. Note that the full picture of voltage regulation is not taken into consideration, e.g. synchronous generators capable of quick response to voltage fluctuation. Large DG plants is also assumed to be required to participate at a higher degree to voltage changes than smaller units. As for this study where mainly smaller PV systems and WT are considered the DG type, it represents some of the challenges. Bidirectional flow of power implies voltage drop and possible voltage rise with respect to distance from the feeder busbar (i.e. voltage drop in the upstream direction). Thus, the power flow "seen" by the HV/MV Transformer (TF) could fluctuate and its Automatic Voltage Regulator (AVR) controller could be in need of re-tuning. The figure shows the fact that the power seen by the MV/LV TF indeed could vary more, if there are DGs present in the LV network. One of the problems is also illustrated by the flow diagram, as the hypothesis of that the voltage supplied to the MV/LV TF could fluctuate more than before, causing a need of more dynamic voltage regulation, as the LV network itself could fluctuate at a higher rate with DGs implemented.

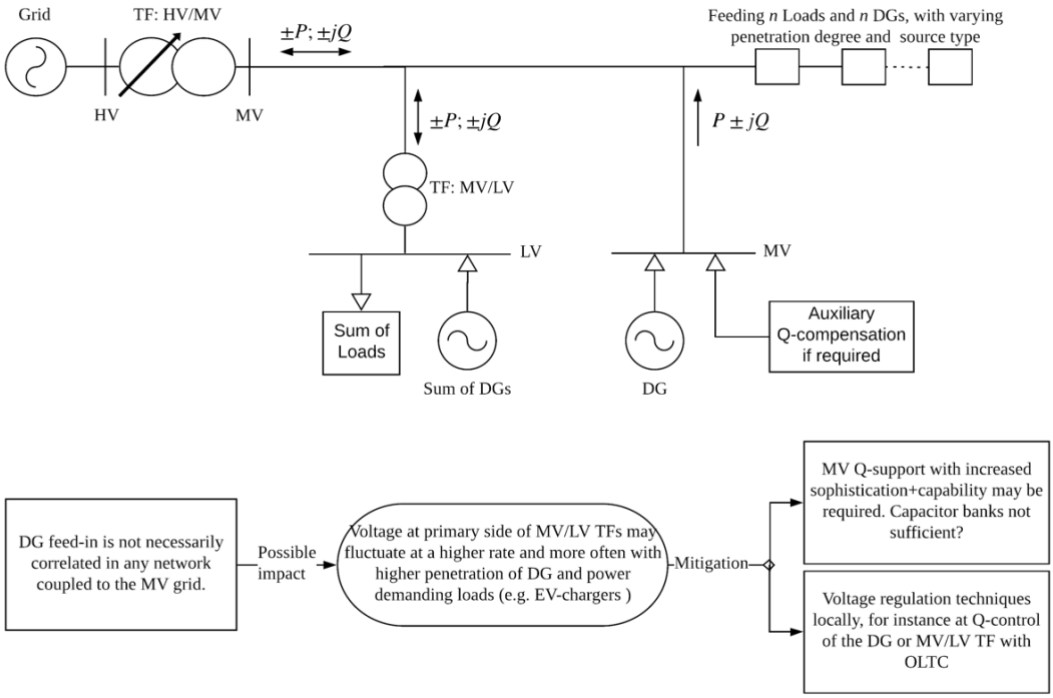

Figure 2: The potential power flow situation in radial distributed MV and LV networks with DGs implemented, including consideration of voltage regulation. All reactive regulation devices are not considered.

Traditionally speaking, switchable capacitor banks (SCB) and OLTC on HV/MV TF are used for regulation but they are normally based on local measurements. Thus, they normally operate without central control. However, the implementation of single-phase regulators for all phases on each feeder is carried out in some cases. In modern cases of power quality enhancement, the utilities test the use of FACTS elements, taking advantage of power electronic devices. For instance, Static var Compensators (SVC) or static synchronous compensators (STATCOM) are able to provide quick reactive power absorption or provision [21].

In order to supply some basis on the problem of voltage regulation, some key definitions and equations are presented in the following. Firstly, the reader should note that all assessments taking the customer node (or bus) into consideration, the point of common coupling (PCC) is the point of which the powers and voltages with subscript *2* are presented, unless otherwise stated. The PCC is the point of interconnection between utility and customer, hence it could represent the border of property.

The inherent reason for voltage regulation is due to the fact that there exists a voltage drop (ΔU) over any impedance as a function of current, which in a power system adds up to a high number of nodes and associated line sections, hence, we obtain different voltage levels (U) all over the network. This drop can be approximated as we know, given in Eq. (2.1) [22];

$$\Delta U = RI\cos\varphi + XI\sin\varphi \tag{2.1}$$

Where the R and X represents the evaluated resistance and reactance, respectively, both expressed in ohms [Ω]. The φ is the phase offset between voltage, V [V] and current, I [A], given in [rad]. In the power system or electrical domain, the $\cos\varphi$ and $\sin\varphi$ elements are often regarded as the *active* and *reactive* element, respectively. This means they are related to the active power P, which is expressed

in Watts [W], and reactive power Q, which is expressed in volt-ampere-reactive [var]. R will always have an absolute value resistance, i.e. always represented by a positive value. However, the X component has two possible characteristics which were the sign alters, depending on if the resultant X is *inductive* or *capacitive*. The *inductive* components (e.g. TFs, induction motor) are associated with a negative phase shift -φ, and thus a lagging Power Factor (PF). The *capacitive* components (e.g. capacitors, cables) are associated with a positive phase shift +φ, which yields a leading PF. The power delivered or supplied by any device could be characterized by their *Apparent power* (S) which is expressed in Volt-Amperes [VA] and their operating PF. This information yields the effect it will have on the power system. Note that only the active power P, does useful work (e.g. lighting, heat and mechanical rotation), and the reactive power Q, does only generate and absorb energy which is related to electric – and electromagnetic fields and its average value over a cycle is *zero*. Thus, the Q is oscillating between source and sink, and the typical end-consumer does not pay any fee for this power, if the PF is within the normally expected range.

The relation between S, Q and P is given by eq. (2.2), and the associated PF is displayed in Eq. (2.3). In addition, the power triangle is presented in Figure 3. The power triangle indicates why typically the active and reactive powers, or components are mathematically presented in, and considered variables in the *imaginary plane*, as the Q and P is represented by the imaginary and real axis, respectively. This further introduce the term *four quadrant power*, which refers to the four possible quadrants of equipment operation, in the P-Q plane.

$$S = \sqrt{P^2+Q^2} \tag{2.2}$$

$$PF = \frac{P}{S} = \cos\varphi \tag{2.3}$$

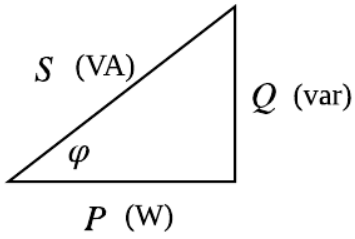

Figure 3: Power triangle depicting the relationship between Apparent (S), Reactive (Q) and Active (P) Power.

An important key in power system dynamics is the flow of active and reactive currents, as they will define the loss in the network, voltage levels and load capacity of the network. As the term of power usually is more convenient in the field of this paper, we can express the voltage drop, or rise amount by presenting Eq. (2.1) with the load components as [23] ;

$$\Delta U = \frac{P_{Load}R+Q_{Load}X}{U_N} \tag{2.4}$$

In Eq. (2.4) the U_N is the nominal or rated line-to-line voltage, P_{Load} and Q_{Load} are the powers drawn (negative sign) by the load. The R and X are the line impedance. If we include the power provided by the DG in the PCC, Eq. (2.4) can be updated, and expressed as;

$$\Delta U = \frac{(P_{Load}+P_{DG})R+(Q_{Load}+Q_{DG})X}{U_N} \quad (2.5)$$

Now, the P_{DG} and Q_{DG} is the active and reactive power flow at the PCC. *It is clearly shown that the DG can have an impact on voltage level in the network, depending on active and reactive power flow and network characteristics.*

For the sake of illustrating the situation, we consider the case of a fixed (i.e. an infinite short-circuit capacity source) supply voltage U_1 at the sending end, an impedance Z consisting of resistance R and reactance X (e.g. aggregated line impedance), and a voltage at receiving end U_2; depending on the active P_2 and reactive Q_2 consumption of the load connected at receiving end. This configuration is depicted in Figure 4. This could represent a three-phase line, 3_ϕ, or a single-phase system, 1_ϕ. As the DN is 3_ϕ, let us assume it depicts a balanced 3_ϕ system and load (i.e. each phase is loaded equally), where U is the line-to-line voltage. By addressing the voltage drop in Figure 4, the following applies [24];

$$U_1 = \sqrt{U_2 + \left(\frac{P_2R+Q_2X}{U_2}\right)^2 + \left(\frac{P_2X-Q_2R}{U_2}\right)^2} \quad (2.6)$$

Eq. (2.6) reflects that there will be a voltage drop ΔU, caused by the consumption of the load, and the impedance of the network element. The figure illustrates that this is the usual case. Nevertheless, manipulation of powers within the network can change this scenario and this fact is further studied throughout this thesis.

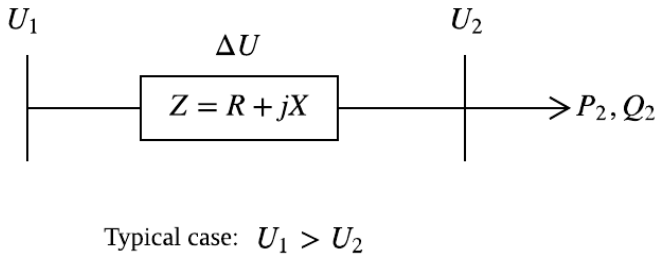

Figure 4: A simplified network supplying power to a load, consuming P_2 and Q_2.

One key element that should be taken into consideration in this regard, is the power loss. The fact that electric heaters consists of a resistance which cause a power loss, dissipated as heat (in this case it is desired, of course) is known to us. In the power system sense, where all the network components have some impedance, there will also exist some power loss at all times, hence, the generator supplying loads in the network must in addition to customer demand cover this power that is lost in the network. The utility bears the cost of these losses, and it is safe to assume they strive to keep these costs at a minimum. The power loss is indeed reasonable to express as two types of loss; one reactive and one active power loss component. Even if the reactive power does not do "useful" work, its current component has to flow in the network, thus causing real power loss. These losses, considered for a defined network area, can be calculated by [25],

$$P_{Loss} = \sum_{i=1}^{n_{br}} |I_i|^2 r_i \quad (2.7)$$

$$Q_{Loss} = \sum_{i=1}^{n_{br}} |I_i|^2 x_i \quad (2.8)$$

Where P_{Loss} and Q_{Loss} is the active and reactive component of the power loss, $|I_i|$ is the magnitude of current flow in branch i, x_i and r_i are the reactance and resistance of branch i, respectively.

Although not focused on in this thesis, it should be mentioned, the measure of phase angle of voltage, of which determines the direction of power flow, and thus the voltage scenario. Here we consider magnitudes of voltage at separate nodes but by controlling the phase angle we can manipulate power flow. This is done by injecting a step in series voltage, which changes the phase angle δ in radians [rad] or degrees [°]. One way to look at this manipulation is that the voltage that "comes first" must send the power to the node with a δ which is lagging in time. This method is more applicable in the transmission system and can be reviewed in [26].

To summarize; the voltage is desirable to keep at a constant value at all times, at all places in the DN, or at least within statutory limits. The apparent power flowing in the network (both P and Q) causes a drop in voltage, ΔU, which may be in need of regulation if predicted or measured out of the desired range. Please note however, it is of great importance to understand that the direction of both powers is the key as to which we consider it to be *raising* (e.g. generator) the voltage or causing a *drop* (e.g. load). In terms of distribution grids; the connection interfaces are dominated by loads absorbing *active power.* Note however, that the *reactive power* could be absorbed or provided (injected into the grid), depending on the equipment connected. As we can control the Q-direction in many cases (and usually not P), the reactive power is both the problem and the solution to keeping voltage where we want it. It should also be mentioned at this point, that the use of per unit (p.u.) representations of numbers and electrical quantities are considered familiar to the reader, as this is used in the report for convenience.

2.2.2 Devices used for Voltage Regulation at the Distributed Level

As the voltage regulation is relatively simple in accordance with its conventional predictability, the main regulating devices are OLTCs, line voltage regulators, and fixed or switched capacitor banks [27] but the following will briefly include some other equipment or methods as well.

Transformer

The *On-Load Tap Changer* (OLTC) TF is considered the most common voltage control technique, and its objective is to keep a stable secondary voltage, here regarded as the MV level. It consists of an Automatic Voltage Regulation (AVR) relay which monitors the output voltage and commands a tap change if the voltage is above pre-set limits. In addition, a *Line Drop Compensation* (LDC) is often included, as of which the function is to compensate an additional voltage drop between the OLTC and a distance from it, e.g. the load location. To avoid a high frequency of tap changes occurring, an intentional time delay is included in the controller. This method is an effective measure of changing the output voltage in steps, and it is described in more detail in Section 3, as it operation is considered of importance in this paper [23]. It should be noted that the TF that supply the secondary LV feeders (e.g. 0.23 or 0.4 kV networks) are normally No-Load Tap Changer (NLTC) TFs, which imply their ratio can be changed (with a limited range) but the TF has to be de-energized while this is taking place.

Generator

If we consider the synchronous generator type DG, they are able to provide reactive power support (lagging or leading) by the use of an AVR relay, but this method can cause unstable operation of the DG, so the Power Factor Control (PFC) has become a desirable control of the synchronous DG. In this configuration, the P/Q is maintained constant, hence there will be a proportional variation in Q if the output P fluctuates. To suppress the impact on PCC voltage, the Q output can be adjusted in the opposite direction [23]. This generator type is common at higher powers and is not further considered in this work. The conventional DN consists often of none generators, and only load demand.

Power curtailment

The use of power curtailment is an effective, yet undesirable technique of mitigating voltage violations. Yet, due to the inflexibility of voltage control strategies, DSOs commonly trip the whole DG from the network to avoid the voltage problem. Of course, this method does waste potential provision of renewable energy into the system and reduce the revenue from DG operation. If implemented on a windfarm say, the active power curtailment could consist of regulating the pitch control [23]. PVs are in many cases requested to disconnect from the DN if undesirable voltage levels are reached, in accordance with the *EN 50438 – Requirements for micro-generating plants to be connected in parallel with public low-voltage distribution networks*. For instance, if PCC voltage exceeds 1.15 p.u. or goes under 0.90 p.u referred to nominal system voltage, the unit is requested to be disconnected within 3 seconds [28].

Capacitor banks and reactors

The capacitor bank is a well-known device in the DN, and it is usually classified as either *fixed capacitor bank* (FCB) or *switchable capacitor bank* (SCB). The SCB can further be considered as switched by mechanical switches or power electronic equipment, e.g., thyristor controlled, termed *Thyristor switched capacitor* (TSC). If a device can control both reactors and capacitors by the use of thyristor switches, a fast and step-less control of reactive power is obtained, termed Static Var Compensator (SVC) [29]. As the reactive power flow causes voltage levels to change, it is desirable and most effective to inject this power locally, near loads with a high reactive consumption (e.g. commercial and industrial customers). Keep in mind that all TFs are acting like an inductor, it is consuming reactive power which has to be balanced by injection somewhere in the grid. The principle of reactive power injection (it could represent a switched device) is depicted in Figure 5, where the comparison is made to illustrate the result of capacitor placement (switching).

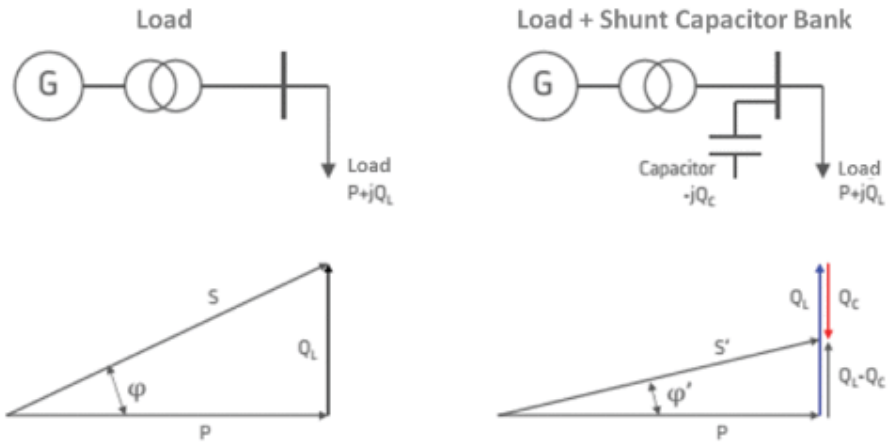

Figure 5: The principle of capacitor implementation, displaying the reactive power flow reduction, and hence, voltage regulation [30].

The shunt capacitors can be coupled in several manners, like delta connection, one wye, double wye and H-bridge, but they are not discussed in detail here [30]. The determination of capacitance (C) when the required amount of var - injection is set is assumed as fairly known to the reader. The principle is the same for shunt reactors (inductors), which could be a requirement if cabled networks provides excess reactive power due to large capacitance.

During the daily operation, switching of these components can be performed in order to keep the voltages within admissible limits. Traditionally, the SCBs are switched by the use of circuit breakers on the command of the DSO. Somewhat more modern systems where a controller monitors the condition of voltage and current can switch the reactive components with higher accuracy, automatically, for instance by the use of contactors. The SVC systems can operate towards a certain setpoint and a deadband, which ensures the node voltage is kept within certain limits. The reactive power flow is inherently a optimization problem where the objective is to maximize voltage quality, while losses, reactive power reserve and loading constraints of devices should be minimized, for instance [31].

2.2.3 Voltage Control Schemes used on Generating Units for Q-support

As we understand, reactive power is a tool we use to regulate voltage in the power system, as the active power output usually is devoted to frequency control (which in essence is active power control). Going through all the relevant theory regarding these subjects are well out of scope of this paper. One important fact to consider is that the reactive power flow in any system is minimized, in order to reduce the losses presented in Eq. (2.7) and (2.8). For a sounder understanding and a good insight in the field of voltage regulation and reactive power control, [32] is recommended. Nevertheless, some of the key regulation schemes are presented in brief;

Constant PF control can be seen as a source which always either is consuming or providing reactive power. This way, its contribution to voltage regulation is always proportional to its delivered active power. This method provides a predictable source seen from the grid. If one unit rated X kVA is to operate with a constant PF, this rated apparent power would never equal the delivered active power, as some capacity is devoted to reactive power. The reactive power will vary when active power varies in order to keep the PF steady.

The voltage control strategy of cos φ (P) control consists of providing the generator unit with a PF command, which is either underexcited (consuming Q) or overexcited (providing Q). In other words, the control variable is the phase difference φ, as a function of how much active power P, the unit delivers. Figure 6 (a) is illustrating this method. It can be seen that the requested PF is usually lagging when the unit delivers high power, in order to suppress voltage rise, and vice versa.

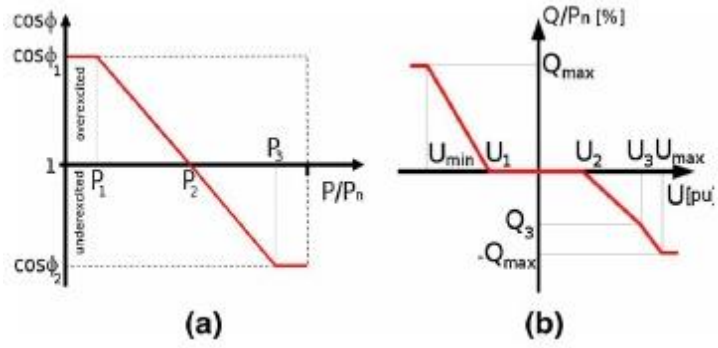

*Figure 6: Example of reactive power curves; (**a**) cos φ (P) curve and (**b**) Q(U) curve [33]*

For all strategies, one must define the thresholds (limiter) of each variable, to secure that the unit does not operate outside the acceptable limits, often associated with thermal limits or instability reasons. In addition, the slopes can indeed have a deadband where the controller is "inactive" or holds one variable constant (e.g. like the deadband in Figure 6 (b)). In this manner; each unit's capability is taken into account and therefore the contribution to network regulation is shared in a rational manner. Figure 6 (b) holds an illustration of Q(U) control, where the reactive power setpoint is a function of the measured voltage. In This manner, the reactive power contributes by a known (determined) amount in both negative and positive direction. For detailed observation of control schemes, [33] is recommended, where mathematical representation, indeed, is included.

2.3 State-of-the-Art Voltage Regulation in the Distributed Network

The topic of this thesis is indeed well documented in the literature. It is a challenge the power systems are facing today, and the problem of voltage regulation is highly relevant. As discussed, several mitigating techniques exists when it comes to overcoming voltage unbalance in the DN. For any problem to be solved, the problem must first be analyzed and understood. The power system is a complex object, and hence several works in literature focus on studying and analyzing the DG impact, to fully understand how we can mitigate it in a rational way.

Several papers focus on what state the voltage regulation in the DN is today, and which challenges we could meet in the future with respect to a higher penetration of DGs.

Reference [34] gives status and future trends in the DN, where the architectures of today and tomorrow are presented. Available methods and optimization strategies for DG impact mitigation are discussed, including demand side management, OLTCs, Q-support, STATCOMs, LDC etc. Several techniques for voltage control in DNs are illustrated in [23], where it is stressed that it is desirable to deploy different techniques as scenarios varies, due to the fact that some methods are more efficient in certain scenarios. The R/X ratio is discussed to have major impact on voltage control techniques. In

[15], challenges regarding DG penetration on MV feeders connected to a busbar controlled by an OLTC, by assessing the current flow the OLTC sees, and thus regulates after. This scenario is reported to cause undesirable control commands by the OLTC. Unbalances in voltage fluctuations, with respect to DGs are discussed in [1], and by the proposed reactive power control, the total capacity of the network before reaching voltages out of bounds is reported to have increased (stability), by using the proposed scheme.

Combined MV and LV reactive power support scheme where OLTC and SCB are controlled in the MV network, and the available reactive power provision in the LV grid through the PVs was implemented in [35]. Active power curtailment is the last resort in the control scheme, yet it showed to have satisfactory effect on the recorded voltage profile, even without curtailment. The paper in [27] takes also the MV and LV networks into account, and strive for them to work in harmony. The control scheme operates all the reactive power reserves, based on the optimal source. OLTCs, shunt capacitor banks, distributed STATCOMs are working together in this novel approach. The highly dynamic regulation provided by a STATCOM is considered essential, and the closest device to the voltage imbalance regulates first. The priority of conventional devices is put first in line. Needless to say, this paper assumes pretty high levels of communication. Several more papers examine approaches of control with Q-support and/or novel OLTC controller schemes [36] [37] [38].

The DGs in LV networks specifically, usually PVs, oppose voltage concerns when the voltage drop is eliminated completely, or in fact, the injection from PVs cause reverse power flow, and thus voltage rise in the network. The impacts of DGs are investigated in numerous papers, such as [33] [39] [40] [41]. The penetration ratio of which becomes critical with respect to voltage levels is often used as a measure of voltage stability. However, it should be noted that numerous definitions of penetration can be observed in the literature, and the need of thorough analysis is necessary.

Several methods exist when integrating mitigating techniques for voltage quality, however, the LV network oppose challenges regarding its R/X ratio as previously stated. This problem has to be addressed in a wide range of network configuration in order to better understand its impact on voltages, loss and loading of the network. In [24], reactive power control methods are compared in terms of sensitivity of injected power for regulation, and losses. Indeed, it shows that LV networks are requiring large amounts of reactive power in order to regulate their voltage. A variable control strategy, consisting of Q(P) and PF-control is proposed in [42], and tested on a LV network, which yielded a control scheme which caused minimum reactive power regulation and satisfactory voltage levels. Furthermore, OLTC implementation and control is a subject of examined approaches to mitigate voltage violations when DG penetration increases. It is considered an effective approach, as it disregards the reactive power control on DGs, if the penetration is within a certain range. The method is investigated in several papers and results indicate its positives outruns other methods used [43] [44] [45] [46] [47] [22]. It should be noted, that [43] considers a hybrid proposition to the control, to provide optimal regulation from both reactive power and the effective measure of tap-changes.

The above discussion is considered to justify the encouragement of going through with the research aims of this thesis, and contributing to increased knowledge on DG integration challenges.

2.4 Regulation and Guidelines for Distributed Generation

Many different regulations or grid codes are active worldwide, and some are applied or adopted in several countries. In the following, just a short selection of some key regulations or guidelines are given;

EN 50438 – Requirements for Micro-generating plants to be connected in parallel with public low voltage distribution network holds requirements for the operation of the DG. This is distributed by CENELEC. The German standard VDE AR-N 4105 holds operative requirements for generation equipment connected to the LV grid, and is adopted by for instance Norway on some points. The *International Electrotechnical Commission* (IEC) develops and publishes international standards.

The standard Application guide for *IEEE 1547.2.2008 – standard for interconnecting distributed resources with electric power systems* available in [2] *,* defines that the DG shall not actively regulate the voltage at PCC. It could support the areas system and it could work in opposition to regulation equipment installed by the DSO. Reactive power support requested by DSO is beyond the scope of IEEE 1547 requirement. Some DSOs request that the DGs should operate at constant PF, and this way the DG will follow the PCC voltage.

The Commission Regulation (EU) 2016/631 Requirements for grid connection of generators [48] is establishing a network code on requirements for grid connection of generators, and it is also known as Requirements for Generators (RfG). It defines classification of generator types and their respective operational characteristics. At higher voltage levels, and powers, the TSO is usually involved in the process of setting the requirements for the generator.

In terms of power quality, the *EN 50160 – Voltage Characteristics in Public Distribution Systems* describes the requirements valid for the countries which have adopted it. As for now, the Norwegian power quality requirements are stated in *Forskrift om leveringskvalitet I kraftsystemet* [49].

3 Voltage Regulation of Transformer by On-load Tap Changing

This Section provides a short introduction to the tap-changing mechanism integrated on TFs at higher voltage levels. The key information is the objective of the OLTC, how it operates and how it can be represented. Only essentials regarding the OLTC is given, and the reader is referred to literature, for instance [50]**,** for an extended understanding of OLTCs, and TFs in general. The majority of the information provided in this Section is obtained from [50] and [39].

3.1 The Objective

The on-load tap changer (OLTC) between HV and MV is conventionally used as the last regulative device downstream, when entering the DN [31], when excluding devices like capacitor banks etc. The TFs which steps the voltage down to normal end-users (e.g., 0.23 kV) are normally adjusted by their no-load tap changers (NLTC), if even adjusted, seasonally in order to match the load differences between summer and winter, for instance. Hence, they must be de-energized before operating their tap-changer. The actual ratio adjustment normally takes place on the HV side of the TF, which makes sense as to lowering the current of which the tap-changer should "break", and reconnect. The turns ratio is the controlled variable on an OLTC, and it is performed mechanically in steps, hence the regulation is discontinuous. A typical regulation bandwidth of such a device can be ±8 steps of 1,25 % each, i.e. a regulation of ±10 % of nominal voltage. Due to obvious reasons, the OLTC allows the interconnection of power systems and a somewhat decoupling of the grid voltage levels takes place.

As discussed, this scheme of regulation could potentially run into challenges when DG penetration increase in the LV and MV grid. The principle of OLTC operation is sketched in Figure 7, where the MV side is regulated in order to deliver admissible voltage when loading is varying in the MV network. The ratio *r* Is the variable used to regulate the secondary voltage.

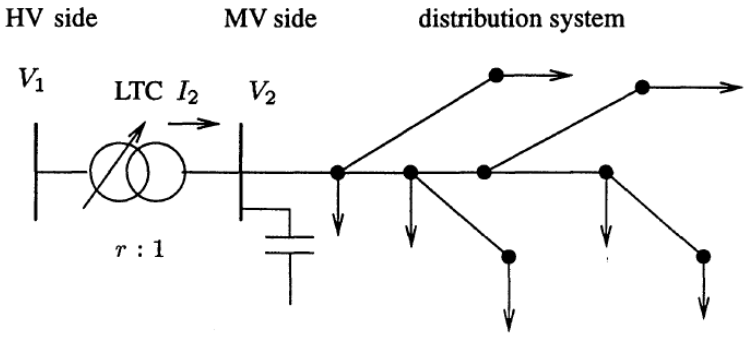

Figure 7: The operative principle of OLTC; where the MV side of the OLTC is regulated [50].

3.2 Voltage control of OLTC

Regulation of the MV busbar voltage is typically performed in accordance with the two principles *constant voltage* and *line drop compensation (LDC)* [36]. The constant voltage regulation compares the

busbar voltage with a setpoint value and commands the tap changer to operate after the offset has occurred after a prescribed period of time. LDC contains a modification of the setpoint voltage, as a function of the current flowing and the node voltage at the controlled side of the transformer. This *compensated voltage* is then provided to the OLTC controller as the desired value. This compensation is thus achieved simply by implementing an LDC calculation into the controller, containing the desirable impedance which to compensate, e.g. approximate distance of line downstream (introduced in the following).

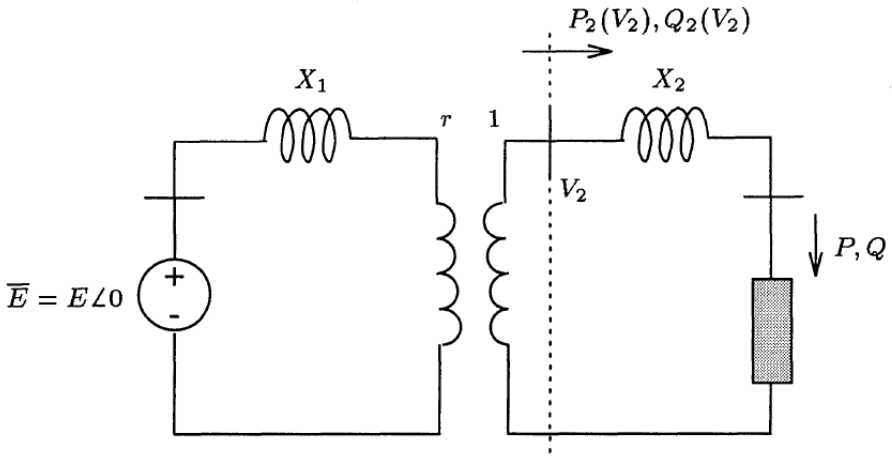

Figure 8: Equivalent circuit of an OLTC, depicting the effect of ratio change on the TF [50].

Figure 8 illustrates an equivalent circuit of the OLTC, where a load consuming power is seen. The reactance's seen on primary and secondary side could represent network reactance, upstream and downstream. Secondary side reactance and the load make up a voltage sensitive load which is depending on the secondary voltage. When an increase in output voltage is sought, the ratio *r* is decreased [50]**.** Inherently, the inductance seen by the primary side grid will vary when the OLTC changes taps, i.e., the impedance is tap-dependent. The switching of the OLTC is performed without stopping the flow of power through the apparatus, however, the discussion of electromechanical aspects of the tap-changer is outside the scope of this work. The OLTC make it possible to operate the power system with electrical distances between load and generators that would otherwise not allow the power to be moved to the loads in the network [50]**.**

In terms of modelling; the OLTC operation could be regarded as discrete (discontinuous), as it steps the ratio by one step instantaneously, by Δr, which is an element of a given range of tap steps. The OLTC can operate at time instants denoted by t_k where *k* is a real number. These time instants are given as;

$$t_{k+1} = t_k + \Delta T_k \tag{3.1}$$

And the ΔT_k, is expressed as;

$$\Delta T_k = T_d \frac{d}{|U_2 - U_{ref}|} + T_f + T_m \tag{3.2}$$

Where U_2 is the controlled voltage, U_{ref} is the setpoint voltage, *d* is half the OLTC deadband (DB), T_d is the maximum time delay for inverse time characteristics (not always a constant), T_f is the intentional

fixed time delay and T_m is indeed the time necessary for the mechanical operation of one switching taking place.

The logic of the tap changer at any instant t_k can be expressed as follows;

$$r_{k+1}\begin{cases} r_k + \Delta r & if \quad U_2 > U_2^0 + d \quad and \quad r_k < r^{max} \\ r_k - \Delta r & if \quad U_2 < U_2^0 - d \quad and \quad r_k > r^{min} \\ r_k & otherwise \end{cases} \tag{3.3}$$

Where r^{min} and r^{max} are the lower and upper tap limits, respectively. The DB of the voltage control is clearly shown. Voltage setpoint must, due to obvious reasons, be within the controller DB.

In Figure 9, an illustration of a block diagram for OLTC control is depicted. The LDC is introduced in the illustration, showing its relation in the controller. The basic elements of the control system are:

- Tap-changing mechanism, driven by a motor unit
- Voltage regulator (measuring unit and time-delay element)
- Line drop compensator (LDC)

The LDC's objective is to provide a voltage setpoint to the regulator, by integrating an additional voltage setpoint of which that projects a voltage setpoint at some distance from the TF, i.e., a projected controlled node. The new voltage provided by the LDC, U_{comp}, can be expressed as

$$U_{comp} = \left|U_{measured} + \left(R_{ref} + jX_{ref}\right) * I_{measured}\right| \tag{3.4}$$

Where $U_{measured}$ is the measured secondary side (typically) voltage, R_{ref} and jX_{ref} are the setpoints for the branch element between the TF and the projected controlled node and $I_{measured}$ is the measured secondary side current. If the assumption of unidirectional power flow is made, the absolute value of $|I_{measured}|$, in Eq. (3.4) can be applied [39].

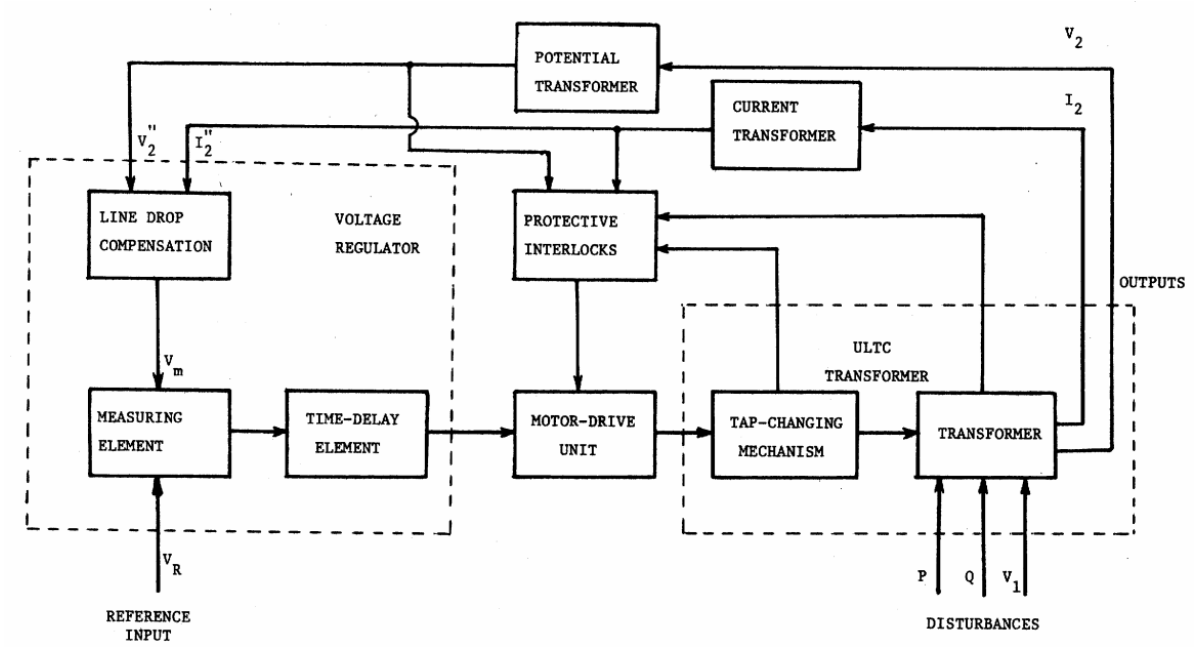

Figure 9: Block diagram of the voltage control on an OLTC, where the block of LDC is included [39].

The LDC signal is fed to the voltage regulator and it is compared with the initial voltage reference to generate a voltage error, like [39].;

$$\Delta v = U_{ref} - U_{comp} \tag{3.5}$$

The measurement element (can be seen in Figure 9) consists of a relationship between measurement unit input Δv, a relay hysteresis band ϵ and the output V_M, as depicted in Figure 10. The sign of the next tap change is determined on behalf of the sign of the voltage error Δv and hysteresis band.

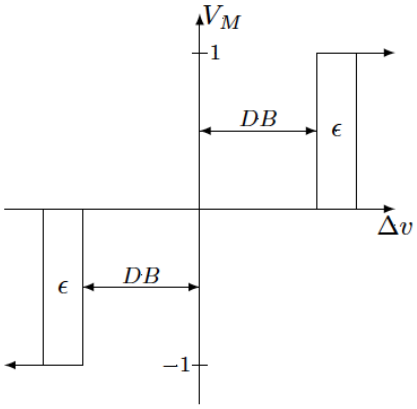

Figure 10: OLTC measuring element [39].

The signal from the measuring element is provided to the time-delay unit, which is an adjustable delay which operates on behalf of the objective to reduce the frequency of tap changes, and not command the motor unit to switch taps when short-term voltage variations take place. By this reasoning, the time delay is given in seconds. However, two different time delays are used, either a constant, $T_d = T_d^0$, or a as a function of DB and voltage error Δv, expressed by Eq. (3.6);

$$T_d = \frac{T_d^0}{|\Delta v / DB|} \tag{3.6}$$

The reasoning of Eq. (3.6) is to reduce the time-delay when the voltage error is considerable, with respect to the controller DB. Finally, the tap changer can operate, by changing its ratio *r.* The discrete step-by -step operation can be expressed as in Eq. (3.7), where the r_k is the OLTC tap position after operation k, r_{k-1} is the previous tap position and Δr_k is the incremental tap change [39].

$$r_k = r_{k-1} + \Delta r_k \tag{3.7}$$

3.3 Coordination of OLTC Operating in Cascade

When operating more than one OLTC in cascade, interactions should be minimized. Consider the radial system in Figure 11, with two OLTCs in cascade. If the ratio r_1 is suddenly reduced, both V_H and V_M are raised, however; when ratio r_2 is reduced (to raise the V_M), the voltage at V_H will get reduced as well.

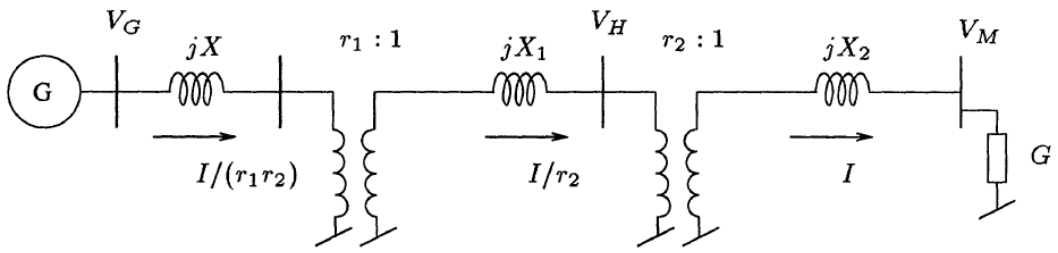

Figure 11: A radial system with cascading OLTCs [50]

To avoid excess interference between the two OLTCs, the OLTC at higher voltage levels is usually set to operate the tap-changer faster than the one downstream. This ensures more effective control, and fewer tap changes. The practical intentional time delay is typically 20-40 seconds larger at the HV/MV OLTC than at the OLTC at higher voltage levels (HV/HV). This rule applies if several OLTCs are installed, they should operate slower when approaching the end customer.

3.4 Practical Considerations

Frequency of tap changes is desirable to keep at a minimum from a mechanical point of view (out of the scope of this paper), to increase the likelihood of long operational lifetime. Maintenance is indeed required within certain time/step intervals just as the car we drive every day. Some manufacturers imply almost maintenance-free solutions, as for the OLTC on the MV/LV transformer in [51], however, the routines will vary with different manufacturers and working principles, indeed.

This leads to the fact that increasing OLTCs role in the future planning and building of the distribution system also could raise concerns. Imagine OLTCs installed at every secondary substation, i.e. at MV/LV TFs, the device is more active and requires more attention and control within the maintenance and operation division in the utility. Various types exist today, and even more sophisticated types will most certainly emerge in the future, which may lead to practical challenges as the utilities are a monopoly and the competition should be withheld for all components, which further strengthening the previous statement of interoperability's importance of our future power system at all voltage levels. This reasoning is based on the thought that several types of different OLTC devices in the distributed network increase the need of individual implementation, controller tuning and verification of operation.

The implementation of OLTCs are assumed to gain more ground at lower voltage levels in the future, as the loading of the lines and potential import of power to the grid alters the dimensioned voltage drop considerably. Amongst other, they could leave room for the reactive voltage regulation to operate first after the OLTC has operated, providing a wider regulation bandwidth in total. It is further assumed, that the HV/MV OLTC might be in need of revision in respect of controller operation, if the concern of high DG penetration in the DN is present.

4 Generator Representation in the Distributed Network

This section presents some introduction of the relevant type DGs and their characteristic considered useful when addressing the method and results in the work of this thesis. Only key elements which are of value are included. Furthermore, some technical grounding in terms of basic reactive power support by the DGs are offered to the reader. Here, the term *plant* represents a total set of generating units seen by the grid, e.g., a Wind Farm with several WTs.

4.1 Photovoltaics

The PV source of power is coupled to the utility through an interface of power electronics, i.e. inverter technology, as the output of solar panels is Direct Current (DC). The inverter (mostly referred to as converter in this paper, as the operation of the Pulse Width Modulation (PWM) is considered) operates with the objective of delivering as pure as possible AC output. The intermittent nature of solar irradiance implies, indeed, that the power output is highly stochastic. However, it can be predicted with some degree of certainty the day-ahead, for instance, based on weather outlooks. This thesis totally neglects or disregards the use of energy storage systems, thus, all power delivered by the PV is either consumed locally or exported to the utility grid if there is excess power at any instant. A generic overview of the converter-based interconnection of PV to the network through the PCC, is depicted in Figure 12. “DE” is simply representing the PV input. Inherently, it operates under the principle of voltage source converters, and the PV system has no rotational inertia or kinetic energy.

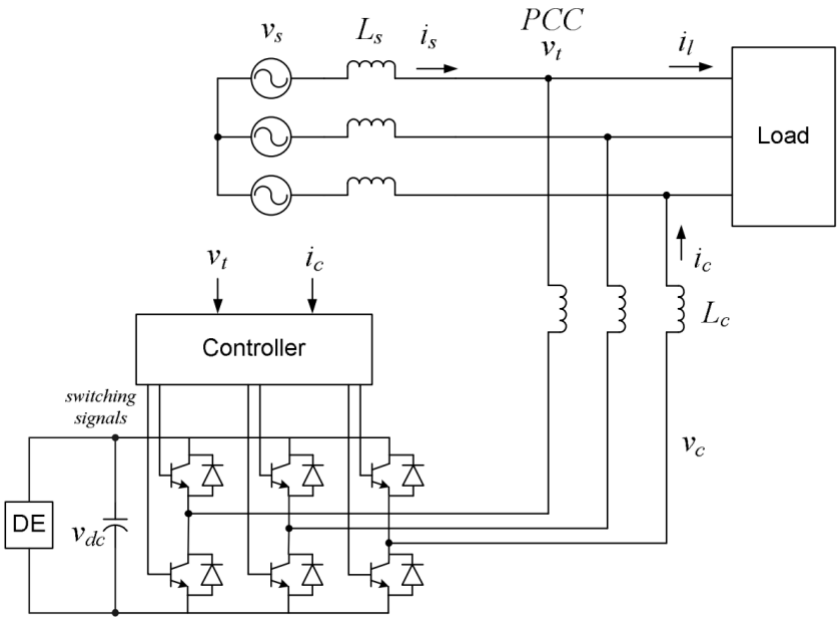

Figure 12: 3-phase PV inverter interconnection to the grid [52]

The inverter typically delivers AC output by the help of PWM in a DC-DC Boost converter and is lastly switched by for instance IGBT or MOSFET switches and smoothed before reaching the output. The controller determining firing angle of switches, as per the reference current, and smoothing components (V_{dc} and L_c) can be seen in Figure 12.

The quality of the sinusoidal wave injected into the network is out of the scope of this paper and is considered to be of sufficient quality. Please note, however, that the operation of inverters in parallel with the network could deteriorate power quality by introducing harmonic distortions.

The power of which the inverter (or the PVs) can deliver to the grid is in addition to solar irradiance reaching the system, affected by operating temperature, soiling and shading of the panels amongst other. As a matter of fact, the capability of the inverter will evidently vary as a result of this. By capability it is referred to the P-Q-diagram of the inverter, which tells us which conditions the unit is allowed to operate in. From a control strategy point of view, the P-Q capability is of great interest, as the DGs contribution to voltage regulation is determined this way. That is, if we consider the generator to inject all its available active power to the grid, and only control its reactive power in a capacitive or inductive manner, according to the network state. The P-Q capability is described further in the following subchapters, as both DGs considered in this paper has the same theoretical opportunities (PV and WT). Note that only balanced three-phase units are considered in this paper. For a more in depth understanding of the operation, control and inverter basics; [53] and [52] are highly recommended.

4.2 Wind Turbine Generator

WTs are based on the kinetic energy input of the wind, which is converted to electrical energy via the mechanical energy of a rotating shaft. The active power output will vary with wind speed, as seen in Figure 13. This will evidently cause the output power to fluctuate as a function of wind speed. Indeed, there will be some delay and "smoothing" of the power output as the rotor has some inertia. Nevertheless, the WTs can be regulated by their controller to operate based on different reference values, e.g., like curtailing active power output in order to follow a power output reference. All details of the operation are obviously not included here, like the description of pitch control of rotor blades (is used both to maximize power harnessing and curtail power output, depending on wind speed), gearbox systems etc. The overview of electrical topologies and characteristics, seen by the grid is in focus, and the considered size order of rating is the MW-range.

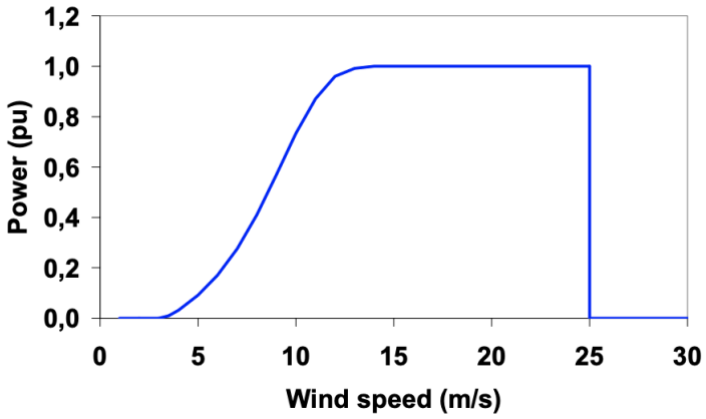

Figure 13: Power output characteristics of a wind turbine with respect to wind speed (illustration) [7]

Clearly, the power injected into the grid is intermittent, and hence, its impact on the grid will be dynamic. Requirements by TSOs regarding dynamic plant characteristics vary, typically with respect to installed power and connected voltage levels. As will be introduced in Section 6.1, the plant power

range of interest is a *Type C* plant according to RfG (Requirements for Generators, by EU, remember). This implies that the plant should be able to dynamically control its operating point in accordance with voltage and output power, for instance. Frequency support should also be implemented, and maximum ramping of power (e.g. MW/s) has to be controlled. These concepts are illustrated in Figure 14, where the control of active and reactive power can be seen. Over-frequency is mitigated by curtailing active power injection, and vice versa. Requirements for the capability and parameter setpoints will in a case like this be governed by regulations, and the TSOs requirements.

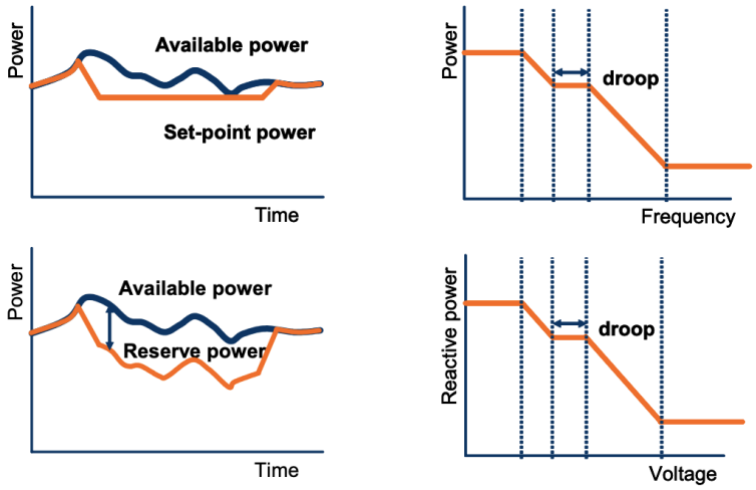

Figure 14: Modern wind farm control options for network stability, varying according to the relevant TSO requirements [7].

We usually consider four different types of Wind Turbine Generators (WTG); the Direct-connected Asynchronous Generator *(Type I),* Wound-rotor Asynchronous Generator with external resistance control *(Type II),* Doubly-fed Asynchronous Generator (DFAG)*(Type III)* and the Variable Speed turbines with Fully-Rated Power Converter *(Type IV).* The main differences of the topologies are the coupling or interconnection with the grid, where the *Type III* and *IV* offers the greatest freedom of control. The *Type I* will inherently follow (has to operate slightly higher) the synchronous frequency of the grid, as it will consume power (motor) rather than deliver it if it operates slower than the network frequency, and it will always consume reactive power. The *Type II* has the option of a variable rotor resistance (available through slip rings) which can be used to control the electromagnetic torque dynamically. *Type III* employ a wound rotor where static power converters are used to drive the field current (rotor), which facilitates operating speeds faster and slower with respect to synchronous speed. It can both supply and absorb reactive power, via its excitation. About 30 % of the power output flows through the converter in *Type III* configuration, hence, the converter is cost effective [54]. The *Type IV* is as its name implies; interconnected to the network through a converter bearing all the power flow. Due to obvious reasons, the latter type, *Type IV* has more freedom in terms of dynamic control, however, the rating of the converters has to be oversized to provide reactive power support when operating at nominal active power [55] [2]. Note that the generators which is not synchronous generators are mostly termed *asynchronous* generators here, instead of *induction* generators. This is due to the fact that the machine does not operate by the *induction principle* as soon as the rotor is available and controlled via slip rings, for instance, because it is then operated by magnetization of the field winding.

A block scheme of a Fully-Rated Converter Generator is depicted in Figure 15. It illustrates the decoupling of the network and the WTG, which enables a wide range of operational speeds, for instance. *It should be stated at this point, that the Fully-Rated Converter WTG is the type of WTG considered in the remainder of this paper.*

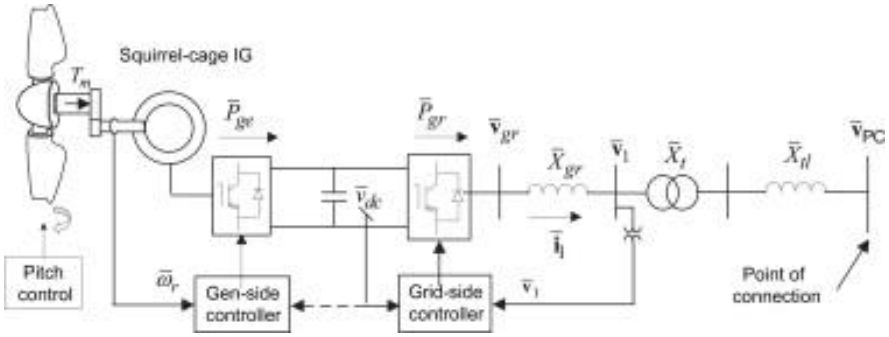

Figure 15: Block diagram of the fully rated converter type wind turbine generator (Type IV), based on asynchronous generator [55].

4.3 Reactive Power Support by Power Electronic Interfaced DG

The converter-based PVs and WTGs can, as is stated in the previous subsections, support the network by regulating its reactive power absorption or provision. Keep in mind that this operation is possible due to the switching of semiconductors and converter operation, in the process of providing an AC output. We recall that the inductive or capacitive operation of any device is coupled to the phase-difference between voltage and current, of which the angle is φ. Thus, by controlling the firing angle (or time of switching) of switches, the current going through the converter can be manipulated to be leading or lagging the voltage at AC-side (PCC). This principle is responsible of providing crucial network support, as it indeed can be controlled with a quick and almost instantaneously response, i.e., within a cycle [54].

The inverters are supplied in certain ratings (e.g. kVA or MVA) and has to be used in accordance with the manufacturer's instructions. Both single-phase and three-phase inverters exist, and the work in this paper is emphasized towards balanced systems, i.e., three-phase loads and sources. The *modules* (meaning the whole power converting device including filters, AC-DC converter if present, DC-DC converter and inverter) can simply be arranged in parallel in order to increase the total rating of any facility. We are here discussing both smaller size inverters for residential PVs and large-sized modules for powers in the MVA-range. *Nevertheless, the principle and key characteristics remain the same.* Recall that protective schemes and fault-ride-through specifications are disregarded in this paper.

It is stressed, that the main factors limiting the capacity is the insulation levels of internal components, the thermal constraints for elements carrying current etc., thus, the operative range is limited by the total apparent power rating. The reactive and active power should be controlled (including when the module is manipulated to operate near unity PF), when voltage support is desired. This is done by the computed switch states, which is calculated thousands of times per cycle for high precision.

The relationship between active and reactive power imposes the limit on current in each phase *i*, as previously introduced. The expression in Eq. (4.1) has to be obeyed at all instants [37];

$$P_i{}^2 + Q_i{}^2 = \left(U_{i,PCC} I_i\right)^2 \tag{4.1}$$

Where all variables represent the magnitudes of the phase *i* measurements, of active power P_i, reactive power Q_i, voltage at PCC $U_{i,PCC}$ and current through the converter I_i. The active and reactive power capability of each phase in the converter can be written as [37];

$$P_i{}^2 + \left(Q_i + \frac{U_{LL,PCC}{}^2}{X_i}\right)^2 = \left(\frac{U_{i,PCC} U_{LL,PCC}}{X_i}\right)^2 \tag{4.2}$$

Where the $U_{LL,PCC}$ is the line voltage at the output.

Maximum reactive power which is available through the module for each phase is [37];

$$Q_{cap,i} = min\{Q_i^c, Q_i^v\} \tag{4.3}$$

Where Q_i^c and Q_i^v are;

$$\begin{cases} Q_i^c = \sqrt{(U_{i,PCC} I_i^{max})^2} \\ Q_i^v = \sqrt{(U_{i,PCC} U_{i,PCC}^{max} X_i)^2 - P_i^2} - \frac{U_{LL,PCC}{}^2}{X_i} \end{cases} \tag{4.4}$$

In Eq. (4.4), the I_i^{max} is the maximum current output the converter is rated for, $U_{i,PCC}^{max}$ is the maximum voltage output of the converter and X_i is the total equivalent phase reactance seen by the converter, between itself and the PCC.

It has been briefly introduced that the grid codes will require the plant to operate within certain zones of the capability, if the plant has a large enough capacity which makes its impact on the network noticeable. If the requirements cannot be met by the converters themselves, ancillary reactive power devices must be installed at the plant busbar, for instance. It has been illustrated that, the reactive power support the converter is able to provide is indeed dependent on the PCC voltage, which as we know, is not a constant value in the power system. In [54], some standards are presented in brief, showing their required capability curves (PQ-diagram). For instance, it is noted that Statnett (Norwegian TSO) demands a lagging and leading capability of PF=0.91 for the whole operational are of the module. In addition, dynamic control is usually requested to provide stability to the network (or mitigate instability if you like), like described in Section 4.2. The dynamics, including active reactive power control to support frequency, grid stability and fault ride through is indeed an interesting matter of control strategies and so on, however, it is out of the scope of this paper.

5 Power Flow Analysis

Power flow calculations of large power networks include a large number of nodes, branches, generators, loads etc., and could by this reasoning be considerable time-consuming if performed by manual calculations. As the reader should be well aware of, it is of utmost importance to be able to calculate currents and voltages at varies locations in the power system. It is essential not only from a design point of view, so components can withstand the stresses they are exposed to; furthermore, the economical operation in minimizing network losses should be strived to be performed at all times. In other words, we need to know which *state* the network is in, at every instant. *In the following subchapters,* [29] *is used, unless otherwise stated, for giving a short introduction to some important analysis measures.*

5.1 Load Flow Problem Formulation

In general terms, the load flow problem is a nonlinear set of equations as

$$\boldsymbol{f}(\boldsymbol{x}, \boldsymbol{u}, \boldsymbol{p}) = 0 \tag{5.1}$$

Where $\boldsymbol{f}$ is an *n*-dimensional (non-linear) function, $\boldsymbol{x}$ is an *n*-dimensional vector containing the state variables, or state, as components. These are indeed the voltage magnitudes and voltage angles of each node in the system. $\boldsymbol{u}$ is a known vector with control outputs, e.g., voltages at generator with voltage control. $\boldsymbol{p}$ is a vector with the network parameters, or components, e.g., line resistances and reactances.

The solving of Eq. (5.1) is performed with respect to $\boldsymbol{x}$. Surely, it is necessary that $\boldsymbol{f}$ and $\boldsymbol{x}$ share a similar dimension, which means that the number of unknowns and equations correspond. However, in the general case, there exists no unique solution, and cases with no solution also exists. Note that if $\boldsymbol{x}$ is known, all other system quantities, as $\boldsymbol{p}$ and $\boldsymbol{u}$, can be obtained. We are usually interested in finding active, reactive flows with respect to flow in lines, generation from machines and consumption by loads. To solve the Eq. (5.1), as it is non-linear, a linearization, given as

$$\frac{\partial \boldsymbol{f}}{\partial \boldsymbol{x}} \Delta \boldsymbol{x} = \Delta \boldsymbol{y} \tag{5.2}$$

Is usually used. In addition, these equations also provide useful information about the network. The Jacobian matrix $\frac{\partial \boldsymbol{f}}{\partial \boldsymbol{x}}$, where each element is given by

$$\left(\frac{\partial \boldsymbol{f}}{\partial \boldsymbol{x}}\right)_{ij} = \frac{\partial f_i}{\partial x_j} \tag{5.3}$$

Can be used for several useful calculations and is considered an important indicator of the conditions of the system. The subscript *i* and *j* represent the node indexing.

As all analysis in the engineering sciences starts with formulation of appropriate models, this aspect is of great importance. In the power system domain, we are always dealing with mathematical models, and there exists several strategies.

The lumped-circuit line models (π-models) and distributed line models for instance, illustrated that there are several models, which has to be justified when choosing the respective model. Selecting the "correct" model for the work to be performed, can often be the most difficult part of any study. A good

engineering practice is normally to use a simple model as possible. The simplifications made and so on, should reflect the need for details in the study. Including numerous complicated factors which may not give any more viable result, could instead only make computations more cumbersome.

5.2 Nodal Formulation of Network Equations

As we speak about nodes in the system, we can consider a power flow from one node to another. We then name the two nodes of interest as *k* and m. For instance, by the Kirchoff's current law, we know that the sum of currents has a given relation in the nodal representation of any network. All currents in a node is calculated by their flow, e.g., flow from *k* to *m.* We must surely include characteristics like impedances, loads and generation. Impedance is commonly expressed I admittance, partially to simplify the process of matrix computations. Admittance in Siemens [S] is expressed like;

$$Y = G + jB \tag{5.4}$$

Where G and B is the conductance and susceptance, in Siemens [S], respectively. A matrix representing all node-to-node admittances, an Y-matrix, is usually used in calculations. It is a $n * n$ matrix in a network with n buses/nodes.

At this stage, the expressions for active and reactive power injections is simply given in Eq. (5.5) and (5.6), respectively. The variables are obvious and in line with previously stated parameters.

$$P_k = U_k \sum_{m \epsilon K} U_m (G_{km} \cos \theta_{km} + B_{km} \sin \theta_{km}) \tag{5.4}$$

$$Q_k = U_k \sum_{m \epsilon K} U_m (G_{km} \sin \theta_{km} + B_{km} \cos \theta_{km}) \tag{5.5}$$

As the problems of realistic load flow cannot be solved analytically, iterative solutions implemented in computers must be used. There are two methods typically used; Gauss-Seidel Iteration and the Newton-Raphson method. The foundation of such calculations is extensive and is left out this paper.

The short discussion above justifies the use of software in the process of analyzing power systems and its components. The user interface is usually better than only seeing a script for instance, more variables are typically accounted for and lastly, the user can observe in a graphical way what he/she is modelling and simulating. For understanding the great dynamics of higher details, for instance about the coupling between demand, production and its mechanical inertial connection, [29] is recommended. The reference holds good formulations and descriptions of many models of network components also.

5.3 DIgSILENT PowerFactory®

The software chosen for this thesis work was DIgSILENT PowerFactory® [56], hereafter noted as PowerFactory. It stood out for the author, in the search for good tools in assessments like the one in question. It was attained through a thesis work/research license request. The quality of equipment library, numerous calculation algorithms easily available and the reporting of results are regarded as a plus within this platform. The platform has in addition a vast number of standards, controllers and devices from several sources and manufacturers. This fact raises the credibility of the results, if the software is used in the right manner.

It is indeed a somewhat time-consuming process when getting to know a new simulation software, so there are of course many underlying hours of playing and testing within the PowerFactory platform. The simulation schemes performed are mainly load flow (steady state) or *Quasi-dynamic* which is a series of load flow calculations. These are the interesting network conditions in this work.

At this stage the reader should bear in mind that there exist many uncertainties and simplifications when using such a software. One must not under any circumstance accept the attained result as the hard fact, but evaluate assumptions and simplifications performed in the process.

5.3.1 External Grid

The *External grid* is used in PowerFactory to represent the grid of which the modelled system is connected to (external networks), and the characteristics of this should be revised per the accuracy, system layout and type of event/events desired to investigate. The types of external grid representation available is *PQ, PV* and *SL* references. Using the *External grid* technical reference [57], these are briefly explained here.

- **PQ**
  The external grid is modelled as a constant source of active P and reactive power Q. A positive value is representing generated power, and a negative value is considered to be consumed power.
- **PV**
  Here the active power infeed is specified (P>0) and by default this power controls the voltage of the busbar which it is connected to.
- **SL**
  The SL type of external grid, can also be referred to as *swing bus* or *slack bus*, as it balances the network connected to its busbar, by both absorbing and providing all power that is required. The SL-type thus represent a reference bus where the voltage and angle are kept constant (V$\angle\delta$).

5.3.2 Static Generator

The generator is implemented by the *static generator* element, which in its simplest manner injects the defined amount of active and reactive power. As steady-state calculations will be used in this work, it simplifies the operation of all components greatly. Control options are available, like Q(U), PF(P), const. Q, const. PF, Q(P) and more. The capability and controller setpoints/droop characteristics have to be set. The controller can act locally on the single generator, or the generator can be added to an external controller which can be applied on several generators. The connection topology can be implemented as 3Ph, 3PH-E, 1Ph and 1Ph-N [58]. In addition, the power can be unequally distributed amongst the phases if desirable. In this paper, the constant power factor is typically used.

5.3.3 General Load

The load element in PowerFactory has a very similar interface to the static generator. The nominal load can be defined a variety of ways, load curves can be included, loading events can be defined etc. The loads are used both as representation of entire feeders or aggregated loads, which is in line with the

documentation [59]. The loads are considered to be a balanced, three-phase, constant impedance load if not any type is defined. This will be the case in this work.

5.3.4 Cables

In the research license attained, only cables were included in the software library, and thus, time were not devoted to implement overhead lines. Instead, it was decided to consider cabled networks, as they might represent more and more of how we will see DNs in the future. Cables with LV ratings (1 kV) were used in the LV DN, and cables with MV rating were used in the MV grids. Insulation levels are always selected larger than the one the respective network operates at. Cross sectional area (in mm^2) of the cables (and their current rating) are selected on the basis of reasonable skill by experience, common sense and some theoretical basis. Note that the cable types integrated by real specifications from cable manufacturers, and makes for a simple integration of cables in the network.

5.3.5 Transformer

The TF device in PowerFactory easily lets the user scroll through several types for various voltage levels. Thus, the selected TF represents real TFs where its datasheet has been used for determining its characteristics.

If the automatic tap-changer (OLTC) is activated, it regulates the busbar voltage at one of the TF sides, or remote busbar, whatever is commanded by the user. The regulation is performed, in essence, like the technique described previously in the theoretical grounding. The tap controller of PowerFactory can be revised in [60], and the three-phase TF in [61].

The OLTC controller includes a tap-hunting detection logic, which stops further tap switches if the voltage fluctuates out of the desired range repeatedly. This would only cause an oscillating effect which could persist for some time.

6 Assessing the Impact of Distributed Generation

In the DIgSILENT® environment, several models are analyzed in terms of voltage quality and losses. In general, the *Load flow* of a steady state scenario was simulated, which represent simplifications from the real point of view, as the considered cases reflects a snapshot of system condition. Any transients or short period fluctuations are neglected. The methodology of the work is presented in the following subchapters. Firstly, some generic information and specifications about the modelled system is presented, which remains the same for all considered cases. Then, the modelled systems and their considered scenarios are briefly described.

6.1 Superior System Description and Evaluated Characteristics

The methodology used and superior description (valid for all systems investigated) of simulations performed is presented in the following. The focus of the thesis is to better understand how the DGs could impact the DN. As this is an extremely wide problem, involving a great number of variables, and depending on many network components and topology; the scope has been narrowed down to the possible problem of voltage constraint violations, and some matter that inherently is a part of this network property that varies every instant, e.g. reactive power regulation, loss and capacity considerations. Furthermore, the network loadability curve could be useful for analyzing when the network reaches the limit where voltage instability could occur. For the purpose of examine some voltage regulation aspects regarding DG, three models are used. The first is a very simplified radial MV distribution grid containing some feeders, loads and DGs. Secondly, a Wind Farm with six WTGs connected to a stiff MV busbar is evaluated in the light of voltage/var regulation. Lastly, several scenarios of PV penetration are investigated in a LV cable network consisting of 19 customers. For analyzing the network in particular, the external grids in this work are always swing buses. All simulations are carried out as balanced, positive sequence AC load flows.

The voltage range of acceptable limits is considered to be in line with the EN 50160 [62] Standard and Norwegian requirements at a minimum but the objective of keeping as flat as possible voltage profile was in mind through the process of simulations carried out. For instance, in [38], the steady state range of voltage at customers end is +6 % and -10 % for the LV grid, and ±5 % for the MV network. Reference [45] reports +10 % and -6 % for the LV grid, which is the exact opposite, and furthermore ±5 % for the MV grid. Other references are indeed used as an input for which requirements are to be met. The absolute minimum steady-state voltage with reference to nominal voltage is given in Table 1. Steady state is here regarded as the minute-scale (In Norway the requirement for steady-state is an average over one minute).

Table 1: Absolute limits for steady-state voltages considered satisfactory.

Grid Level	ΔU_{lim} *[p.u.]*
Low Voltage	± 0.10
Medium Voltage	± 0.05

6.1.1 Superior Load and Line Specification

The loads are in all studied systems and cases implemented as a load with two of the properties P, S, PF or Q specified. The input represents the rated load power and operating point. For static analysis, this is considered sufficient in this work. Neither are voltage dependency of loads included in any of the cases. Voltage dependency of loads was under testing found to not have notable impact on the results and was therefore neglected throughout this work.

Loads are represented by a constant impedance, balanced three-phase, unless otherwise stated. For load flow analysis this is sufficient.

It is noted here, as cables can be seen as a load to some degree, that the operational temperature of cables is always set to maximum when simulating. This is performed to further provoke some of the "worst case" scenarios. The utilities have to plan and dimension the network in accordance to predicted maximum power flows (not very short transients of course), to secure the lifetime of network components and safety aspects, for instance. Hence, it is rational to examine these conditions, although they may not happen often in practice. All lines (branches) are modelled as a π-equivalent line, where the characteristics are distributed at the branch start and end, in addition to a series element.

6.1.2 Superior Generator Specification

As stated, the generator types considered in this paper; is PV and WT. The PV are regarded as small generators installed in residential homes and the WT are installed in the MV DN, say near a substation or on a primary MV feeder which has the capacity to allow the connection of a WT park. The reactive power capability (characteristics), if present, follows the course of software templates of power equipment. The specification of generators is based on the same principle as loads, where two of the properties P, S, PF or Q are specified. The numerical value inserted here represents their nominal power. In addition, several methods for Q – control are available, for instance const. $\cos\varphi$, const. Q, $Q(U)$, $\cos\varphi(P)$ to mention some of them. These schemes are described in the respective section where it is relevant, if used in this work.

In regard of ENTSO-E in their draft Network Code *Requirements for Generators* (RfG) , the generating modules considered in this paper are classified as *Type A* (P>0.8 kW, U_N<110 kV) and *Type C* (P>10 MW, U_N<110 kV), by their voltage level connection point and their Power Capability, for the Nordic Power System. Hence, the requirements and guidelines/grid codes could be used as an overall basis of the capabilities of the generators. The main difference is the minimization of supervision and control of the *Type A*, and the wider dynamic responses required for *Type C* [63]. This can also be found in the *Commision Regulation (EU)* 2016/631 [48] which are operative. For the relevance in Norway, the reader can refer to [64], where the Norwegian TSO drafts its understanding and implementation considerations in terms of the RfG. Note that this implementation will complicate many operations, e.g. that most of generators with nominal power exceeding 0.8 kW will mainly be installed in the distributed network (DN). Today, there exists no regulating and constraining guidelines by the TSO in Norway for production modules with nominal power less than 1 MVA, unless the module is causing great and demanding impacts on the regional, or transmission grids [65]. Hence, the DSO is responsible for the implementation of these modules and their connection arrangements.

6.2 Medium Voltage Radial Distribution Network

Firstly, to illustrate and evaluate the impact of an increasing penetration of DG, a highly simplified model of some radial MV feeders was developed within the software platform. It is a 22 kV network supplied from a stiff external grid, represented by a 132 kV substation (swing bus). The objective was primarily to analyze the voltage variations with respect to varying degree of DG penetration and load scenarios. Penetration level of rated DG power was in this case taken as the S – rating of the total aggregated load on the respective bus, i.e. 100%. The developed MV radial network used for initial studies is depicted in Figure 16, which clearly shows that there is a varying level of DGs installed on each feeder. Detailed element description and ratings will be given in the following and in the Appendix A.3 (Network and Line characteristics) and A.2 (Transformer data, LDC). The Feeders are maximum 23 km in length (Feeder A and B), and Feeders A and B have identical topology, if the penetration of DG is disregarded. In this section, the term *network* is used for the MV side of the TF, i.e., MV1 and downstream. It should be noted that all loads and DGs are balanced, i.e., a symmetrical system not taken into account the possible negative effects of an unbalanced network. No reactive power compensation is installed, unless otherwise stated.

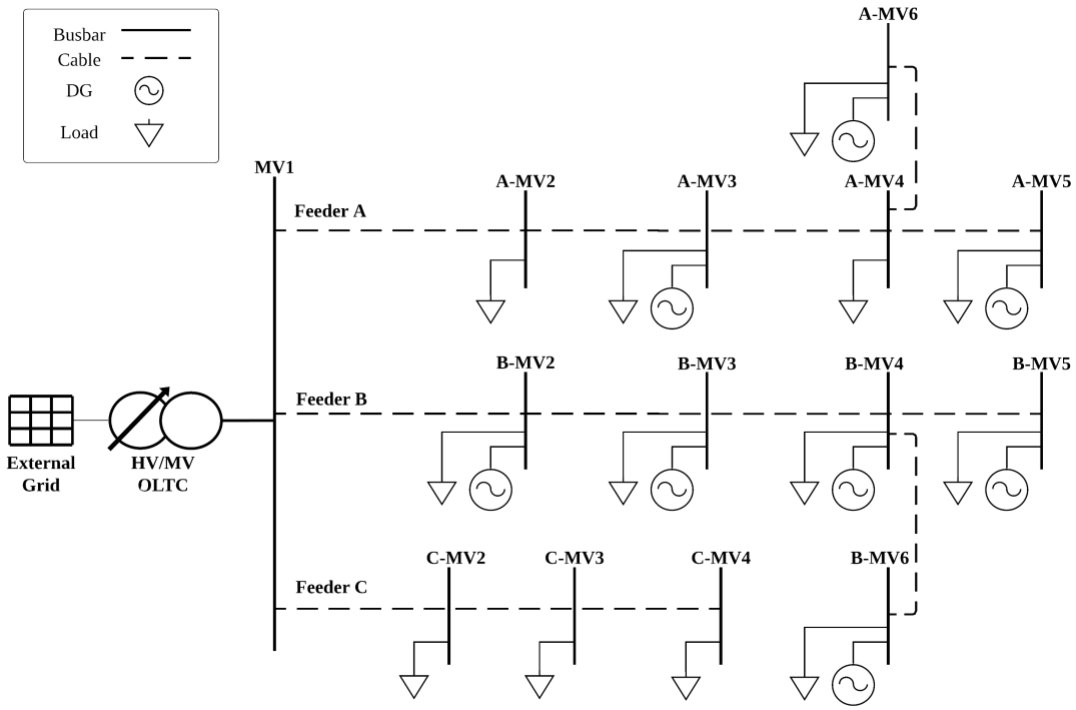

Figure 16: The developed MV radial network used for initial study.

For comparing between the results, some indexes are defined regarding voltage profile, losses and penetration level of DGs. They are inspired by [39] and presented in the following;

Penetration index [%], denoted $PEN_{\%}$ is here defined as the ratio between the sum of connected DG plants with respect to the sum of real power load and loss in the base case, as illustrated by Eq. (6.1);

$$PEN_{\%} = \frac{\sum_{i=1}^{n_{DG}} P_{DG}}{P_L^0 + P_{Loss}^0} \times 100\% \tag{6.1}$$

Where P_L^0 is the sum of real power load and P_{Loss}^0 is the recorded real power loss in for the base case and $\sum_{i=1}^{n_{DG}} P_{DG}$ represents the sum of DG installed real power capacity.

When evaluating variations between the operation scenarios, it would be beneficial to easily present the change in voltage conditions in the analyzed network. For this purpose; an index for voltage variations is defined as follows. The maximum difference in voltage in the network is noted for each operation scenario and compared to that of the base case. This way, an index for voltage profile *flattening* or *increasement* in voltage profile is set, $I_{\Delta V}$[p.u.], as shown in Eq. (6.2).

$$I_{\Delta V} = \left(V_{max}^0 - V_{min}^0\right) - (V_{max} - V_{min}) \tag{6.2}$$

Where V_{max}^0 and V_{min}^0 are the maximum and minimum voltage [p.u.] recorded in base case, respectively. V_{max} and V_{min} represent the actual maximum and minimum voltage [p.u.] measured in the assessed case, respectively.

With this form, the $I_{\Delta V}$ will be positive if a flattening result is obtained, and negative if the voltage deviation is increased with respect to the base case.

Loss considerations are an important factor in network planning and optimization, thus the impacts on power loss is of interest in this work. For this cause, a loss index, I_{Loss} [-] is defined, as;

$$I_{Loss} = 1 - \frac{P_{Loss}}{P_{Loss}^0} \tag{6.3}$$

Where P_{Loss}^0 and P_{Loss} are the active power loss [W] for base case, and the examined case, respectively. Near unity values imply a positive effect of DG penetration (minimization) and negative values reflect an increased power loss.

6.2.1 Generators, Transformer and Loads in MV radial feeder system

In the developed system, the generators and loads are simply implemented by the Library equipment *Static Generator* and *General Load*, respectively. The ratings of both is noted within the properties for each component.

Load

Loading of the system is simply implemented as an aggregated load at each bus, located as per the schematic in Figure 16. It is set to represent mainly residential areas (LV networks) and hence, some distribution TFs. The PFs is set to around 0.95 lagging. The stationary power drawn from the network is adjusted by load scaling. For complete aggregated load characteristics for all buses, please refer to Appendix A.3. No capacitor bank (switched or static) or any var-compensating device is installed. The cabled network will inject some reactive power, but this is not expected to be in large quantities, yet it is interesting to see how much the cables will impact on reactive power balance.

Generators

The generators are in this system simply set with an operating dispatched power, which is constant, unless otherwise stated. The *PF are unity for all DGs*, i.e., delivering only active power, according to the generating scale in percentage *(i.e., DG=100 % does in this case mean that all DGs are operating at rated power*). The DGs can be seen as power electronic interfaced sources delivering power at unity PF in steady state. Refer to Appendix A.3 for generator ratings.

Transformer

The substation TF was implemented as two parallel operating TFs, due to convenience within the library components. It has an OLTC integrated and the setpoint, deadband and time constant can be set. It should be noted that the used TFs are identical, and their OLTC will operate together. Furthermore, it has rated frequency 60 Hz, which is a mismatch with respect to the system frequency, which is considered to be 50 Hz. Yet, this is considered to mostly affect the loadability of the TF, and that in particular is not of high interest in this section. They can be roughly seen as one TF operating with their total capacity (40 MVA), sharing the load perfectly. Some basic specifications on the TF is given in Table 2. The tap changer is operating on HV-side, and the controlled node is the LV-side busbar, unless otherwise stated. In addition, the chosen nominal voltage at HV side (external grid) was 132 kV, thus some adjustment has to be performed to get the desired voltage at LV side of the TF. OLTC control setpoints are briefly noted in Table 3.

Table 2: Some basic specifications on the identical HV/MV transformers installed in parallel in the MV developed grid. With respect to simulations, they can be regarded as one TF with the double capacity.

Spec.	*Value*
Rated voltage [kV]	138/23.1
Rated power [MVA]	20
Rated frequency [Hz]	60
Fabrication	WEG
OLTC range [%]	±8x1.25
LDC	None (deactivated)

Table 3: Initial controller setpoints for the HV/MV OLTC in MV system with several feeders.

Control setpoint	*Value*
Voltage setpoint [p.u.]	1.00
Lower bound [p.u.]	0.99
Upper bound [p.u.	1.01
Time constant [s]	0.5

6.2.2 Line models

The feeders represent feeders of considerable length, i.e. 23 km is the farthest point from the substation. All lengths given are wire lengths. In the modelling aspect, the PI-equivalent (π) was deployed on all lines. The characteristics of each line segment (branch) is strived chosen on a rational basis but relies mainly on theoretical and practical insight. Thus, the capacity, i.e. the current rating and cross-sectional area of each branch is in harmony with the power which is expected to flow in the respective branch. On Feeders A and B; the size of cable is kept constant all the way to the end (MV5), in order to represent the feeder "backbone" which could, say for instance in reality, be further expanded in the future. Feeder C is thought to be excluded from future expanding and has decreasing cable size downstream. It is stressed, that all branches in the model are cables, i.e. underground cables laid in a row formation (e.g. 3x1x500 mm^2). Overhead lines were preferable to the author as they are assumed to represent a larger part of installed MV feeders in Europe for instance, and indeed in rural areas which is of great interest in voltage quality studies. However, it should then be considered as a somewhat "futuristic" network, with say, for esthetic reasons has been installed as an underground network. This can cause a higher degree of reliability as it is not that prone to weather conditions (e.g., lightning, snow, falling trees). It is however considered to have a larger component of capacitance than overhead lines. The X/R ratio of the feeders are ca. 1.3 (varying a little between the feeders), implying reactive power regulation has a more dominant effect on voltage levels. The cable types used, along with some basic data, e.g. resistance and reactance of the branches are presented in Appendix A.3

6.2.3 Operation scenarios

For visualizing voltage drop in the system, some *operational scenarios* were performed. Load flow calculations where used to obtain voltage profiles on the respective primary MV feeders.

Two of the scenarios simulated are regarded as the *high load no production* (HLNP) and *low load high production* (LLHP), which can be thought of as the "worst case" operation of the network in terms of steady state voltage profiles, hence, they are useful to analyze, even in this simplified manner. This is due to the fact that the HLNP will cause the most severe voltage drop, and the LLHP introduces the possibility for reverse power flow and thus the chance for increased voltages with respect to distance from substation. The operation scenarios evaluated are listed in Table 4.

Table 4: Operation scenario description for the MV network

Scenario index	*Load [%]*	*DG [%]*	*Abbreviation*
1 (Base case)	60	0	
2	100	0	HLNP
3	100	100	
4	20	100	LLHP

6.3 Wind Farm Connected to Medium Voltage Network

A wind farm was analyzed with respect to voltage control. The whole system model was taken from the DIgSILENT library *("Wind Farm Example")* and contains six 2.5 MW WTGs delivering power to a wind farm busbar (collecting 2 cables from two and four WTGs), which is then connected to the MV grid through the PCC (0.2 km between Wind Farm and MV substation busbar/PCC). It represents interconnection almost directly to the stiff MV (20 kV) grid, i.e. the substation in this thought case, which is represented by a *SL* bus reference (swing bus) at 1.0 p.u. V. For evaluating voltage control; the model is customized, and the reactive power control (voltage and PF) is studied in detail. Each P-Q capability is the same, and it can operate over a wide range of PF as it is a *fully converter interfaced generator*. In this section, the term *plant* is used when referring to the whole generating module, i.e., what the overlying grid "sees" at PCC. The general specifications of the plant are given in Appendix B.2

The model was later customized further, for studying the impact of PV in a LV network connected to a feeder (20 km cable) on the same MV source as the wind farm. Their interaction was expected to be neglectable, but this was performed to leave room for potentially further altering the placement of the WT park on a MV feeder, in addition to residential networks and analyze their interactions. This scenario could be compared to the Figure 2 in Section 2.2.1, where the DG connected to MV line represents the WT park. The Wind Farm is depicted in Figure 17. Note that a capacitor bank exists on the plant busbar. Please refer to Appendix B.1 for network and TF characteristics.

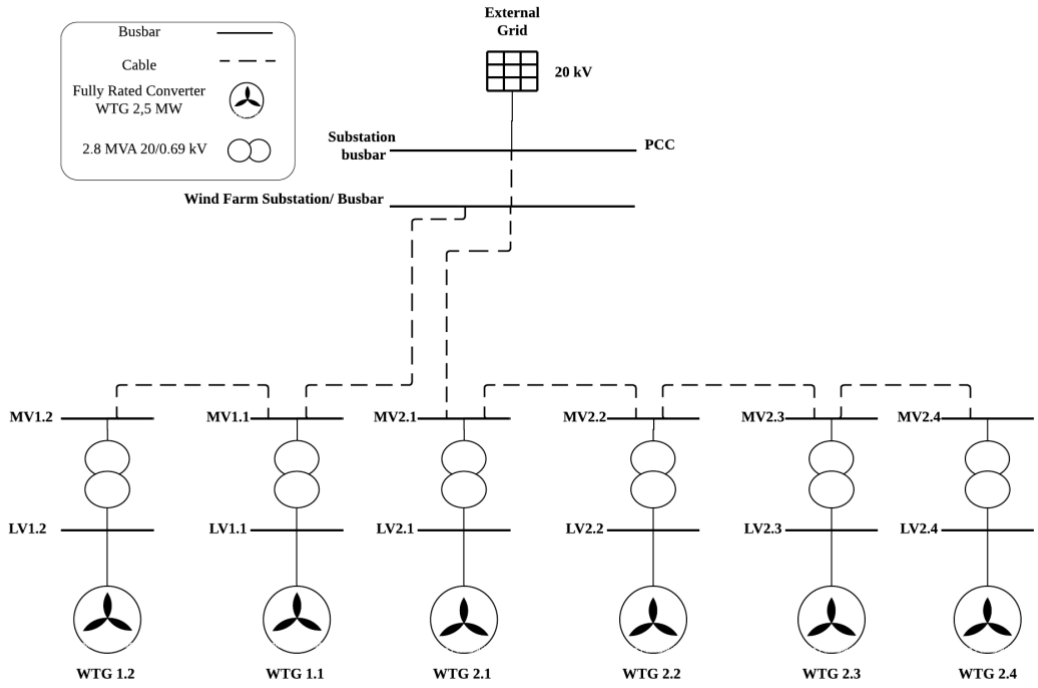

Figure 17: Schematic of the simulated Wind Farm Plant, consisting of six 2,5 MW Fully rated converter WTGs. The MV and LV side of the plant has nominal voltage 20 kV and 0.69 kV, respectively.

The wind speed vs. active power output for each WTG an essential characteristic which tells the operator of the turbine what power outputs is achievable at the respective wind speeds [m/s]. This

power curve, which is the same for every WTG, is included in Appendix B.3. Active power can be utilized when wind speeds are above 3 m/s. The WTGs reach nominal output power at 15 m/s, and is brought to a stall when wind speed > 25 m/s, i.e., power output is zero at wind speeds over 25 m/s. As we have seen previously, the curve is not linear between minimum and nominal power output.

6.3.1 Wind Turbine Generator and Local Control

The WTG used is one of the templates available within the PowerFactory platform, the *Fully Rated Converter WTG* template [66]. This model represents a fully rated converter interface, i.e. only the grid side converter is "seen" in the model. In this matter, this is suitable because the mechanics (e.g. rotor, gearbox) is decoupled from the grid. Furthermore, this topology is considered favorable with respect to the electrical freedom which exists when decoupling grid and mechanics. The potential pros and cons regarding the lack rotational inertia is not included here.

Each WTG has a rating per the description in Table 5.

Table 5: Rating of each wind turbine generator

Parameter	*Value*	*Comment*
S_{WTG} [MVA]	2.778	3_{ϕ} - Fully Rated Converter
PF_{rated} [-]	0.9	
Number of WTGs	6	Total P= 15 MW

Steady-state Controller

The WTGs operate with a supervisory controller for the whole Wind Farm, which is referred to as *Plant controller*. Reactive power is shared equally between all WTGs, i.e., each WTG contribute 16.667 % to the total regulation which is performed at the wind farm MV busbar. The protection scheme makes sure that disconnection occurs if the guidelines in the separate case are violated. The steady-state controller is operating in PF-mode and is controlling the output via $\cos\varphi(P)$- characteristic curve. This is a fairly simple approach as the power output is affecting voltage, and this impact is proportional to injected power. The required reactive power compensation demand will as known vary with injected active power, to suppress voltage variations. The controller characteristics of the PF-control is briefly presented in Table 6. The PF setpoint varies linearly between the two points stated in the Table, i.e. the plant is operating more and more underexcited when active power injection grows towards the nominal value. This controller is the one which is operative in the simulations performed, unless otherwise is stated.

Table 6: Wind Farm: Park controller reference setpoints for PF-control as a function of active power injection

Parameter	*Min. PF [-]*	*Active power [MW]*
Overexcited (inductive)	1.0	7.5
Underexcited (capacitive)	0.95	15

The controller PF setpoints implies that it is set to absorb reactive power whenever the WT farm active power output is above the threshold of $P_{WT\ Farm}$ = 7.5 MW. It is never operating in overexcited region in steady-state, this is implemented in the dynamic controller, which is not discussed here. The regulated node is the PCC, i.e., where the cable from the plant meets the breaker at the substation, 0.2 km from the plant.

6.3.2 P-Q Capability of each Wind Turbine Generator

Each WTG has a capability curve integrated which defines the absolute limits for operational conditions with respect to PF or reactive power flow. The P-Q diagram is depicted in Figure 18, where, within the area constrained by the red lines in the Q – and P plane shows the operational area of the generator. Maximum active power is indeed 0.9 p.u. of rated power.

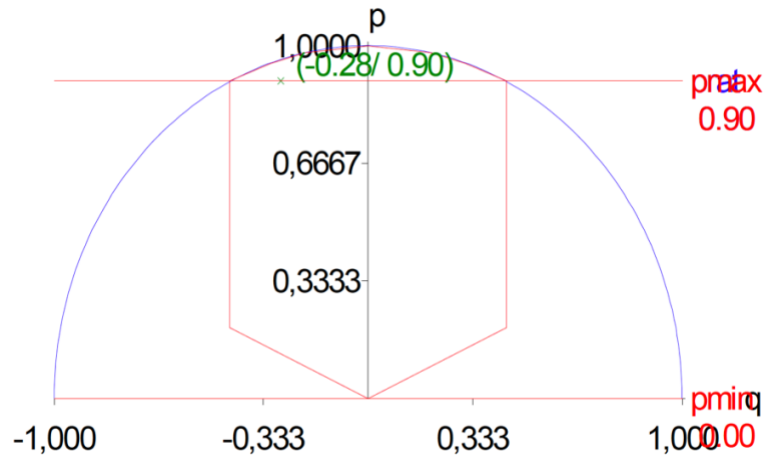

Figure 18: Capability curve of each WTG. Maximum limit of reactive power is the same in under-excited and overexcited state. The vertical and horizontal planes represent P and Q, respectively. It is illustrated that the WTG has a wide range of Q support and can regulate Q even when active power output is equal to rated.

The capability changes with the voltage level at the PCC, as showed in Figure 19. This is a consequence of the relationship between voltage and current. The diagram is not presented in detail; however, it follows the default setting of the *Wind Farm example* in PowerFactory, which is used here.

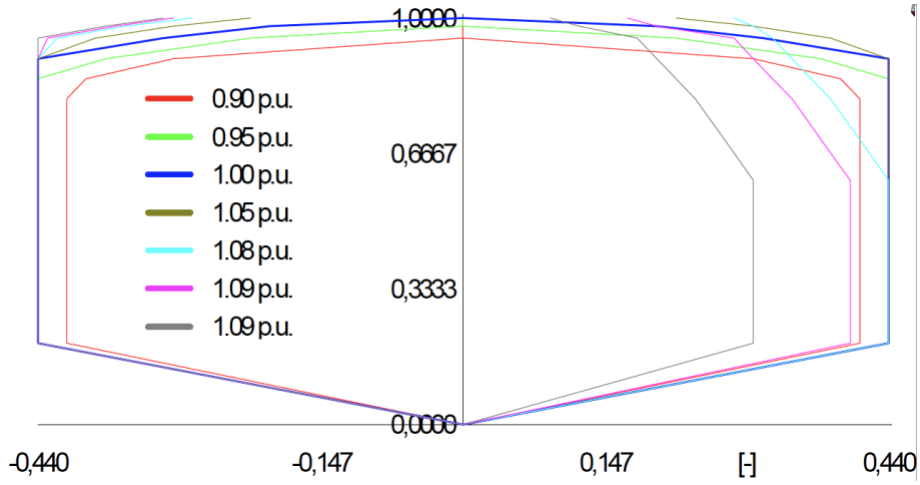

Figure 19: P-Q Capability diagram determined with a range of PCC voltages (displayed in legend). P-axis and Q-axis is vertical and horizontal, respectively.

6.3.3 Local reactive power compensation

The plant has in addition a capacitor bank which is switchable (SCB) connected to the plant busbar through one 20/0.4 kV TF. The bank is connected in star configuration, and has a total capacity of 2.5 Mvar divided in 10 equal steps. This is installed to provide ancillary reactive power support when low voltages take place, and the capability of the park is reduced. This is due to the fact that the capability can change with respect to voltage at the PCC, as the thermal constraints will be reached before sufficient reactive power support per the requirements is achieved. With the SCB injecting reactive power, the WTGs have to consume more reactive power in order to deliver the desirable PF of 0.95 when active power output is nominal. The SCB is injecting 1 Mvar, unless otherwise stated.

The WTG converters has to be oversized in order to provide Q-support even at full active power output. This is, as understood from the previous theoretical background presented, due to the fact that both the reactive and active current has to be carried by the converter, thus thermal and electrical constraints exist. The significance of this is that topologies like this can provide wide reactive power support, but it can be costly to oversize the components.

6.3.4 Wind Speed Sweep for examining Performance

In order to examine the operation of the plant as a function of varying wind speed, it is found reasonable to execute a *Wind speed sweep,* which run the model through a range of wind speed inputs. A sweep from zero to 30 m/s wind speed was conducted in order to analyze the individual WTG contribution to regulation, and the plant bulk power at PCC. The step wind speed was 0.25 m/s.

6.3.5 Active Power Injection and Impact on Voltage at Wind Farm Busbar

In order to observe some dynamics (meaning a series of load flow simulations in this case), a scaling curve is implemented in the WTG elements. This means that the active power output is controlled by a power profile, and thus, it indirectly represents wind speed changes. However, the curve consists of values with a step time of 15 minutes. Simulation time will be a whole day, i.e., 24 hours. The SCB is disconnected in this investigation, the only reactive power regulation will come from the WTGs. The scaling curve (relative values with respect to nominal power) is given in Appendix B.4

6.4 Low Voltage Radial Network with PV at PCCs

In order to study the impact of increasing DG penetration with respect to photovoltaics (PV), a domestic LV network was developed for this purpose (a secondary distribution system). The distribution TF supplying the LV DN was connected to the same "substation" busbar as the wind farm (stiff source), with a 20 kV cable (20 km) to the position of the LV grid. In order to investigate the scenarios which are of interest to the author, in particular sunny and partially cloudy weekdays where most residents within a domestic grid typically are at work or school, the implementation of some dynamics were performed. However, the dynamic simulations are performed with the *Quasi-Dynamic Load Flow* calculation within the software**.** This algorithm uses the static load flow characteristics, i.e. it does not include transient and fast variations. However, the steady state scenarios are of interest in this thesis, hence the method is sufficient. The MV side of the TF has no load attached, unless otherwise stated. The Appendices regarding this subsection is Appendix C.

The developed domestic grid; consists of residential customers in what is considered a typical LV radial in underground cable networks (more than 90% cables). The LV grid is modelled as a $U_{n,L-L}$ = 0.4 kV TN-C-S network, which is connected to a delta - grounded star-connected distribution TF, providing customers with three phases (L1, L2, L3) and *PEN*-conductor. The PEN-conductor is indeed split into earth (PE) and neutral wire (N) at customers PCC, and 3-phase power is assumed to be both drawn and injected between phase-neutral (L-N), i.e, 0.23 kV rated equipment. *All loads and PV systems are modelled as perfectly balanced*, *which is a significant simplification.* But it could represent a network where all customers have installed (or have been requested by the DSO) 3-phase PV systems, due to the rating. Furthermore, the PV systems are indeed rated higher than the threshold for which single-phase connection is allowed (16 A per phase) by many utilities [67] [68].

It is assumed all customers let their power flow uncontrolled in the PCC, i.e., surplus power will be fed to the grid, and the AMI-meter measures power in both directions (*no battery storage*). In addition, it is assumed PVs operate at constant PF=1, only providing active power, unless otherwise is stated. The network consists of 19 customers connected to 5 cable cabinets installed on the ground, which distributes cables downstream to each house. Please note that all PVs and loads represents one household; and they are all identical in both nominal power and their daily scale curve (load – and feed-in curves for 24 h). In Figure 20, the developed system is depicted, where cable types and length, busbar indexing and so on are included. It shows, that bus (cabinet) LV5 has the longest distance from the TF, which is 300 m from the TF secondary side. Extended data on cables and distribution TF, along with rated power of loads and PVs are included in Appendix C.1 and C.3.

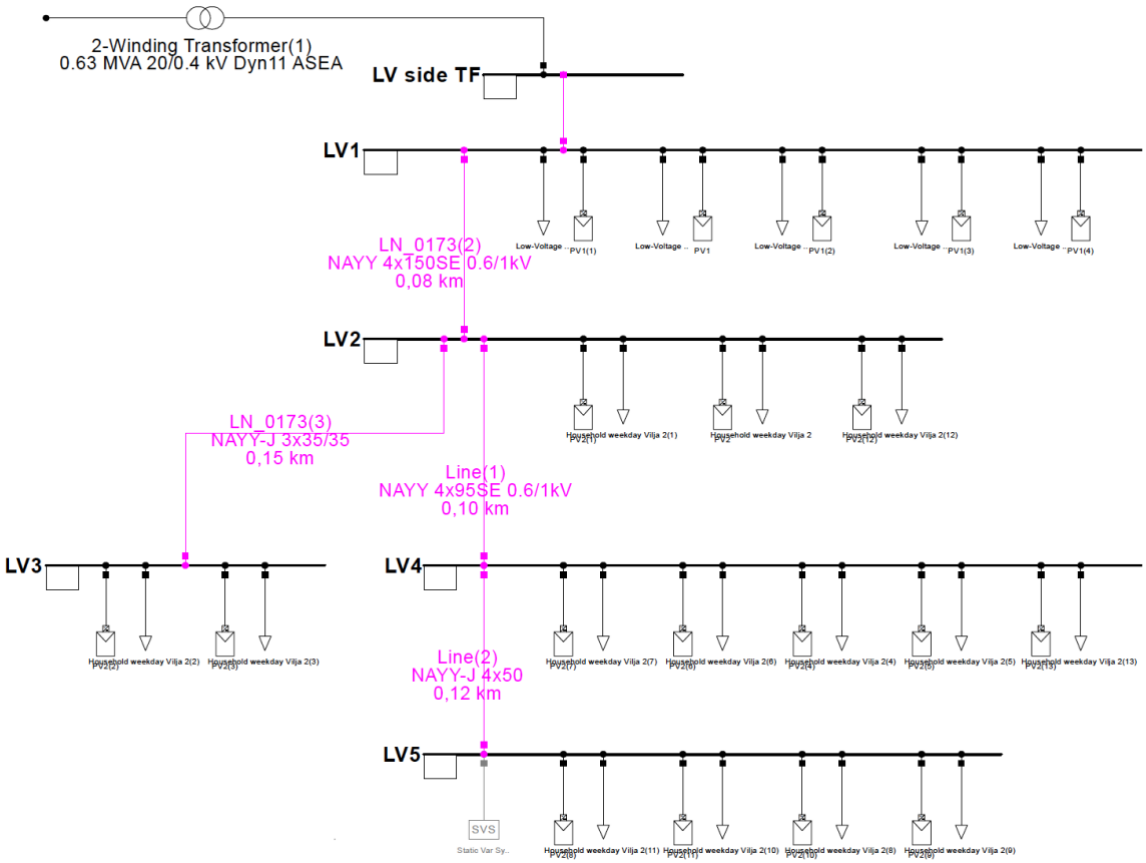

Figure 20: Schematic of the developed LV cable network. It is supplying 19 customers via 5 cable-cabinets. The first cabinet downstream is connected straight after the LV-side on the TF. Every customer is represented by one load – and one PV system symbol.

6.4.1 Input data in Quasi-Dynamic simulations

For investigating the voltage profile on the course of a day, scale curves were implemented on both loads and PVs. The load curve represents a weekday load scenario of a households, and the curve is taken from the PowerFactory library, and further modified. The modification performed on load profile was in order to achieve very low load mid-day. Although the load profile is the same for every house in this work, this correlation of load in such a network can happen in theory. Furthermore, the likelihood for this happening is assumed to be inversely proportional to the number of customers connected to the same distribution TF (residential customers). The term *network* is in this section used when referring to the developed LV network, which is galvanically separated from the MV grid.

The residential loads and PV systems are implemented as the same library equipment's as previously. PV output power P_{PV}, is following the Power-curve, which is both executed as a "sunny day" and a "partly cloudy". These two curves are obtained from the PowerFactory library but is modified to represent the two hypothetical cases of solar irradiance. As the power output is directly scaled by the dynamic profile, the solar irradiance is indirectly included. The rating is regarded as a quite large PV-system in the residential aspect, but it is chosen in an effort to simulate a scenario which may take place in practice. Note that all curves are self-modified, but it is considered to represent plausible scenarios.

Loads are considered to have a constant PF = 0.95 lagging (inductive) to account for some reactive consumption and a total rated active power approximately equivalent to each house having a 3x32 A circuit-breaker in this 0.4 kV grid. In words of power, if a residential PCC is drawing maximum current, the power drawn from the grid, P_{Load}, is 22 kW if the PF is unity (balanced). The ratings of the key elements in this network are listed in Table 7. It illustrates that the PV inverter is rated 11 kVA with a PF=0.9. This implies the inverter is somewhat oversized, in order to provide reactive power support if it is found necessary in this study.

Table 7: Power ratings of the key elements in the LV grid. Refer to schematic of grid for bus indexing. All houses are modelled with a PV system installed.

Parameter	*Value*	*Comment*
P_{Load} [kW]	20	Rated PF=0.95 ind.
P_{PV} [kWp]	9.9	Inverter S= 11 kVA, PF=0.9
Number of customers	19	Refer to schematic for topology

The TF is of type NLTC, thus it has to be de-energized in order to adjust its winding ratio. But if the simulations show it could be favorable, it is possible to test OLTC operation within the specs of the TF. The rating of the TF is 20/0.4 kV, 0.63 MVA. The NLTC has 5 taps and regulation ±2x2.5 % (neutral position is 0). Its rating is exceeding the total maximum demand in this particular network, but one can regard it as if only this radial LV feeder is modelled. The TF might supply other loads as well, e.g., public road lights, more LV feeders etc. If it is found preferable, the OLTC will be activated on the MV/LV TF, thus representing a TF with retrofitted OLTC or a newly installed TF with this solution implemented. Please note that in such a case the available taps (and hence the regulation of each tap), must remain unchanged from the original library component. This is due to the fact that TF types within PowerFactory library are “read only”. Furthermore, this would not reveal the real OLTC performance by simulation as the time resolution is too low. The effect of tap changes is in such a case considered to be the key study, not the investigation of “rapid” tap changes.
Key TF data are presented in Appendix C.1

In order to assess the local property of voltage, it is found reasonable to simulate the course of a day, i.e., 24 hours. Therefore, when simulating on this respective system, a Quasi-Dynamic simulation is performed, which in essence is a series of load flow calculations as previously described. This way, the varying power injection by the PV systems can be easily visualized. The step time of each iteration is set to 15 minutes. The key simulation information is listed in Table 8.

Table 8: Key information about the simulations performed on low voltage network. Valid for all simulations within this section.

Spec.	*Value*	*Comment*
Simulation type	Quasi-Dynamic	
Step time [min]	15	i.e. 96 calculations per day
Total simulation time [h]	24	From 00:00 until 24:00
Resolution: scale curves [min]	15	PV and load (power)
f_{rated} [Hz]	50	
Voltage dependency, loads	NO	

6.4.2 Residential load and PV systems – Dynamic profile

This subsection briefly presents the dynamic scale-profiles implemented for all residential loads and PV systems. These respective curves are valid for all simulations on this network, unless otherwise is presented. Some other scenarios are of interest, but they will be explicitly described if carried out within the recorded results. These curves have a resolution of 15 minutes, i.e., every set value has a duration of 15 minutes. This is indeed a great simplification as the load and PV in reality will be highly dynamic in some cases but is considered sufficient. All load and production scaling curves; can be found in tabulated form in Appendix C.3.

The load curve is representing customers demand at the PCC. The two peaks can be seen as the "morning rush" and the afternoon where typically power demanding kitchen equipment is in operation for some time, and water heater for instance are active. No special consideration towards the scenario of EV-charging is included here, however it could be a part of the demand. The minimum demand is 2 kW and can be regarded as some base load (e.g., water heater). The maximum demand is by this relative scale approximately 15 kW. The scale curve of the residential load is depicted in Figure 21.

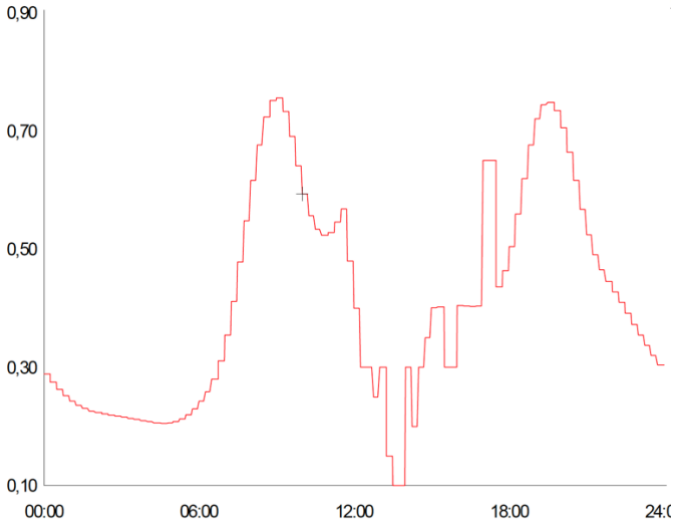

Figure 21: Load curve used as input when scaling the residential load referred to its rated value. Y - and X- axis does therefore represent the p.u. power (relative) and time of day [hh:mm], respectively. Minimum is 0.1 and maximum is ca. 0.75.

The scenario of a sunny summer-day is imitated by setting relative power setpoints for the PV system at all times through a 24-hour period. This curve is based on inspiration from literature but mostly the curve is intuitively set by considering a sunny summer-day. According to its rating, the maximum active power injected by one PV system is 9.9 kW. It is stressed that using this curve on all PVs, assume that all customers have identical geographical orientation, PV system rating and efficiency. Furthermore, no shading or soiling is present. This has to be considered a modelling simplification and the results has to be perpetrated as such. The PV scaling curve for a sunny day is illustrated in Figure 22.

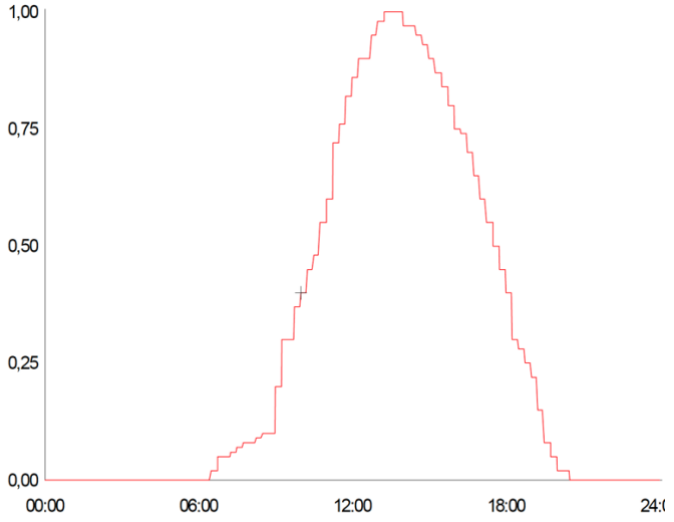

Figure 22: PV power curve on a sunny summer-day used as input when scaling the residential PV system referred to its rated value. Y - and X- axis does therefore represent the p.u. power (relative) and time of day [hh:mm], respectively. Maximum power is 1.p.u. mid-day.

For taking a partly cloudy day (the season is undefined) into consideration and investigate the impact the spontaneous injection of power by the PV system; the scale curve depicted in Figure 23 is applied. This profile is based on the “sunny day profile” and modified with random low setpoints, to represent

the blocking of solar irradiance reaching the residential PV systems. The steps in relative power output is quite high, it is considered to be a sunny day with dense clouds blocking the sun intermittently.

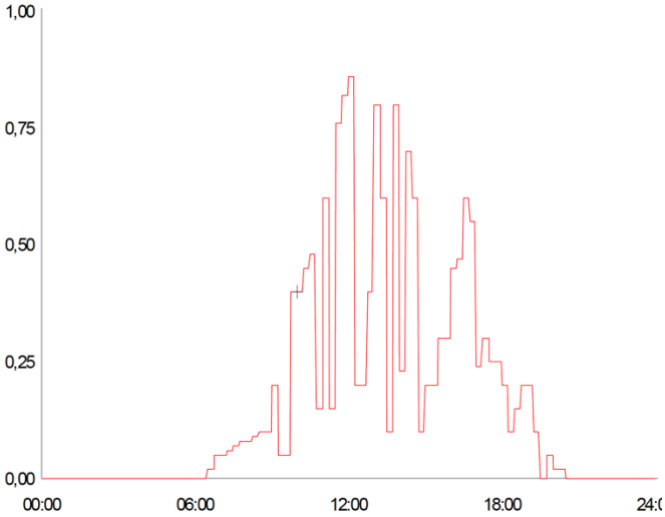

Figure 23: PV power curve on a partly cloudy day used as input when scaling the residential PV system referred to its rated value. Y - and X- axis does therefore represent the p.u. power (relative) and time of day [hh:mm], respectively. The intention is to represent the stochastic nature of the PV system.

Two penetration ratios in *percentage* are defined, in order to keep track of how aggressive the penetration in the local network is. The previously defined penetration index is not used as the loss in the network is neglected when considering the LV network. Taking a ratio associated with the TF rating is in this case not desirable, as it would reflect a low penetration ratio, because the simulated network is only a part of the network this TF in practice is thought to supply. The two ratios consider the maximum installed apparent rating of the inverters installed within the network, to the sum of maximum installed load for all customers. This gives a ratio, PEN_{PV} [%], which is associated with the limitation of the circuit-breaker for all customers (the power allowed to be drawn) in the local LV grid. The second ratio PEN_{Load} [%] simply imply how many customers in the network who have PVs installed. The two expressions are defined as follows;

$$PEN_{PV} = \frac{\sum S_{PV,installed}}{n_{Loads} * S^{max}_{Load,installed}} * 100 \tag{6.4}$$

$$PEN_{Load} = \frac{n_{PV}}{n_{Loads}} * 100 \tag{6.5}$$

Where $\sum S_{PV,installed}$ is the sum of all PV inverter ratings installed in the LV network [VA], $S^{max}_{Load,installed}$ is the maximum apparent power allowed to be consumed by each customer, which is calculated using the rated values previously given. n_{Loads} and n_{PV} simply represents the number of loads (customers) and PV systems installed in the network, respectively.

6.4.3 Operation scenarios

In this subsection, the methodology for evaluating the performance of the LV network is presented. In brief; the initial determination of desirable tap position on the NLTC (transformer) was conducted disregarding any production in the network. Then, this tap position was used, unless otherwise stated, throughout the remainder of the simulations, thus imitating a conventional MV/LV secondary

distribution TF. Then, the cases of some different sizes of the connected PV systems are executed (all PV systems are still delivering the same power each, P_{PV}), i.e. scaling the PV curve itself, which could represent PV systems of higher or lower rating. Furthermore, the topic of clustering within the local network is of interest, hence some clustering scenarios are performed (e.g., only some PVs at the end of the LV feeder).

As stated, the initial study is how the network behaves without any PV connected to any PCCs. This indeed to address the impact PVs have on the network, by having some foundation to compare results with.

- *Case A (Base case)* was considered to be the scenario where the network has zero PVs connected, i.e. PEN_{PV} =0. All loads are operating according to the described load profile. The TF tap position (NLTC) will be adjusted by justification from simulations performed.

- *Case B* involves all customers having a PV system installed, per the described ratings. Only active power P_{PV}, is injected by the PVs, i.e., operating at unity PF. Scenarios of both sunny day and partly cloudy day is examined. This case represents penetration ratios PEN_{PV}= 52.25 % and PEN_{Load}= 100 %.

- *Case C* investigates clustering impacts on the network, where PVs are concentrated in one topological area of the network. Here, the PVs are clustered at the LV feeder end, at LV4 and LV5. This case represents penetration ratios PEN_{PV}= 19.25 % and PEN_{Load}= 36.84 %.

- *Case D* investigates the impact of clustering close to the TF. This case represents penetration ratios PEN_{PV}= 19.25 % and PEN_{Load}= 36.84 %. The penetration is identical in Case C and D.

- *Case E* is simulated with the Wind Farm active and placed halfway down the MV feeder which is supplying the LV network. The MV feeder cable is 20 km, thus the Wind Farm is placed at 10 km downstream from the substation. The objective is to examine voltage fluctuations on the MV feeder when the Wind Farm is delivering power of varying magnitude (wind curve applied). With respect to the LV network, the *Case B* and scenario of *sunny day* is performed.

- Furthermore, regulation techniques might be tested on the LV network if found necessary or preferable, due to violations of admissible voltage levels. The results will be clearly listed by their respective subsection index.

7 Simulation Results

In this Section, the recorded results are presented, and briefly discussed where it is found reasonable. Any discussion of higher significance and summations of the findings is given in Section 8. The presentation of results is executed by using Matlab, as PowerFactory figures provided too low quality with respect to visuality of numbers and axis information. Colors are used in the figures of this work, instead of different black lines. This is to provide the reader a picture which is easier to interpret.

7.1 Medium Voltage Radial Distribution Network

The MV radial feeder network with Feeder A, B and C was simulated in some cases to evaluate the simple case of voltage drop in the MV grid. Simulations performed and their respective yield is briefly presented in the following. When evaluating the power balance, the busbar MV1 was used as the balanced node, i.e., the power imported or exported into the MV network is what the TFs "see" on their secondary (LV) side. When summation is performed on the MV1 busbar, negative sign means export from the network (generation > consumption) and positive sign means import to the network from the overlying grid.

7.1.1 Load scenarios without DG

In the Base case, the loading of the network was set to 60 % with respect to the nominal load, at all buses. All consumed power was indeed delivered by the overlying grid, trough the TFs.

If the MV1 was kept at 1.00 p.u., the minimum voltage in the network was recorded to be 0.97 p.u. the OLTC was tapped into position Tap_{pos}= -3 for delivering a voltage of 1.02 p.u. at the busbar in the substation. This position provided the voltage band of 1.02 p.u. (U_{max}) to 0.99 p.u. (U_{min}) within the whole network. Some key results are noted in Table 19. For a diagram of the voltages at each bus, please refer to Appendix A.1.

Table 9: Key results fro MV grid Base case simulation (60% Load, 0% DG), displaying voltages and powers.

Parameter	*Value*	*Unit*	*Comment*
U_{max}	1.02	p.u.	ΔU_{max}= 0.03 p.u.
U_{min}	0.99	p.u.	
P^0_{Load}	23.29	MW	Sum of P, all loads
P^0_{Loss}	0.71	MW	Network loss (P)
Q^0_{Load}	7.33	Mvar	Sum of Q, all loads
$\sum Q^0_{MV1}$	5.00	Mvar	Import to network
$\sum P^0_{MV1}$	24.00	MW	Import to network

Almost all loads have a PF=0.95 lagging, and it should be noted that in this case the resulting PF seen by the TF is PF=0.978 lagging. Thus, the cable network has injected reactive power and is in this manner compensating for some of the consumption of reactive power at each bus. As it is assumed that the majority of loads in reality has an inductive nature, it seems like it could be beneficial to let the cables in the network inject reactive power (as they inherently do at this voltage level). This way, in broad scale, the need of mechanically switched (MSCB) or thyristor (TSCB)capacitor banks could be reduced. In this case, the problem of resonance should be carefully considered, if the reactance and capacitance in the network may be equal in some scenario. At that point, the admittance will be at a maximum, causing low losses but however, reduces the opportunity to regulate reactive power as normal, i.e., all compensation will oscillate between sources of reactive power, which in such a case would be only generating modules.

It is worth noting, that for a load scaled to 20 % on the network, indeed provokes the OLTC to command several tap changes and reaches the desired operating point at Tap_{pos}= 1. Comparing to Base case, it has switched 4 taps. Not worth mentioning, the network operates well within statutory voltage limits.

For the operation scenario indexed 2 (HLNP), the initial result gave a substation busbar voltage of U_{MV1}= 1.02 p.u. and the lowest network voltage U_{min}= 0.95 p.u., which surely is on the limit of satisfactory. One way to solve this which was tested, was including the LDC on the OLTC by setting the R and X controller parameters to the value of the calculated impedance of the line going from the substation to MV2 on Feeder A. Feeder A is the feeder which is loaded most heavily, and therefore it is used. The OLTC and LDC setting in this case is depicted in Appendix A.2. These settings yielded U_{MV1}= 1.03 p.u. and U_{min}= 0.97 p.u., and the controlled node, A-MV2, was attained in accordance with the LDC control.

In addition, optimal OLTC tap position was determined with the help of the *Voltage Profile Optimisation* tool within PowerFactory, as Tap_{pos}= -5. This algorithm considers both consumption and production case simultaneously, and this tap position yielded a voltage at the MV1 busbar equal to U_{MV1}= 1.03 p.u. and the lowest network voltage recorded was U_{min}= 0.97 p.u. It is clear, that the maximum deviation in this condition is ΔU_{max}= 0.06 p.u., which is the double of that in the Base case. For the operation scenario 2, this particular voltage diagram, and key results from the HLNP case can be found in Appendix A.1.

The results from HLNP simulation shows that the bulk reactive power provided by the cables in the network is reduced from($\sum Q^0_{MV1}$ - Q^0_{Load}) = -2.33 Mvars in Base case, to ($\sum Q_{MV1}$- Q_{Load}) = -1.42 Mvars in HLNP scenario, causing the PF seen by the TF to be 0.965, i.e., less compensated than Base case. In MV and HV networks where cables are used, one must remember the, in some cases, considerable quantities of reactive power provided by the network itself [69].

7.1.2 Impact of Distributed Generation in the Medium Voltage Network

Operation scenarios 3 and 4 displayed some effects the DGs have on the network and is briefly described hereunder. The LDC is deactivated if not otherwise stated.

In operation scenario 3, the DGs are scaled to deliver 100 % of their nominal power, with a unity PF, i.e., only real power is injected. This disregards all impedances which may be aggregated by all the DGs, instead this aspect is assumed to be included in the load element. Keep in mind, 100 % of DG in this

network does not imply a 100 % *penetration* ($PEN_{\%}$) in the network. As the network has varying degree of maximum DG penetration with respect to the different feeders, the voltage profile will not be similar. This fact is true in the other cases as well, but the potential effect of DG was expected to strengthen this hypothesis.

For Operation scenario 3, where both loads and DG are set do operate at their nominal power, the loading of the external grid decreases. As the DGs do not deliver nor consume reactive power, the bulk Mvars still has to be delivered by sources upstream. The loading of cables, needless to say, decreases significantly due to the locally produced power within the network. Eventually, causing TF loading to reach half of what in the HLNP scenario.

The OLTC was switched to Tap_{pos}= -4, yielding a voltage at the substation busbar of 1.0 p.u. On all feeders there is a voltage drop present, and Feeder A experiences the largest drop, as the U_{A-MV6} = U_{A-MV6}= 0.97 p.u. Feeder B which has DG at every bus, holds an almost completely flat voltage profile, i.e., 0.99 p.u. at all buses. Feeder C has no DG connected and a voltage profile which is flat at 0.99 p.u. The scenario causes Feeder B to inject 0.7 MW into the substation yet drawing 3.2 Mvars. *It is clearly illustrated that the variation of DG penetration with respect to several feeders connected to OLTC busbar will cause the voltage profiles to fluctuate more than what is predicted in the conventional case.*

As for the LLHP scenario, revealed a tap change command from tap -4 to position 1. In this state, the MV1 voltage was 0.99 p.u. This was indeed within what is assumed to be favorable in such a scenario, but the OLTC was switched to investigate the effects. Tap_{pos} = -2 caused voltage limits to be violated along the feeder, and the Tap_{pos}= -1 was commanded, which showed satisfactory results, however, the highest voltage, now at B-MV6 (Feeder B, farthest from the substation) was recorded to be 1.04 p.u. This is an acceptable voltage rise, but it does not leave any room for further voltage rises.

The OLTC control setpoints in this case was updated to a setpoint of 1.01 p.u. at the MV busbar, and the lower and upper bound was 0.99 and 1.02 p.u., respectively.

These control setpoints provided a tap position of Tap_{pos}= -1, yielding MV1 voltage of U_{MV1}=1.02 p.u., thus it is operated as a voltage drop is predicted, like the conventional scenario. However, this MV1 voltage opens the door of voltage rise downstream on the feeders which have DGs installed, which could be out of the desired range. The highest voltage in the system was recorded to be U_{max}= 1.04 p.u. which still is acceptable. Note that the table have turned in this scenario, the maximum voltage is now measured at B-MV6, which is the farthest point from the TF on Feeder B. Feeder B has indeed the maximum penetration of DG of the considered feeders, and hence it is rational that it should provide the largest voltage rise in such a situation. As the reactive power load is low, the system itself provides all reactive power consumed (2.44 Mvar), i.e., the TF sees zero reactive power flow. And of course, active power is exported from the network and has to flow through the TF (export), where the largest part of active power comes from Feeder B (11.4 MW) as it has DG at every bus.

Setting the OLTC at Tap_{pos}= -2, i.e., providing one more tap change in direction of further increasing secondary voltage, was tested to see if this one tap change would give undesirable voltages anywhere in the network. The voltage on the substation busbar U_{MV1}=1.03 p.u., which is considered to be a reasonable value if the utility would expect heavy loading and voltage drop on any of the feeders. This situation did cause the maximum voltage in the network to be U_{max}= 1.06 p.u. (Feeder B – MV6), which is considered unacceptable here, thus the significant importance of OLTC is illustrated.

At this stage, the illustration of voltages on the feeders for various scenarios is considered unnecessary, as the voltage profiles did not vary significantly. This is assumed to be because the network is quite "stiff", i.e. it has a reference source providing and absorbing whatever the network requires right at the primary side of the TF, and impedances are kept low within the network. In addition, the feeders are at most 23 km in length, which is assumed to be quite long in this aspect, but still within reach so the resulting impedances are not getting very high. However, please note that only cable impedance, and no other components which will have some impedance in reality, is included in the model. To conclude this section, some key results are listed in Table 10. The loss and voltage indexes (I_{Loss}, $I_{\Delta V}$) are showing how loss and voltage profile has been affected with respect to base case. Loss index is negative if the loss has increased, and a positive voltage index gives a flattening of voltage profile in the network. The total maximum recorded tap-changes is between the HLNP and LLHP scenario, which is 6 tap changes. The results show the significance of the OLTC, and that the implementation of DG might challenge its operation further as it has to regulate in "both directions", not only between the load considered to be nominal and the high load scenario.

Table 10: Key results from the simple simulations performed on the MV network. The essential information is considered to be changes in loss and tap position. Maximum recorded variation in tap position is 6 taps, between HLNP and LLHP.

Parameter	*Scen. 1(Base)*	*Scen. 2(HLNP)*	*Scen. 3*	*Scen. 4 (LLHP)*
ΔU_{max} [p.u.]	0.03	0.06	0.03	0.02
$I_{\Delta V}$ [p.u.]	-	-0.03	0	+0.01
$PEN_{\%}$ [%]	0	0	90	90
I_{Loss} [-]	-	-0.66	0.60	0.53
P_{Load} [MW]	23.92	38.82	38.82	7.76
P_{Loss} [MW]	0.71	1.18	0.28	0.33
Q_{Load} [Mvar]	7.33	12.22	12.22	2.44
$\sum Q_{MV1}$ [Mvar]	5.00	10.80	9.80	0.00
$\sum P_{MV1}$ [MW]	24.00	40.00	17.00	-14.20
Tap_{pos} [-]	-3	-5	-4	-1/1

7.2 Wind Farm Operation when Integrated in Medium Voltage Network

The WT park and the WTGs individually were inspected in light of reactive power control and impacts on voltage. Some simulation results are presented in the following, which include some discussion. Discussion of higher significance are presented in Section 8.

7.2.1 Wind Speed Sweep – Output of Plant and WTG

By applying a *Wind speed sweep* script available in the PowerFactory Wind Farm, the characteristics of the plant as a function of active power output is easily illustrated. As stated in Section 6.3.4, the curves swipes the wind speed from zero to 25 m/s, in 0,25 m/s steps. The plant controller's objective is shown in Figure 24, where the reactive power absorption (left) and the $\cos(\varphi)$ (right) can be seen as active power output varies. These measurements are taken at the PCC; thus, they illustrate what the plant delivers to the utility. Bear in mind that these plots represent a wind speed which is steadily increasing and is only for illustrating the plants performance. In practice, the actual output of the plant is highly stochastic in nature.

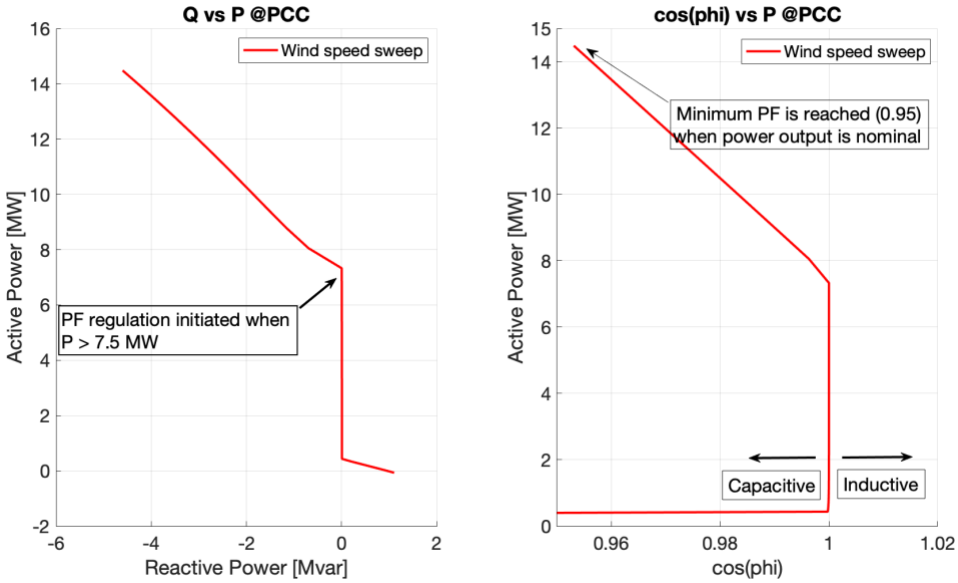

Figure 24: Wind speed sweep: reactive power consumption (left) and cos(φ) (right) with respect to active output power at the PCC.

The power output and losses seen from the PCC are displayed in Figure 25. It can be seen that the plant reaches maximum output when the wind speed is ca. 15 m/s or higher. At lower wind speeds, the power output will be highly influenced by the wind speed. The wind speed is only swept up to 25 m/s, thus, the WTGs brought to a stall is not included.

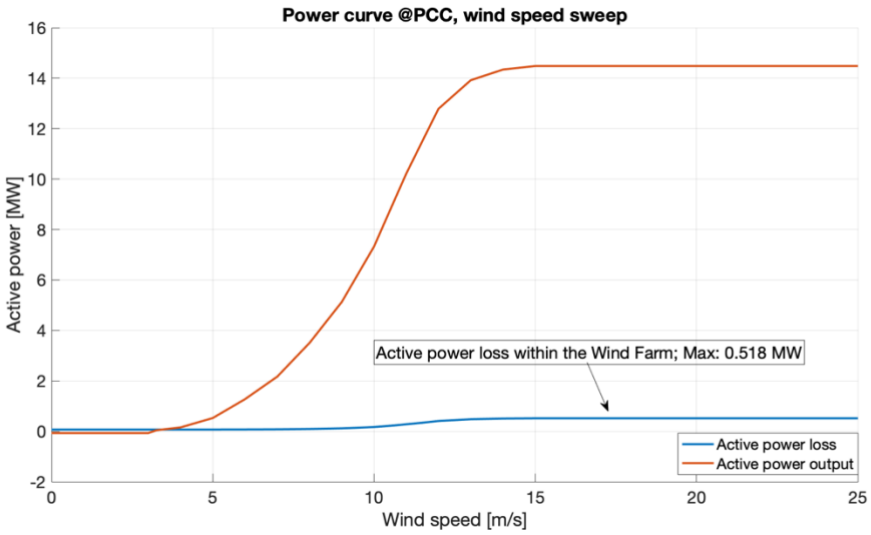

Figure 25: Power curve for the plant, wind speed swept from 0 to 25 m/s. Active power output and power loss within the plant are shown.

7.2.2 P-Q Capability when PCC Voltage Changes

The P-Q capability will as previously stated vary with the PCC voltage. This is not presented by graphical plots, yet it is stated for the sake of the reader. As the maximum capability of the converter is limited by the voltage it sees, amongst other, the maximum reactive power available for support changes with voltage. The reasoning behind the SCB installed on the Wind Farm busbar is indeed the objective of delivering sufficient amounts of reactive power (injection) when the PCC voltage is lower than nominal. When it is needed the most, the capability of the plant decreases. Yet the SCB is a static device and is rated for a certain Mvar power, for instance. Indeed, ancillary reactive power equipment installed at the Wind Farm busbar could participate in voltage support, and ensuring the plant is capable of operating within the requirements at all times.

7.2.3 Varying Power Output and its Impact on Plant Busbar Voltage

As the power output of the individual WTGs vary, the power seen by the PCC will vary. The effect this has on busbar voltage within the plant is of interest, as this could potentially be considered to be connected to a MV feeder, for instance. In this simulation the SCB is put out of service, or disconnected, thus all reactive power regulation has to come from the WTGs and they do not need to consume more than necessary in order to cancel out the injection by the SCB. The total active power output of the plant, total reactive power absorption by WTGs and the voltage measured at the plant busbar have been recorded and are displayed in Figure 26. Clearly, the reactive power consumption is initiated as a result of active power output reaching more than 7.5 MW, as per the request of the plant controller. However, the PF of 0.95 capacitive was never reached in this case, as the power output did not reach nominal, i.e., 15 MW. The minimum PF recorded in this simulation was PF= 0.965, seen from the PCC. Note that the voltage variation on the plant busbar in Figure 26 is not considered to be high, however it can tell us that voltage could fluctuate up and down when active power output varies. Hence, cascading impacts may be present.

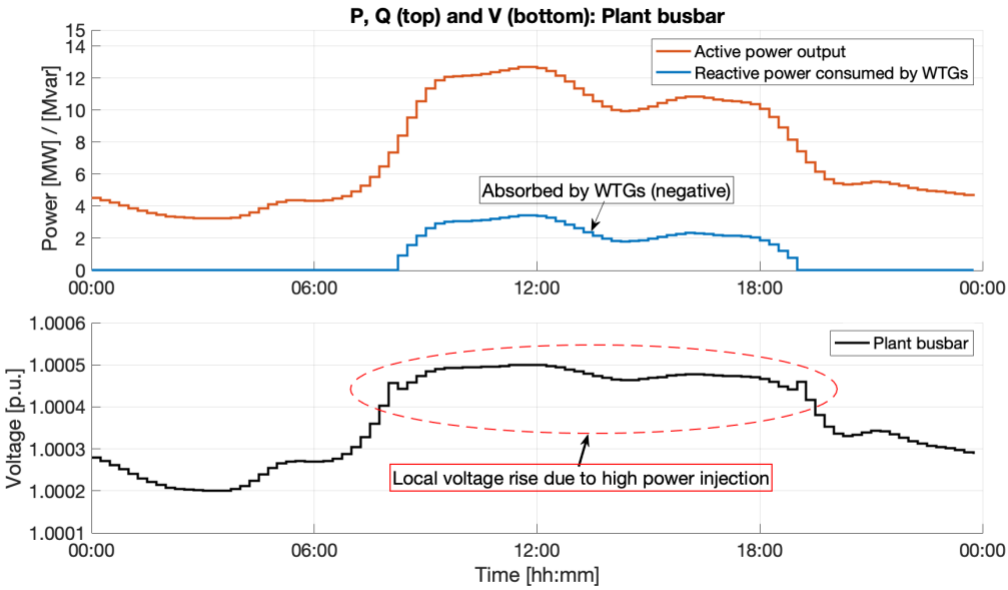

Figure 26: Active and reactive power (top) and voltage at the plant busbar (bottom) when active power output is adjusted by a curve. Reactive power is absorbed by WTGs in order to suppress voltage rise.

If the SCB is in service at say 1 or 2 Mvar, the WTGs have to consume an additional amount of reactive power (equally divided between all WTGs). The SCB can facilitate a better P-Q capability when operating at low voltages, or at all when it comes to injecting reactive power. A remark at this point could be the observed reactive power by the SCB, which is seen to vary as the voltage at the bus of which it is connected fluctuates. The reactive provision is increasing when voltage rise (i.e., *Q* output is proportional to bus voltage). Thus, the SCB principle as we know it, works to some degree against itself, as it can contribute to voltage rises above the desirable. This is in accordance with previously presented theoretical grounding.

7.3 Low Voltage Radial Distribution Feeder

PV power P_{PV}, is following the power-curve, which is both executed as a "sunny day" and a "partly cloudy" day. As the power output is directly scaled by the dynamic profile, the solar irradiance is indirectly included. The rating is regarded as a quite large PV-system in the residential aspect, but it is chosen in an effort to simulate a scenario which may take place in real-life. Note that all curves are self-modified, but it is considered to represent plausible scenarios.

As for the plotting of voltages, it is found preferable to include the MV side voltage also, which is as stated 20 km from the substation (cable), but has no load connected on MV side, unless otherwise is presented. This is to show the steadier voltage profile of the MV network.

Loads are considered to have a constant PF = 0.95 lagging (inductive) and a total rated power approximately equivalent to each house having a 3x32 A circuit-breaker in this 0.4 kV grid. In words of power, if a residential PCC is drawing maximum current, the power drawn from the grid, P_{Load}, is approximately 20 kW for the simulations.

7.3.1 Case A - Load and No PV Connected

The initial simulations on the LV network was performed to evaluate the performance without PV connected to any customers PCCs, it is by this reason also referred to as *Base case*. The NLTC was set to Tap_{pos}= 0 initially. Table 11 presents some data on the recorded voltages on the nodes in the network which have the lowest and highest voltage, i.e., LV1 and LV5. The energy flowing into LV1 through the course of a day is also included for the purpose of having it available for later use. The table clearly shows that steady-state voltages are as good as within spec in all scenarios of the tap position. For instance, the tap position provides a voltage at the farthest bus (LV5) which is out of statutory limits 2.5 hours per day with the simulated load profile. This could be neglected maybe but bear in mind this load profile does not draw full power (for which the customers circuit-breakers are rated), thus it is considered necessary to not neglect this. Hence, the tap position Tap_{pos}= -2 stand out as the correct alternative in this matter.

Table 11: Key results from tests on the LV network, Base case; testing of NLTC tap positions.

Property	*Tap 0*	*Tap -1*	*Tap -2*
LV1 energy [MWh]	+4.425	+4.415	+4.405
U_{LV1} (max, min)	1.00; 0.98	1.03; 1.01	1.05; 1.04
U_{LV5} (max, min)	0.98; 0.86	1.01; 0.89	1.03; 0,92

To provide some foundation for the scenarios studied in the following, plots of bus voltages for Base case and tap positions -1 and -2 is shown. In Figure 27 the bus voltages are illustrated, and one can clearly see that LV5 is out of the statutory limit.

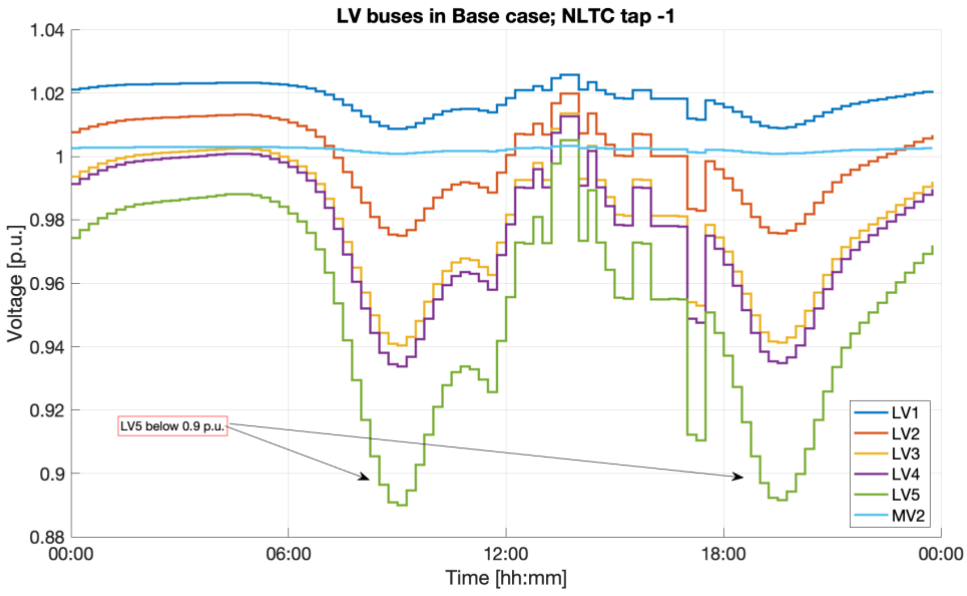

Figure 27: Voltages for each bus as described in the legend; for the Base case in LV network. NLTC tap position is -1.

As the tap position Tap_{pos}= -1 provided undesirable low voltage, the NLTC is adjusted further in the negative direction (thus increasing output voltage). It has been previously described that this TF has a regulation of ±2x2.5 %, which tells us we have no more regulation freedom in this direction. Therefore, the TF is now set to Tap_{pos}= -2. This adjustment yields the bus voltages depicted in Figure 28, which illustrates that all buses have voltages through the course of a day, that is within limits, and justifies the NLTC setting. As there exists only load in this case, the voltage drop will indeed occur in downstream direction. However, the LV1 voltage is kept at a voltage which is about 5 % higher than the nominal value.

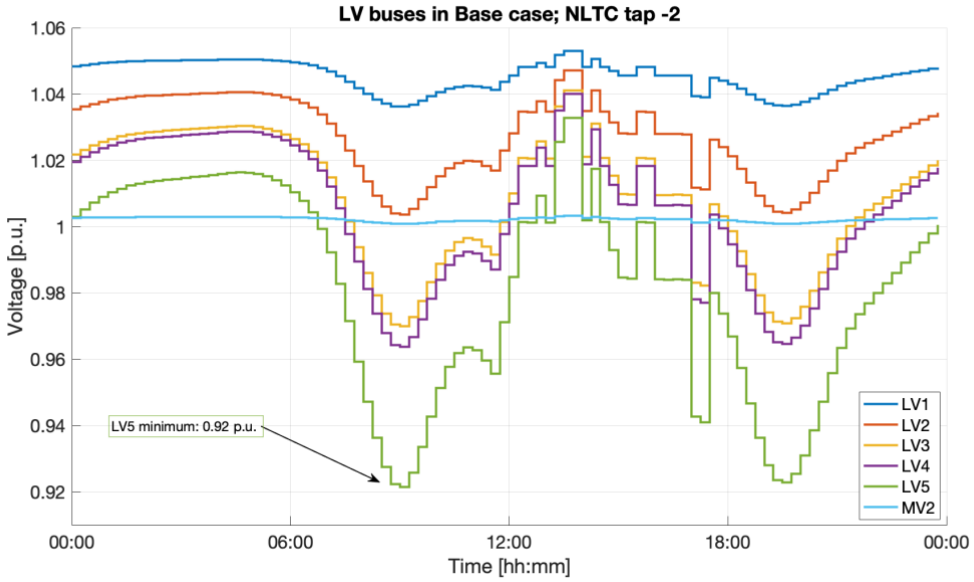

Figure 28: Voltages for each bus as described in the legend; for the Base case in LV network. NLTC tap position is -2.

It could be mentioned that the loading of the TF could be seen as identical in the Base case for both tap position -1 and -2. Furthermore, the power flowing in or out of the network (referred to TF secondary side) is of interest as foundation for further simulations. It is not included here, but it is worth mentioning, that the maximum reactive power flow recorded into the LV network in the Base case is $Q^{LV}_{max,import}$= 109 kvar, as the loads consume some reactive power. The active power flowing into the network can be useful for further studies, yet it is not plotted as it inherently follows the exact same curve as the load scaling curve previously presented. It will, however, be used when comparing scenarios.

7.3.2 Case B - PV at all PCCs in the Network

The Case B, where all customers have PV systems installed was analyzed in search for the network performance in such a case. Both scenarios with respect to power output from the PV systems was simulated. Recall that all PVs inject power at unity PF at this stage. The power output is set to exactly follow the scaling curve. The scenario where all customers have PVs installed yielded the voltage profile depicted in Figure 29, by using the PV curve for a *sunny day*. The simulation reveals that the voltage profile with respect to distance from the first busbar (LV1) shifts direction when PVs inject large amounts of active power simultaneously as the load demand is at its minimum, i.e., LV5 has the highest voltage mid-day and is actually touching the limit of 1.1 p.u. in the simulation. Furthermore, the

minimum voltage is recorded as 0.93 p.u., i.e., there is a 0.17 p.u., or 17 % variation of voltage in the course of a day! Energy import to the network, referred to the LV side of the TF, is $E_{PV@allPCC}^{sunny}$ =3.41 MWh in this case, a clear reduction from the base case of E_{Base}^{0}= 4.40 MWh.

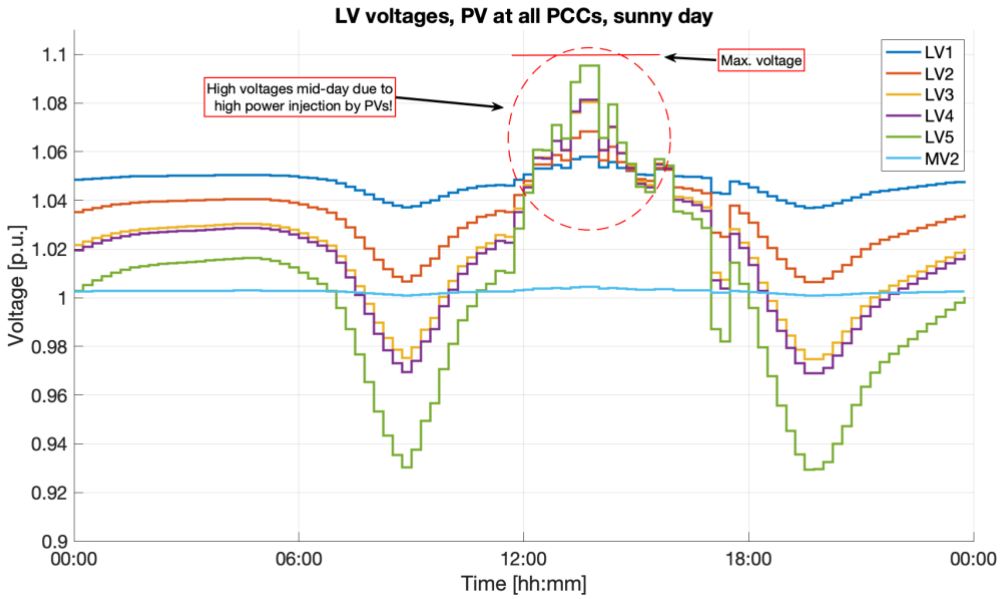

Figure 29: Voltages at each bus per the description within legend. PV at all PCCS, injecting power on a sunny day. Voltages are clearly affected and are near to the statutory limit mid-day.

The PV curve representing a partly cloudy day was also applied, giving the voltage profile as showed in Figure 30. This scenario shows indeed very similar results as the sunny day, yet the fluctuation of the injected power is an important matter to understand. These simulations are based on a fairly "slow" step time; thus, it could be even more fluctuating in practice. See how the intermittency cause the voltages to vary with great relative values mid-day. In addition, note that the LV1 voltage has the same maximum and minimum voltages in both scenarios. However, the LV5 voltage maximum value is recorded to 1.09 p.u., and the minimum to 0.92 p.u. Energy import at TF secondary side is $E_{PV@allPCC}^{cloudy}$= 3.70 MWh.

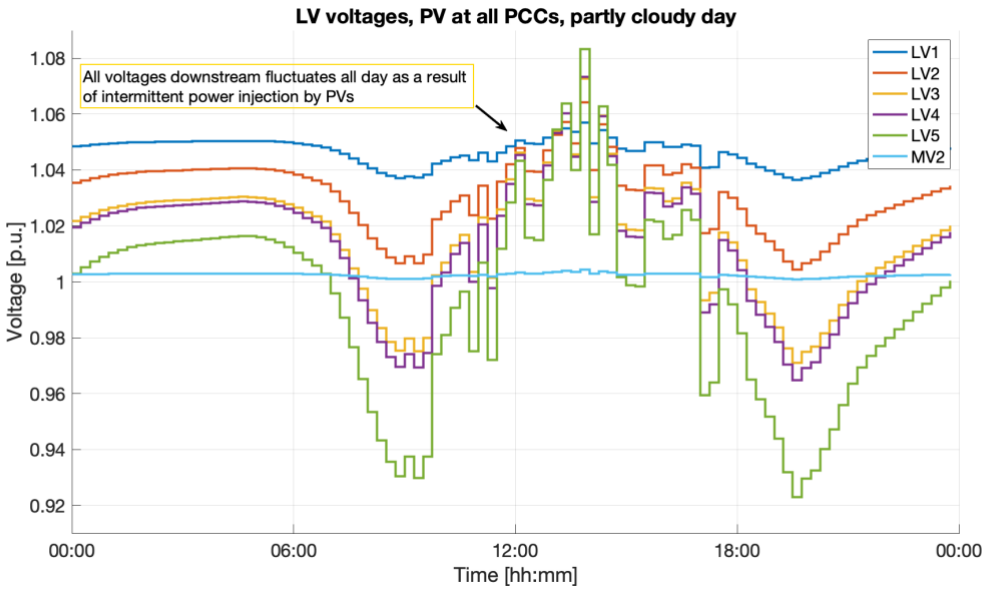

Figure 30: Voltages at each bus per the description within legend. PV at all PCCs (Case B), injecting power on a partly cloudy day.

These scenarios of different degree of intermittency yields two different load scenarios seen by the TF, of course. Figure 31 illustrates the active power flow seen by the TF at secondary side. It can be seen that the partly cloudy day affects the power flow in such a way that it is fluctuating between import and export. Indeed, the two scenarios reveals that the overlying grid will see the LV network as a source of active power, and a sink for reactive power for some periods, in this case.

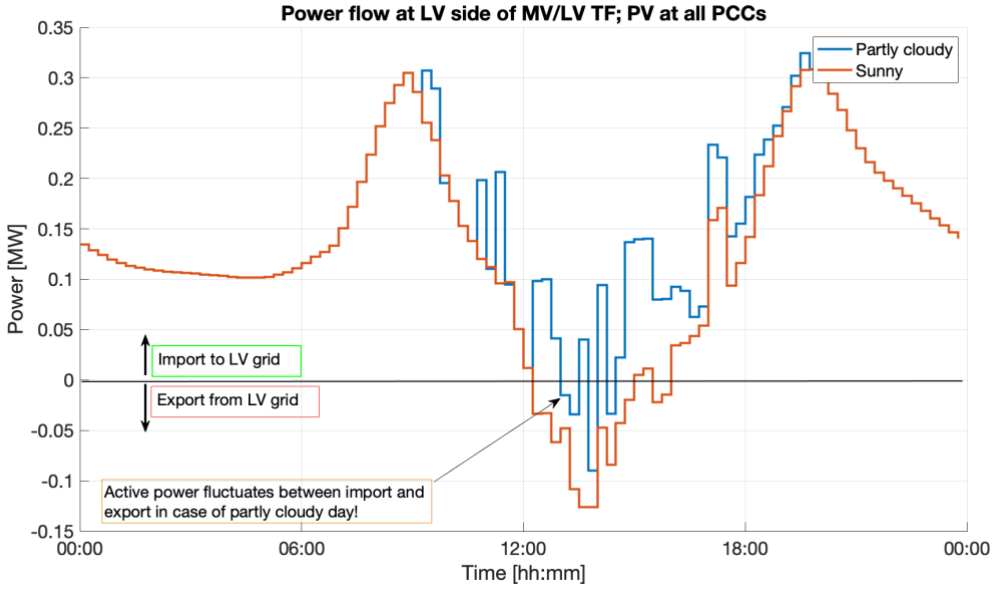

Figure 31: Active power flow seen by the TF secondary side in LV network, with PV at all PCCs (Case B). The difference between sunny and cloudy day is clearly illustrated.

7.3.3 Case B – Mitigation of Voltage variation due to PVs by Droop Control of TF

As the Case B cause the voltages downstream in the network to vary of a total 17 % during the day, mitigation of this PV impact was tested. The TF is a component which is existing between all MV and LV networks, and instrumentation of this could be executed in the process of AMI-installation. For instance, the current and voltage could be logged and sent to the DSO, providing useful information, such as some DSOs are doing today [70]. This way, the TF has the potential to either be retrofitted with an OLTC or reinvested if found necessary. Nevertheless, the techno-economics are not taken into consideration here, only *the principle of operation*. The sampling resolution is not taken into account here.

The technique of using the measured power flowing through the TF was considered as a strategy to improve the performance of the network. This could be regarded as a droop control of the transformer, which commands a tap change on basis of the measured power and the voltage and compare it to the desired voltage at the respective power flow.

The compensation is on the TF termed *current compounding,* and the apparent power flow was chosen as the measured value which determines the desired voltage. The time controller constant was kept at its default value; 0.5 seconds. The simple technique used, was the use of the predictable maximum import and export apparent power flows at the LV side of the TF. These values were simply calculated using the ratings of PV systems and loads, thus obtaining a VA power flow. The setpoints of voltage are quite aggressive but bear in mind these scenarios are really not expected to happen in practice. The applied control setpoints are listed in Table 12, and are illustrated by their slope in Figure 32.

Table 12: Setpoints for apparent power droop voltage control of TF

Parameter	*Predicted power flow [MVA]*	*Desirable LV1 voltage [p.u.]*
Maximum export	- 0.2	0.92
Maximum import	0.4	1.08
Tolerance [%]	-	2

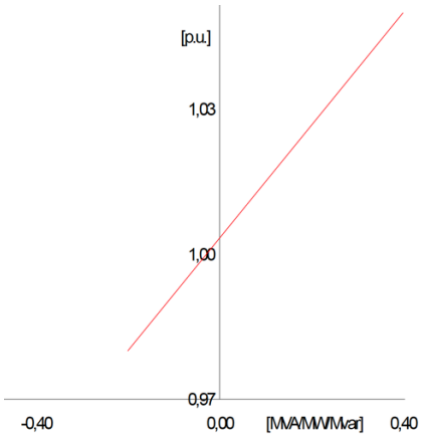

Figure 32: Illustration of the applied droop curve on TF. MVA values are used as setpoints.

Relaxing the setpoint of voltages, i.e., adjusting them in direction of 1 p.u., caused the OLTC to change taps in a pace which was not as aggressive as in the recorded results. Yet, the illustration of such a mitigation technique is the objective and thus a tighter voltage band is desirable. The regulation strategy was applied in the *sunny day* scenario, and yielded the results depicted in Figure 33. The voltage at bus LV1 was in the interval 0.97 to 1.04 p.u., and the LV5 voltage was in the interval 0.93 to 1.02 p.u. Clearly, the situation has improved by a large margin, as especially the maximum voltage at LV5 is lowered mid-day when power injection is at a maximum.

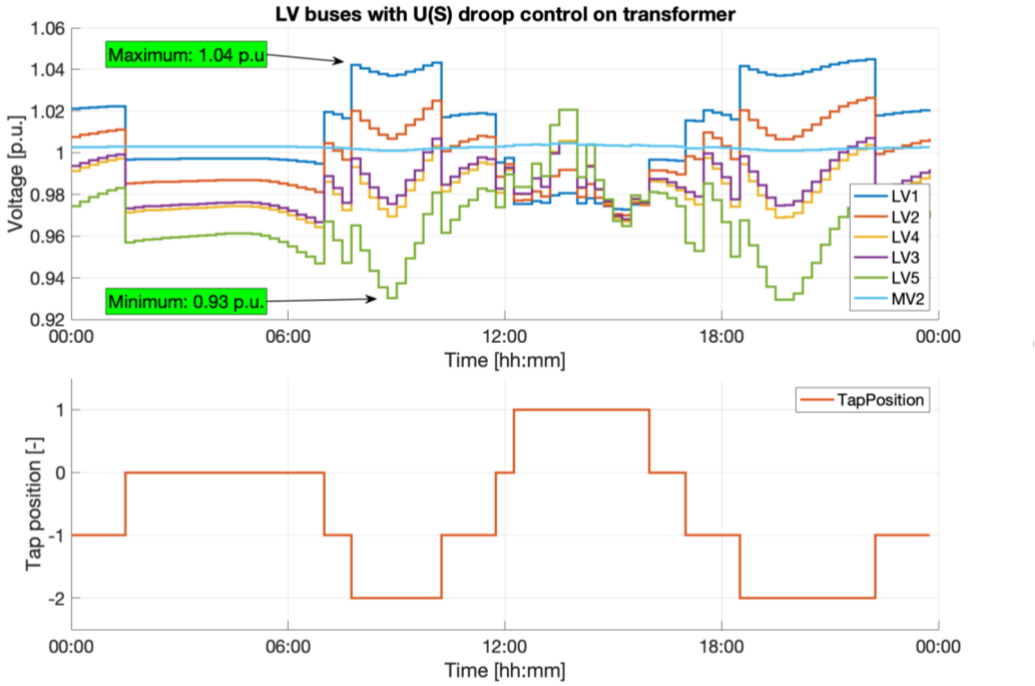

Figure 33: LV bus results and tap position on the TF when operating in U(S) droop curve mode.

The number of tap changes through the course of this day is recorded to be 10, and in some periods one tap change is not maintained in a long period until the controller requests another tap change. The number of tap changes which are acceptable, and the fact that voltages increase by large amounts in a very short time is a topic which should be addressed. The rate of which the voltage changes is a factor to consider when maintaining operation within statutory limits. These results show that the application of a linearized droop curve containing apparent power flows and the determined voltage setpoints, improves the dynamic voltage profile in the course of a sunny day, where the network is exposed to both relatively heavy loading and reverse power flow with respect to TF secondary side.

7.3.4 Case C – PV clustered at feeder end

For case C, the TF is reset to its tap position of -2 and the control of output voltage is deactivated. This was done in order to examine the conventional layout and compare with the base case. The LV4 and LV5 buses was considered to have PV systems installed, operating on a sunny day. Two of the PVs on bus LV4 was put out of service, along with the PV on bus LV1, LV2 and LV3. The voltage is of interest in this case, and the measurements showed that the profile is very similar to the Case B in terms of the voltage maximum and minimum values. The voltage range of LV5 was 0.93 to 1.08 p.u. throughout the day, and this is indeed equivalent to the *Case B* without modification on the TF. The recorded bus voltages are presented in Figure 34.

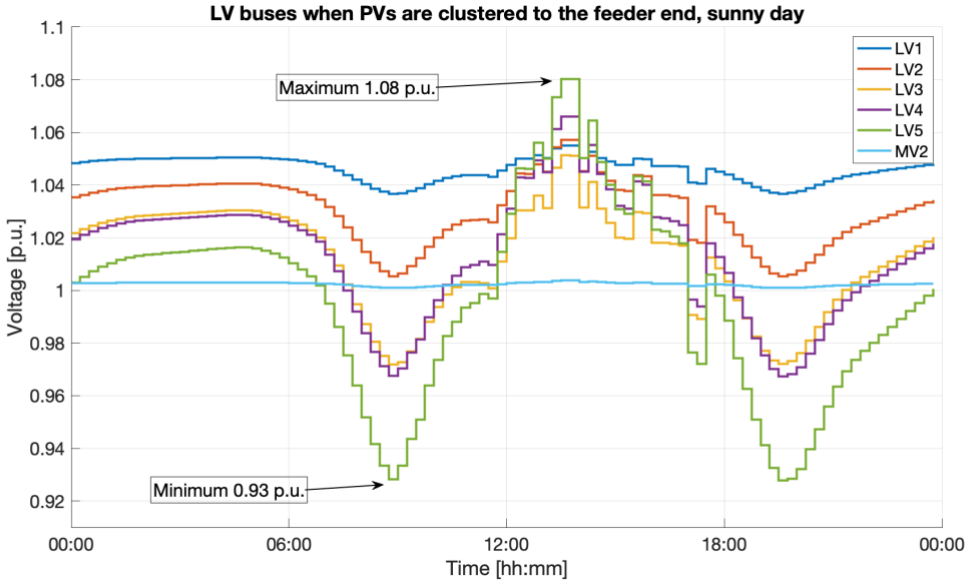

Figure 34: LV bus voltages in the case of clustering at the feeder end, Case C, sunny day.

7.3.5 Case D – PV clustered close to transformer

For Case D, the PVs are clustered in the opposite nature of Case C, i.e., concentrated at the bus close to the TF. Keep in mind that the penetration of PV is equivalent to the Case C, only the topological placement of the PVs is changed. All PVs at LV1 are active, and two PVs on LV2 is also delivering power. The simulation yielded a voltage profile which clearly suppresses the voltage rise LV5 has been responsible for in all cases where PV are installed on the LV5 bus. The secondary side of the TF (LV1) now holds the highest voltage in the course of a day, which is similar to the conventional case. The voltage at LV5 is at its highest 1.03 p.u. No voltage violations are taking place in this case, as the voltage rise is cancelled by the fact that the injected power is essentially injecting directly into the TF secondary side, where the voltage is determined by the TF. Downstream towards the feeder end the consumption is not high enough to cause a considerable voltage drop, and thus, the excess power is exported to the MV grid.

In this case, it was found that the installed capacity of the PVs can be raised to the apparent power limited by the customers circuit-breaker, without causing undesirable voltage levels. This means that $P_{PV} = S_{Load}$. In terms of simulation, this is equivalent to setting the generating percentage to 220 %, which will cause the maximum delivered power by PVs to increase to 21.8 kWp. Furthermore, this is equivalent to PEN_{PV} = 42.35 % (220 % increasement from the initial Case D), which is considered high when only 7 out of 19 customers have PVs. This exaggeration of PV system ratings yields the voltage profile as presented in the next subsection. Only the *sunny day* results are showed, as they represent the "worst case" scenario with respect to potential voltage rise.

7.3.6 Comparison of 220% PV rating for Case B and D; sunny day

The comparison of Case B and Case D, when PVs are rated with the same apparent power as the allowable maximum customer load (circuit breaker) is presented in the following, as it shows the sensitivity of voltage quality in terms of installed PV system ratings in the network. It is repeated that this layout causes each PV to have a rating of 21.8 kWp, and it operates at unity PF as before. Thus, it

is still assumed the PV is not disconnected but is simply following the voltage level at its node. The Case B and Case D voltage recordings are depicted in Figure 35 (top) and (bottom), respectively.

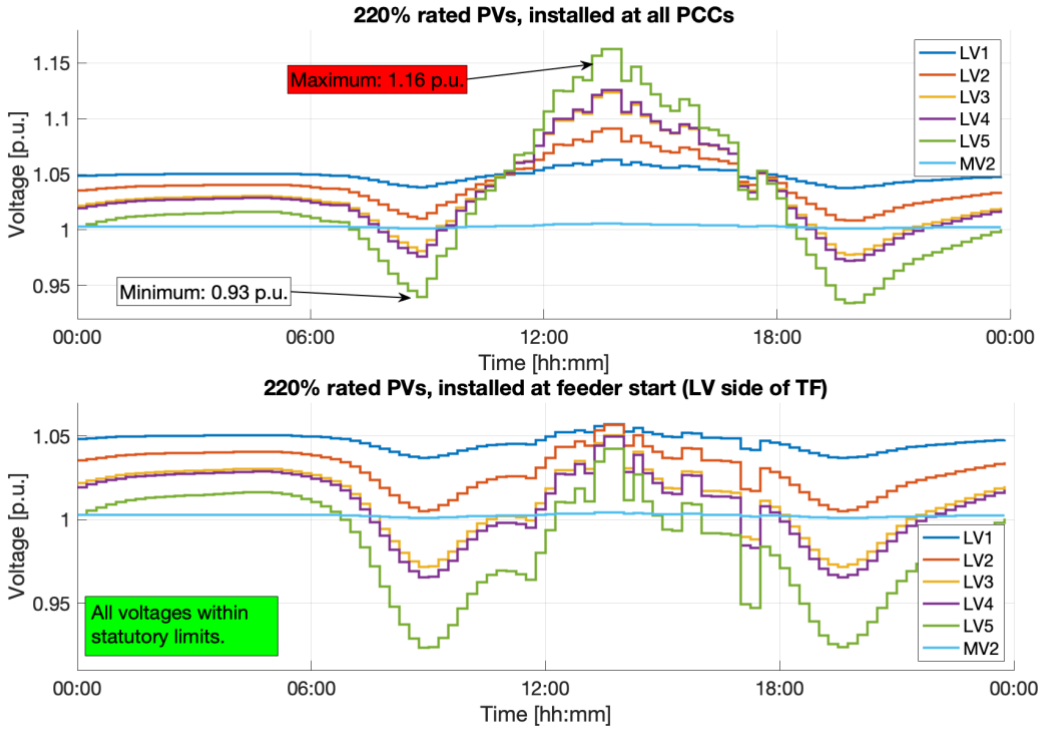

Figure 35: Voltages recorded when PV is rated 220% of it nominal (initial) power rating on a sunny day. Case B (top) and Case D (bottom).

It is clearly shown that for an increased PV rating, the *Case D* is most compatible in regard of voltage levels within the network, in the *sunny day* scenario. Case B reaches unsatisfactory voltages in such a case and voltage regulation revision is required. Case C with this setup is not reported but shows the effect of the export power flow, which is taking place when the injection is higher than the consumption at the buses at the feeder end. In regard of penetration, the Case B simulation corresponds to PEN_{PV}= 100 % and PEN_{Load}= 100 %.

7.3.7 Testing Constant Power Factor Control to Mitigate Voltage Rise on a Sunny Day

It was decided, on basis of the voltage rises recorded for the *Case B* mid-day, the PVs should be exposed to constant PF control. This test would reveal the networks response to reactive power regulation, and its correlation to the network's X/R ratio. Several PFs was tested on the PVs, ranging from 0.95 to 0.7 capacitive, and the results were obtained for each scenario. The active energy flow into the network was also included, although with few decimals, to see if the regulation caused excess active power import. The recorded results are summarized in Table 13, where the bold fonts show the crucial information.

Table 13: Result comparison of constant $cos(\varphi)$ control on PVs for Case B on a sunny day.

Property	*PF=1*	*PF=0.95 cap.*	*PF=0.9 cap.*	*PF=0.8 cap.*	*PF=0.7 cap.*
Energy import [MWh]	+3.410	+3.418	+3.419	+3.422	+3.425
$I_{\Delta V}$ **[p.u.]**	Reference case	0	0.01	0.02	0.03
$Q^{LV}_{max,import}$ [kvar]	109(Ref. case)	124 (+13%)	145 (+33%)	187 (+71%)	235(+115%)
$U_{LV1}(max;\ min)$ [p.u.]	1.06; 1.04	1.05; 1.04	1.05; 1.04	1.05; 1.03	1.05; 1.03
$U_{LV5}(max;\ min)$ [p.u.]	1.08; 0.92	1.09; 0.93	1.08; 0.93	1.07; 0.93	1.06; 0.93

The results show that the voltage rise mitigation by constant PF control has minimal effect on this network (see Table 13), as extremely low PFs do not lower the voltage by considerable amounts mid-day. The active energy import is proportional to the reactive power import, as it has to cover the excess power losses, with respect to the reference case, i.e., Case B and PF=1.

The objective of this comparison and exaggeration of constant PF control, is to obtain the relative changes in network performance with respect to PV operation. The PF seen by the TF on the LV side for instance, is not included here as numerical values. This is because it has not been explicitly evaluated but note that the power flow when the PVs operate at low PFs is approaching a value which is around 0.25, when PVs operate at PF=0.7 capacitive. This is in addition outside the PVs rating, and is performed as an experiment only, as the capability (P-Q) has not been defined for the PVs. Even when PVs operate at PF=0.95 capacitive, the PF seen by the TF is dipping down to PF=0.20 lagging for short periods of time, twice a day, i.e., when PV are approaching and going down from their maximum power delivery. In rough, it stays at ca. PF=0.8 lagging, seen by the TF.

Clearly, the TF loading will increase as a result of the higher reactive demand within the LV network. *Keep in mind, please, that if the domestic reactive demand was "in phase" with the time the PVs inject large amounts of active power, and thus consuming reactive power; the total reactive demand seen by the TF could increase significantly.* TF overload has to be carefully considered. The differences in reactive power flow are displayed in Figure 36, for a selection of the constant PFs.

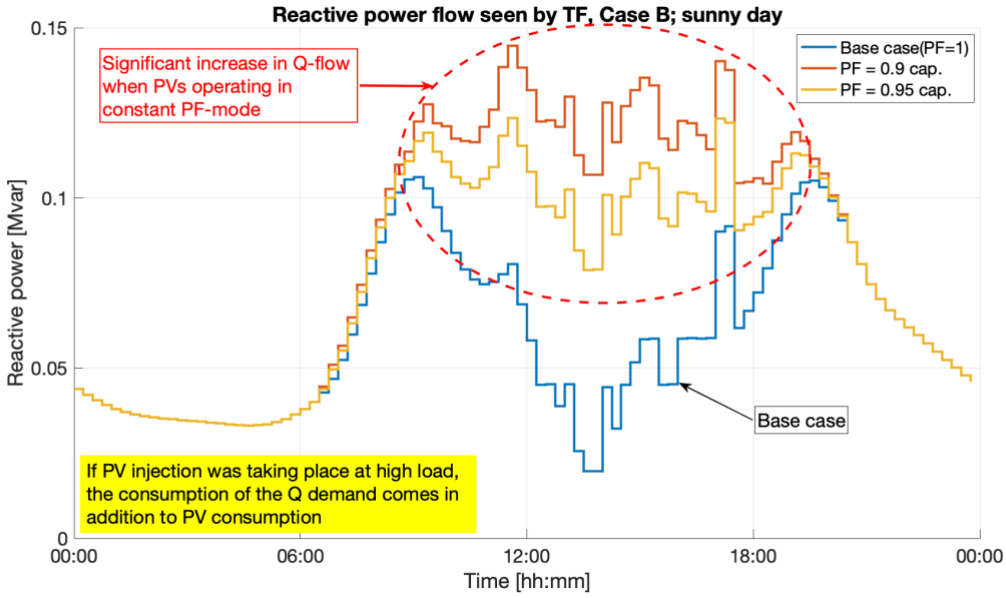

Figure 36: Reactive power flow comparison for Case B, PVs operating with constant PFs of 1, 0.95 cap. and 0.9 cap. The scenario is a sunny day.

7.3.8 Case E – Wind Farm connected on MV feeder supplying the LV network

In Case E the Wind Farm previously evaluated in brief, is connected to the MV feeder (20 km) of which the LV network is connected to, in fact it is connected exactly halfway (10 km) from the substation. Keep in mind, that the substation voltage is a reference busbar simulated as a SL-bus with a stiff voltage at 1.0 p.u.

- Firstly, the Wind Farm was connected, and delivering nominal power, i.e., steady state operation through the 24 h period of simulation.
- Secondly, the output of the Wind Farm was modified in accordance with a curve representing the *scale* of output power. This means that the curve indirectly represents the wind speed and WTG operation, as it is the electrical output which is following a curve in the simulations. The impact this scenario has on the performance is interesting with respect to integrating Wind Farms. The step time of both the power injection curve and the simulation was still 15 minutes.
- In addition, to conclude, a load is connected to the MV side of the MV/LV TF (at node MV2), to represent some other loading of the MV feeder, and observe the impact on voltage levels.

Please note, that all PCCs in the LV DN has PVs installed, in accordance with the Case B.

The Wind Farm was initially operated at maximum output power. The SCB was disconnected in all of the following simulations. In terms of weather scenario, the PVs are simulated with the power output curve of a sunny day, and the PF control is deleted, i.e., the PVs are reset to operate at PF= 1. NLTC tap position is as before, set to -2, which was found to be the most appropriate position in the Base case.

When the Wind Farm delivered nominal power in steady state, the voltage levels in the LV network was as suspected, all raised. The voltage at the Wind Farm busbar fluctuated by a neglectable amount, but it is was observed that it followed the pattern of load in the LV DN (i.e., higher bus voltage when the demand in the LV DN is at a minimum). The primary side of the MV/LV TF now, due to obvious reasons,

had a higher voltage than the previous cases. The maximum MV2 voltage was 1.03 p.u., and in terms of voltages in the LV network, this higher MV voltage caused cascading effects. The maximum LV1 voltage was recorded to be 1.08 p.u. with this configuration, which indeed leaves little or no room for voltage conditions arising due to DGs in the LV network. The bus LV5 reach 1.12 p.u. mid-day, breaking out of admissible limits (PVs do not disconnect in this paper, remember). However, when adjusting the NLTC one tap, to position -1, the conditions change for the better. The comparison is depicted in Figure 37.

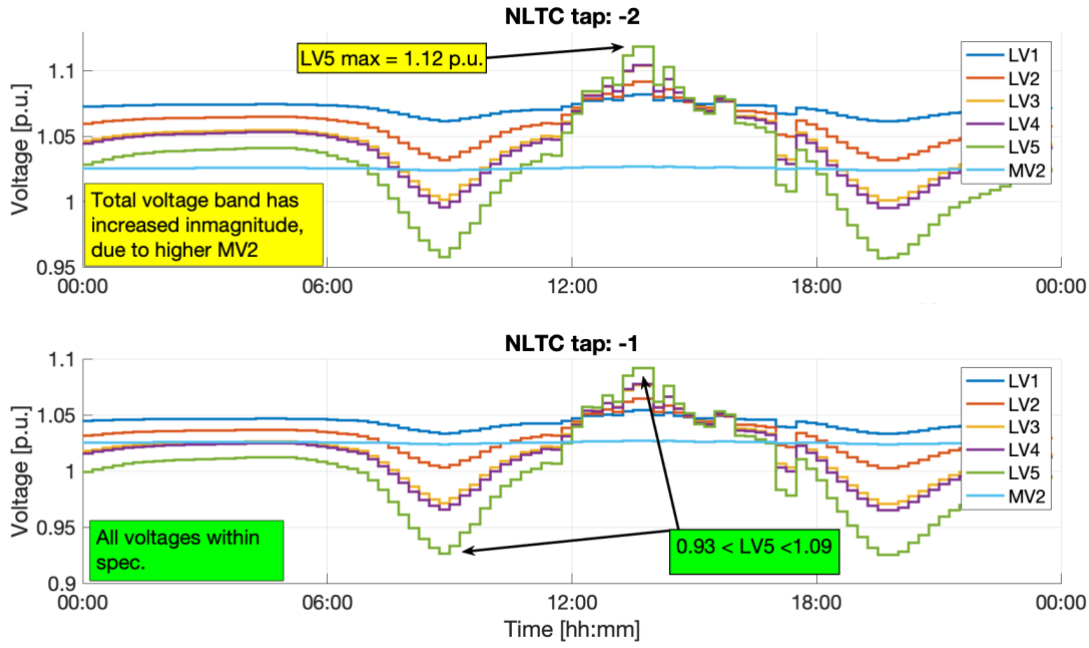

Figure 37: LV network voltages when the Wind Farm is delivering nominal power (steady state), comparison of tap positions on the MV/LV TF; tap -2 (top) and position -1 (bottom).

Clearly, it can be seen that the result indicates a tap change should be made in such a case. This is a process which in practice would involve de-energizing and outage for customers, which is not desirable.

Changing to tap position 0 (neutral), did not yield voltages within statutory limits. The LV1 voltage could be preferable to decrease, and facilitate room for voltage rise but, this tap position caused LV5 to drop too low when the network was heavily loaded twice a day in the simulation.

It should be noted that the margins are small for voltage violations when they are regarded as “ok” only by being inside the statutory limits. It was tested to apply a load at the MV side of the TF supplying the LV grid, which demanded nominal power of 5 MW with a PF = 0.95 inductive. This demand was further customized to be scaled by a load curve throughout the day in order to observe some dynamics. By adding this load, for instance, the voltage levels within the LV network was at the highest 1.10 p.u. (LV5), due to the voltage reduction on the MV side of the TF as a result of increased power demand.

Now, the Wind Farm was modified to operate in accordance with the output power scaling curve introduced in Section 6.3.5. Furthermore, the load discussed above is kept connected to MV side of the MV/LV TF, in order to simulate dynamic loading of the MV feeder. This load’s scaling curve is reaching

its peak demand a little after the peak of Wind Farm output power. The load curve, in relative values to its nominal value, is presented in tabular form in Appendix C.4. The peak demand is ca. 0.3 p.u., which is not more than 1.6 MW. Nevertheless, it was expected to influence the results.

In this configuration, NLTC position of -2 caused the voltages to be outside of admissible limits. When Switching to tap position -1, voltages are barely within specifications, however, it was decided to pursue simulations with tap position -1. Voltages of the primary side of the MV/LV TF (MV2) and the Wind Farm busbar are depicted in Figure 38, which also includes the power output by the Wind Farm and the loads simulated. The voltage increase on the MV feeder can clearly be observed when the Wind Farm injects high amounts of active power. Keep in mind that the Wind Farm absorb reactive power per the plant controller's PF-controller, in order to suppress voltage rise.

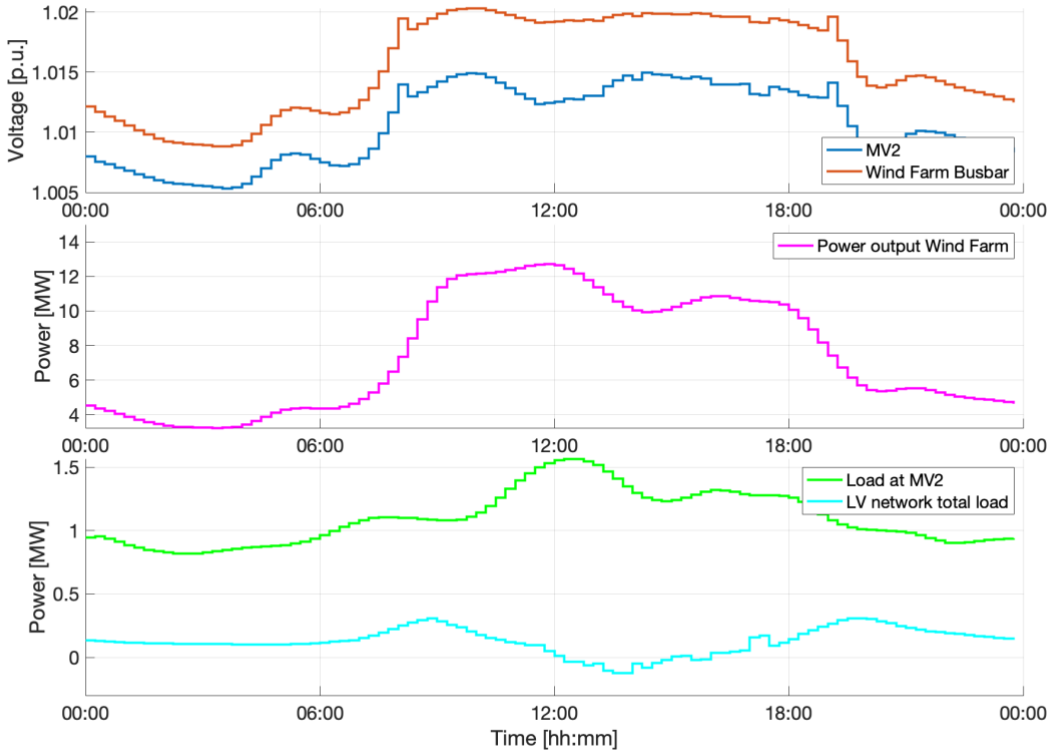

Figure 38: From top to bottom; MV2 and Wind Farm busbar voltage, Wind Farm power output and Loads in the V and LV network, resepctively. Impact on voltage is clearly illustrated.

An experiment was conducted, by modifying the Park controller of the Wind Farm to operate in capacitive PF mode between 1 and 0.95 (linearly) between power setpoints 6 and 10 MW, i.e., it operates at PF=0.95 underexcited when power output is equal to, or above 10 MW. It was observed, that the voltage fluctuation on the Wind Farm busbar was reduced, thus also reducing voltage at MV2 due to higher consumption of reactive power. In this condition, all LV voltages were within admissible limits. *The remarks stated here, illustrates the significant role of the reactive power control in the DN.* Note that cable loading is in this case disregarded.

8 Discussion of Key Results and their Significance

This Section presents some brief discussions on results obtained, and other sightings needing some attention. Each model examined is discussed explicitly.

8.1 Medium Voltage Radial Distribution Network

The MV radial DN which is modelled and studied in this paper is, as previously states, highly simplified, and hence the results should be considered with care. However, this DN's aim is to observe and illustrate the bulk impacts of DGs in the DN. Furthermore, the objective is also to show the significance of the OLTC, and the fact that it might have to operate in a wider range than before, when DGs are implemented. Challenges regarding different voltage profiles are also observed, in the light of DG integration.

8.1.1 Simulated Scenarios and Topology

The scenarios and topology simulated is chosen on the reasonable basis of literature, and worst-case scenarios from the grid perspective. It should be stressed that the network is not influenced directly by any real grid. In practice, the radials may be connected by open breakers to different radials, in such a way that they could be energized from another substation. That is however, neglected, and the capacity of the TFs in the substation is at full load when the network is heavily loaded. Ratings of DGs is equal to the total apparent power load at the respective bus where it is placed a DG, which would imply an extremely high, and most likely very unrealistic penetration ratio (no matter how the penetration is defined). Recall, that the initial plan was to conduct studies on rural overhead line feeders (this goes for the LV network as well), but the cabled network was used, and reasonably justification was given early in the work, when it showed that overhead lines was not included in this license. The cables were chosen by the author, yet the rating and insulation levels are installed with some range of potential future expanding of the network. Although, maybe not in such a degree a DSO would have done, in order to be sure that replacement of the cables not should be provoked by some expanding, which is assumed to always be taken into consideration. The lengths of lines and the aggregation of loads and DGs are placed by convenience and does in practice not represent how a typical MV radial feeder is configurated.

No reactive power compensation or controlled voltage support devices are installed in the network. This could might be seen as unrealistic, yet it was performed to observe the behavior of the network when this is the case. The installment of, say some fixed or switch capacitor banks, could have affected the results, and yielded higher voltages in some cases. In other words, the results could have been affected in a positive way by including the reactive power compensation. However, it was interesting to see how much vars the cables provided. It was found that the cables provided less vars when the network was heavily loaded, in the HLNP case. This has been considered to have a correlation with the higher current flowing in the network, which causes the highest voltage deviation for all of the cases. As the reactive power is dependent on voltage, like;

$$Q = \frac{U^2}{X} \tag{8.1}$$

It shows that the obtained results make sense, as the voltage drops, the reactive power output will be quadratically proportional to voltage level. As the network is cabled, it could have been reasonable to

install a reactor, nevertheless no such consideration has been performed. It usually is desired to have close to unity PF near the substation, to facilitate clean breaker operation in the case of disconnection or fault, however, this has been neglected in this paper.

The load level, which is simulated defines the grounding for comparisons made, thus their values are of importance. For instance, the low load scenario (LLNP), is in this paper considered to be 20 % of nominal power. However, in reality, this "low load" power might be something totally different. The PowerFactory software recommend 25 % load as low load, for the record. This fact leads to that the comparisons made has to be observed with care. On the other hand, 100 % load is considered "high load", and are studied as it represents one of the worst-case voltage drop scenarios on any feeder.

8.1.2 Voltage Recordings

With respect to voltage recordings, it should be noted that the simulations performed is steady-state, and real recordings would most likely be both higher and lower than for the simulations. The OLTC is suspected to have struggled in some load flow calculations, as it appeared to have been set to a certain tap position by the user. But for the cases reported, it operated if the voltages were out of the limits so that the controller commanded a tap change. The OLTC controller setpoints was not changed unless otherwise stated, thus, they were default through the most of simulations. This may have caused unrealistic results with respect to what the typical utility would use as setpoints in such a situation. This will of course depend on predicted loading levels, how close to the substation customers are connected and so on.

One mayor factor to keep in mind when evaluating reportings, is that the HV side of the TFs is simulated as a stiff source, i.e., the voltage is constant at 1 p.u. In real life, however, this will not be the case. At higher voltage levels (say the HV represents some regional grid of 132 kV) there exists voltage variations, indeed, yet they are considered to be smaller than the ones one would find in the MV grid, for instance. As a result of this, the OLTC, and the MV voltage will be affected by the HV voltage deviations which cascade downstream in the grid. The HV levels are themselves regulated by OLTCs and other regulating devices, so voltage variations will take place over time, and in sudden small jumps, when the OLTC at higher levels upstream are operating. This cascading control has been discussed in Section 3. The significance of this is that for a realistic simulation of high quality, this should be represented. Nevertheless, the main objective of these simulations does not depend on the MV busbar variations in the dynamic perspective, as it is expected to be regulated by the OLTC anyways. In addition, no action is made to secure the OLTC operation when power is exported from the MV network, as no problems related to this surfaced.

In reality the voltage drop is actually expected to be higher than the one simulated, as breakers, insulator connections, surge arrestors, undesirable discharges, connections made at MV/LV TFs and aging of other galvanic connections are expected to increase the total impedance on any MV feeder. Hence, the evaluated admissible limits when simulating a network like this, may have to be more aggressive (tighter voltage band) than the one considered in this paper, in order to make room for the realistic voltage drop. Nevertheless, this reasonable assumption could might hold ground or the voltage drop could be less than simulated, depending on the real network characteristics. In addition, LDC might be more typically used than what has been assumed in this paper and may cause the credibility of this voltage regulation scheme to decrease.

8.1.3 Distributed Generation Penetration and its Impact

It is shined a light on the different level of DG penetration of each feeder, (i.e., Feeder B has DG at all buses, Feeder A has some DGs and Feeder C has no DG), and its impact on voltage profiles. This is considered by the author to maybe become a challenge in the times to come. In this paper, the relative loading of the whole network, i.e., all loads are regulated when simulations are performed. Thus, Feeder A and B would have an identical voltage drop in the case of no DG production. The significance of this is that the challenge is not fully examined, as the Feeder C has considerable smaller length, and thus smaller voltage drop. Even changes on the same feeder will take place in reality (in terms of load and production), and this can cause over-voltages or voltage sags. The reasoning behind this is that, say if some loads near the substation was drawing power while at the feeder end; the DG production level is high. This scenario might cause over-voltages which may be in need of regulation. This problem and how it could be mitigated should definitely be addressed in further studies. In [71] the interference between domestic loads and a generating plant connected to a MV feeder has to be revised, as correlation between capacitor switching on the feeder and generator tripping in the plant is determined. The DSO had to revise the control scheme, install voltage regulators on the feeder and lower the step size on the capacitor banks in order to reach satisfactory operation. The problem, which is discussed here, is in a general matter, addressed in [15], and the concern which is considered is indeed of the same nature as the one discussed above. In addition, undesirable voltage levels are recorded when DG injects power close to the OLTC, where it makes a misinterpretation in terms of the power being injected into the feeder. It sees a small downstream power flow and regulates its tap position based on the current reading, as it does not see the fact that the DG itself is feeding almost the whole feeder. Thus, the voltage drop is still present downstream, but the OLTC commands a tap position which lowers the busbar voltage. In terms of this discussion, the contribution of this paper is that the DGs are found to have positive impacts (flatter voltage profile, lower losses) on the network in the scenarios which have been simulated, yet the total tap position changes are increased, when comparing network layout with and without DG. The OLTC usually regulates between low and high load. With DG integrated, it has been showed that the OLTC must operate to satisfy the voltage condition when DGs inject rated power. The OLTC lifetime and electromechanical wear is also a topic which should be included in this discussion.

Modelled DGs are not specified in type, hence, they could in theory represent converter-based DGs, operating at a unity PF. It is however, assumed some of the DGs in reality would have been for instance asynchronous or synchronous generators. This means that in reality, it is assumed, voltage regulation would take place in the MV grid. This have to be somewhat coordinated with the DSO requirements, so it does not interfere and cause oscillations between itself and existing reactive power regulative devices on the feeders.

8.2 Wind Farm Connected to Medium Voltage Network

A short discussion is presented, regarding the modelling and simulation of the Wind Farm. The main objective of these simulations was to investigate what the grid sees when plant of this size is connected. However, dynamics were not included. The series of steady-state calculations and the

impact on the MV network was found to be interesting, introducing new doors that should be further addressed.

8.2.1 Power Fluctuation and Grid Stability

The WTGs in this work are considered only in brief, to obtain knowledge about their integration and how they could impact the DN. In terms of stability and dynamics, the simulated cases did not provide sufficient recordings of such. Their output is expected to fluctuate as the wind speed varies (especially below the nominal power is reached), and thus, their impact on the DN is constantly fluctuating itself. However, the intermittency of the plant was observed and the control actions to prevent over-voltages was recorded. The controller for dynamic operation was not examined as the research license attained did not support RMS simulation which is appropriate for these simulations. It would be interesting to implement the Wind Farm into a more complex power system, where regulation devices, like the OLTC, are operated in a realistic manner. In the performed study, the PCC is a stiff reference bus with 1.0 p.u. voltage at all instants. This limits the impact which can be observed by the WTGs significantly, as the power is fed almost directly to the bus which simply absorb and provide whatever is asked of it. However, it was shown that even with this configuration, the voltage varies at the Wind Farm busbar, although by a small amount. Keep in mind that the only “freedom” the voltage has to change on is the 0.2 km cable from the PCC to the Wind Farm busbar. Hence, the voltage will vary to cover the voltage drop across this small cable segment. Yet the Wind Farm was observed in a simple manner, it has provided some crucial insight, and the recommendation of connecting Wind Farms of this size to the utility via devoted feeders was quite easily justified by the results reported.

The very important real-life event which is neglected in this paper, is the variation of voltage at the “substation”. This voltage will be controlled by an OLTC in reality (typically), just like what has been described regarding the discussion of MV feeders. Sudden imbalances (which takes place all the time) will cause the loading and voltage to vary, and the OLTC will command tap changes. In the case of the Wind Farm, this would be dependent on the type, and how many feeders was connected to the MV busbar.

The reader should be very aware, that if highly dynamic characteristics were included, including a real recorded wind speed data-set as input to the WTGs; the results are expected to have revealed a more severe impact on the MV network. As already addressed, the MV busbar at the substation would have to be modelled in a more realistic manner to provoke the levels of detail desired.

Nevertheless, the Fully rated converter WTGs is considered to be sublime in regard of voltage support, although they are in need of being over-sized to provide reactive power support even at nominal active power.

8.2.2 Possible Issues when Feeding Power into Substation

In the process of simulating the operation of the Wind Farm, the case of power injection into the substation (this is the desired operation, indeed) caused a concern regarding the stability of the conventional OLTCs installed. Say the OLTC regulates a MV busbar which is galvanically connected to several feeders leaving the substation and the Wind Farm injecting several MWs in nominal operation. Could the injection of power, and thus the changing power flow within the busbar, cause undesirable conditions; as the Wind Farm output fluctuates by large amount as a result of the wind speed? The HV

grid or busbar connected to the OLTC, or the OLTC itself if you like, will "see" a demand that is highly variable. Depending on the nature of the loads connected to the MV feeders, the power flow through the OLTC is assumed to be fluctuating more than that of the conventional case, as the Wind Farm supplies a portion of the load, say, of the MV feeders. The concern which may be in need of addressing, is that this scenario will increase the frequency of tap changes and thus might speed up aging (or at least maintenance routines) on the OLTC? In such a case the need for individual voltage regulation of the Wind Farm could be evident.

8.2.3 Topological Placement of the PCC of Wind Farms

It is illustrated that the topological placement of the point of which the generating plant is connected, affects the local voltage levels. This is in accordance to theoretical grounding presented. If there exist other customers connected to the same feeder, the conventional predicted voltage drop and so on is expected to change. Hence, the network may be in need of revision with respect to all connected customers and evaluate if the power delivered is of admissible quality.

For the networks simulated, it is shown that the Wind Farm injection of active power indeed alters the voltage seen by the MV/LV distribution TF which is supplying the LV network and residential customers. However, the network is simplified in a high degree, not representing all practical scenarios. A MV feeder will typically deliver power to numerous customers, and not just one LV grid, which is connected to the feeder end (although a small MV load was included). Nevertheless, this founding is further enlightening the need of careful analysis when integrating WTs or PVs in the DN. In [71], this problem was evaluated in practice, when the DSO experienced voltage issues, and the local voltage regulation by capacitor banks interfered with a DG plant connected on a rural MV feeder with domestic customers connected. This case was solved by installing an individual voltage step regulator for the feeder, which applied the principle of LDC and the projected regulation point was the point of interconnection on the back-bone feeder, i.e., where the plant meets the utility feeder back-bone. This showed to be a good techno-economic solution compared with building a separate feeder to the plant.

Nevertheless, by observations, the reactive power capability of the plant was seen as positive in terms of network support. The converters can respond quickly and mitigate cascading fluctuations of instabilities for instance.

It is further stressed that the most rational solution of WTG implementation with respect to voltage quality seems to be interconnection with the utility through a designated feeder.

8.3 Low Voltage Network with PVs Implemented

The LV radial feeder with PVs implemented was briefly assessed in terms of voltage levels, and some key discussions are presented in the following. Where comparisons to the literature are found reasonable, they are presented.

8.3.1 Simulated Scenarios

Load and Production curves

The scenarios simulated must be considered simplified and the results is only valid for such conditions. PV maximum output is never in "phase" with the demand here, which results in reverse power flow if the production is higher than network demand and line losses. If the demand curve applied consisted

of high demand mid-day, the recorded results would likely indicate that the voltage levels are within admissible limits all day. The practical scenario will vary all the time, and by this reason it is reasonable to plan for the worst-case scenario. This is due to the fact that the power system has to tolerate maximum power without taking damage. But if one stretches this to the bone, the simulations performed does not represent the "worst-case" scenario, as there is a minimum demand of 2 kW at each PCC, which is not zero. All though, the simulated scenarios are considered to be rational as zero load on several PCCs have a low likelihood of happening, with the modern households of today.

Maximum customer demand can by some be seen as high, and yes, conventionally these amplitudes of power demand might not be that common. Nevertheless, with modern loads (e.g. heating pumps, EV-chargers, induction heaters etc.) the power demand increases dramatically. The maximum circuit breaker at a customer PCC is based on the predicted and assumed loads common in a household (and regulations in terms of number of sockets for instance). The factor of which the installed equipment and variable loads are to be connected simultaneously (a factor between 0 and 1) determines the total thermal overload circuit breaker. This factor is assumed to increase with the modern society and thus causing higher strains on distribution TFs for instance.

Furthermore, this implies that the voltage deviation recorded in the course of a day will increase, given that there is adequate impedance between the customer and the TF. The results indicate that a voltage rise is taking place when the network is lightly loaded but there is a high in-feed of active power by PVs. Hence, accounting for the voltage rise, the voltage deviation recorder through the course of a day (i.e., a sunny or partly cloudy) is considered to reach serious fluctuations of voltage magnitude.

The discussion assumes the conventional layout where the MV/LV TF does not have OLTC.

PV curve similar for every PV system

The thesis assumes all customers who have PV, have the same rating, that they operate at the same exact power output at all times, thus they must be 100% equal in type, efficiency etc. Not real-world-like, where these factors would vary significantly. It can be, however, regarded as a cluster of houses which are sold with similar PV systems of the shelf. Keep in mind solar conditions would affect each houses power output greatly, i.e., the simulated cases would not reflect reality even here. They are three-phase interfaced, i.e., their output is balanced. Note that, the ratings are considered to be somewhat high from a residential point of view, but they are used as this could be the case in a LV grid with large houses and "environmental aware" customers. The economically rational size of a PV system is assumed to be lower than the one simulated, thus the impacts on the local LV network are assumed to be lower.

PV inverter rating in practice

The tests performed with a very low PF of 0.7 and such is just for experimental purposes. It is not rational to oversize the inverters more than is needed. By this reason, and others, the regulation scheme, if applicable via the PV inverters, should be defined. The R/X ratio in DNs are a subject of discussion! The DN is not suitable to be as "dynamic" as other voltage levels, due to the fact that the networks are dominated by resistance, which provokes voltage control should be more able to control the active power output. Customers, in the normal sense, who install DGs, they are assumed to desire to deliver all power to the grid, if they do not have any energy storage. The authors opinion that this

fact further encourages the research of OLTC integration in DN (MV/LV TF), yet the practical issues might suppress the implementation of the solution.

8.3.2 Network Topology and Characteristics

Cable size reductions like the ones executed in this work may not be in harmony with common practices, as the entrepreneur will to some degree use what is practically convenient, in such case exceeding the required ampacity for the respective cable, of course. This may decrease the voltage drop/rise along the secondary LV distribution network, as the impedances will change.

The cable cross sectional area is in fact based on reasoning with respect to its current – and voltage rating, and it is strived to oversize to some degree, in order to facilitate the practical view of future expansions. However, this leads to the conclusion that presented results must be evaluated in a critical manner by the reader, as the network may not be equivalent to what the utilities would have installed. Nevertheless, networks are all built with different components as per the requirements by the utility in that particular case. In other words, simulated networks should not be considered to be stating the fact, they should be interpreted with special care. *Relatively small adjustments in network topology and equipment can cause significant differences in results (even when simulation tool insecurities are neglected).* The network is a strongly simplified grid, yet it is based on reasonable skills and what could be considered "typical". The number of customers is kept low for convenience. For instance, a study on PV penetration ratios was conducted in [72], by using a somewhat similar network, although with more customers attached. Please, bear in mind that the simulations do not take into account the extra impedance one can assume the different components introduce to the feeder, e.g., cabinet connections, maybe a bad cable joint here and there, and so on.

As the Wind Farm model was used as a base line for the integration of this network, the cable between the MV busbar and the LV network, was as described 20 km long. This length was randomly selected to facilitate some voltage variations on the MV side, although they were indeed neglectable when only the LV network was connected. When the Wind Farm was connected halfway (i.e., 10 km) from the substation, this configuration seemed reasonable, as it would mitigate some of the real network characteristics.

8.3.3 Voltage Recordings

The reported voltages have to be examined with some reasonable critical view, as previously stated. This is due to the several simplifications made, the network type and the power injected. Reactive power control of DGs could in theory be implemented, but the effect of reactive power-support will change according to which network level the unit is connected. This is indicated by the obtained results, by trying to suppress voltage rise mid-day with reactive power absorption. However, the tested constant PF-control is in line with literature which stress the fact that constant PF-control is favorable in terms of minimal interference with existing voltage regulation in the DN [3]. This subject is not examined in detail, for instance by analyzing OLTC operation, but is indirectly seen by the fact that the reactive power flow in local networks increase the demand for reactive power. This reactive power may in many cases have to go through the OLTC, thus affecting the apparent current seen by the OLTC. The dynamic and stochastic nature of PV output for instance, could demand a higher degree of adjustability and real-time control of reactive power sources at MV level (e.g. capacitor banks)

Nevertheless, if the OLTC operates by measuring bus voltage, the thermal limits will be reached earlier if high amounts of reactive power flows through. More detailed discussion of voltage readings follows.

8.3.4 Permissible Penetration Levels of PV

When clustered to the feeder end, as little as a penetration ratio PEN_{PV} of ca. 20 % caused serious voltage rises to around 1.08 p.u., which illustrates the sensitivity of penetration and placement of the PV system. It is stressed that the maximum voltages recorded for clustering at feeder end and PVs at all PCCs is fairly similar. When PVs where clustered at the feeder start, the PEN_{PV} could be increased to the double (42 %) without causing any seriously high voltages within the network. The PVs in this case was the same as the maximum allowable load of the customer. When all customers have PV installed, a PEN_{PV} of 52 %, caused voltages out of the permissible limit of 1.1 p.u. A doubling of PEN_{PV}, to 100 % caused maximum voltage to increase to 1.16 p.u., some 5 % higher maximum voltage for a 50 % increase in PEN_{PV}. The work conducted, illustrates how sensitive the network might be for PV penetration with respect to the topological placement of the PV. It has not been focused intensely enough on this single matter, and the determination of critical penetration ratios should be addressed with a special focus. The definition and formulation of DG penetration ratio in LV and MV networks should be agreed by researchers contributing to the literature, in order to simplify the comparison of result and thus bring the research faster towards any consensus about penetration levels. Due to obvious reasons, the formulation should be different for LV and MV networks, as more details should be included at the MV level. From the DSOs perspective, it is reasonable to assume that a ratio related to the maximum permissible load demand of the customers (constrained by their approved circuit breaker rating by the DSO themselves) could be beneficial. However, customers have different types of connection types (e.g. single-phase and three-phase) or circuit breakers, limiting their allowed power demand, and thus, complicating the penetration ratio formulation. Nevertheless, it is recommended it is formulated as a sum of the maximum customer demand, and the maximum installed capacity of DG. The apparent values should be used, as those are the ones limited by breakers, lines and so on. One additional recommendation, for detailed analysis, is to weight the different PCCs by how much they affect voltage levels, e.g., PCCs connected to long feeder segments connected to the feeder backbone, should be weighted heavier because they will have a higher impact on voltage levels, as shown in this paper. Customers close to the backbone of the feeder or close to the TF will have a lower weighting, due to obvious reasons at this point.

In [33], a penetration ratio with respect to maximum apparent load was found to cause problems at around 60 %. However, in [39], the penetration levels are indicated as totally safe up to 100 %. Not before a ratio of 225 % are problems reported due to high voltages. Note that the formulation of penetration used here is found more suitable for instance in MV networks, as it includes losses and a base case load. The base case load limits the comparative aspect of the results, in the view of this paper's author. This is because the base case load is considered fairly low, and penetration ratios related to it will seem high. Critical voltages were reported already below 10 % penetration of PVs in [40], if the units were "quite large", i.e., 8.7 kW. If the installed rating was decreased by 50 %, the permissible penetration was determined to be 60 %. The network had a 100 kVA TF and load profiles of a maximum 2.5 kW which is considered very low today. The voltage range was "tighter" than the one considered in this paper, as the maximum voltage was set to be 1.016 p.u.

The reasoning of the discussion above is in essence to point out how much the penetration ratios that are deemed "ok" will vary, as all networks are dissimilar. Due to obvious reasons, the line types, lengths, load pattern and ratings of the PVs govern their own impact on the network (recall, energy storage is neglected in this paper). *Plotting of the penetration ratio as it varies through the day would be a good record to have, yet it was not performed in this thesis. It is by this reason strongly encouraged for further work*. Furthermore, it is noted that many reportings in the literature are lacking sufficient information on the topological placement of DGs in the LV network. This is, as indicated by the observation of this paper, of great importance.

8.3.5 Reactive Power Control at Low Voltage Level

The results indicate that the technique of operating PV with capacitive PF (i.e., consuming Q) cause serious increase of reactive power flow, without providing sufficient voltage suppression. In particular, this is considered within the LV DN, where the R/X ratio usually are higher than unity, and the voltage level is low. Depending on the network configuration (e.g. rural radial feeders, urban feeders), LV DNs are considered to not be optimal for Q regulation, as per the founding in this report. In literature, there seem to be insufficient consensus regarding this topic, as some encourage Q control schemes in LV networks [42] [73], and some find results corresponding to the findings of this work, which shines light on the possible issues [3] [33] . Furthermore, results presented in this work indicate that PVs clustered at the feeder start would in such a case not be required to operate in Q-supportive mode; this observation provides grounding for $Q(U)$ control at the PVs, so the PVs close to the TF do not consume excess reactive power, as voltage here is more stable. However, this configuration will cause reactive power flow seen by the TF to decrease, might leading to voltages downstream rising to unsatisfactory levels in the case of high amounts of PV clustering at the feeder end. A constant absorption of reactive power could mitigate voltage rise in some cases, but the impact is considered to be small. For instance, for *Case B,* when operating all PVs at a PF=0.9 capacitive, resulted in a voltage profile flattening index of only $I_{\Delta V}$=0.01 but yielded a maximum reactive power import to the network to increase with 33 % ($Q^{LV}_{max,import}$) referred to the Base case. This is due to the high reactive consumption by the PVs. *Nevertheless, the significance of the discussion above is that regulation strategy (if implemented) and fairness between Q - supportive PVs in the network has to be examined further, as the inverters experiencing higher voltage deviation in theory have to be over-sized to provide reactive power support.* The PVs at the feeder end, if operated with a lightly loaded network, will have the highest demand of reactive power control if operated in Q(U) mode for instance. A "fairness" approach of control was conducted in [74], where a dynamically computed gain for a Q(U) controller at each PV was sent to the PV and deployed in order to let all PVs contribute equally to voltage control. Indeed, it was stated to be feasible, as it reduced tap changes on the MV/LV OLTC. The need of addressing this problem further is well justified, as TF loading has been shown to increase as a result of Q-control on the PVs. A thorough comparison between methods based on OLTC, Q-control at PVs and ancillary devices installed by the DSO has to be performed, or a combination of the above. As a matter of fact, this becomes a techno-economic matter from the DSO's perspective.

If PVs are to regulate Q as a function of the voltage deviation, it has been showed that the oversizing of inverters can be relaxed as the PCCs approach the LV side of the TF. Active power curtailment (or disconnection) should be considered as the last resort, and this method is not illustrated in this work. In addition, the additional reactive power demand by PVs (highly dynamic) must be met by reactive

power sources in the MV or overlying grid, which could lead to a faster response time and accuracy to be desirable. Thus, ancillary state-of-the-art devices should be investigated for integration in the MV network.

TF loading is considered to be "overlooked" or left out of some reporting's. The results indicate that if PV penetration levels are high and they provide Q-support, the loading of the TF can become critical, as this newly introduced consumption is coming on top of normal load which conventionally was predicted. This is especially the case when loads consume reactive power simultaneously with the PVs high output (i.e., high reactive power absorption if operated in constant cap. PF mode). If single-phase PVs are not evenly distributed amongst the phases, the potential asymmetrical reactive power consumption could, in addition to unbalanced voltages, cause thermal limits on the TF to be violated at a lower penetration level. Hence, the lifetime (or wear) of the TF and its loading constraints are a topic to take into careful consideration when analyzing DG integration in LV networks.

8.3.6 OLTC Integration on MV/LV Transformer

OLTC operation was in this work briefly touched by using the strategy of apparent power measurement to determine the desired voltage (S-V droop slope). This method is mainly encouraged when the PVs do not regulate its reactive power output. The principle remains the same independent of the controller input. The improvement of voltage profile was illustrated in this paper, however, the potential wear, and minimization of tap changes on such a device has to be further investigated.

The OLTC alternative on the MV/LV TF is by the author seen as a good alternative as it effectively changes the voltage profile of the whole network. The option of implementing OLTC on the MV/LV TF is strongly recommended as further work. Several reportings in the literature investigate this type of novel voltage regulation (with respect to LV networks), and many results indicate that it is a preferable solution when penetration of PVs become sufficiently high [43] [44] [45] [46] [47]. *However, please note that there exists a serious challenge in the fact that most LV loads, and PVs of smaller size are single-phase interfaced, meaning that their impact on voltage levels vary significantly*. Even if PVs was almost evenly distributed among the three phases, different ratings and solar conditions of the installed systems, would cause the voltage drop reduction (or in fact voltage rise) to not be in synchronism amongst the phases.

OLTC with controller measurements locally on the TF is assumed to be an easier implementation process than strategies containing data from the customers PCCs, as the AMI data typically log data and report to the DSO at certain points in time throughout the day. MV/LV TFs which already measure voltage and current could be "simple" to further modernize to operate a retrofitted or newly installed OLTC, which for instance could be controlled by a power reading as an average over some seconds. Or it could, control a critical node in the LV network by LDC or "real-time" measurements from the actual node. However, this would include the determination of the most appropriate node of which to control. Note that the evaluation and discussion regarding OLTC retrofitting or reinvestment is out of the scope of this thesis. The available solutions and the economics would have to be analyzed thoroughly.

In addition, economically positives are associated with PV integration, as bulk power delivered from the MV network are lowered, and thus, decreasing losses in the network.

8.3.7 When WTGs are included in LV simulation

With the configuration where the Wind Farm was injecting (at 10 km) its power through the MV cable connected to both the LV network (at 20 km) and the substation (0 km); a rise in voltage level was indeed recorded. This was in line with expected results, as per the theoretical grounding presented in Section 2. Keep in mind the substation voltage is constant at 1.0 p.u. so the power will spontaneously flow into the substation without raising any voltage locally there. However, the raised voltage at the MV side of the MV/LV TF did indeed cause the voltages within the network to break out of permissible borders when the NLTC was stationary in tap position -2 (recall, the LV network was simulated as the Case B). As a result of this, a tap change on the NLTC was in fact requested to adjust the voltage band of the whole LV grid into satisfactory voltages. The significance of this observation; is the indication towards the measures might be necessary to take, when implementing large DGs in the MV network. In other words, the DGs of some substantial size, will affect voltage levels and then "push" some of the voltages in LV networks outside statutory limits (it may not be in every case, of course). However, it was also experimented, and presented in writing; that "tightening" of the PF-controller of the Wind Farm (setting it to start PF-control earlier and then hold PF=0.95 cap. stable) provided a more narrow voltage plot on the Wind Farm busbar, thus mitigating the impact on other networks connected to the same galvanic MV feeder. Nevertheless, the integration of DG in the MV network could provoke the scenario where the NLTC on the MV/LV TFs might have to be de-energized and a tap change has to be executed, or at least be thoroughly investigated, as the DG impact on the MV network will fluctuate as the output of large intermittent plants fluctuates itself.

9 Sources of Error and Challenges

9.1 Modelling Aspects

Modelling and simulation of a system which is to represent a real-life system and its electrical parameters; must not be considered the "whole truth", as it always holds simplification and assumptions. However, the degree of inaccuracy will always vary with the sophistication of the algorithm or software used. Round-off errors will most certainly occur within the software, and it is stressed that the number of decimals used in all analysis is quite scarce. This is however considered "ok" as simulation results itself has to be interpreted with care, as they are not said to be in harmony with the real-life conditions.

9.1.1 Load model Influencing Result

The modelling of loads can be performed in several ways, it depends on the algorithm and variables taken into account. In [50], for instance, short comparisons are made for some load models and reporting their differences. However, in the aspect of simplified analysis like the ones performed in this thesis, the models used are considered sufficient.

The TFs use in the MV network model is a 60 Hz TF as stated. This is only considered to affect its practical rating or capacity, and in addition the voltage levels were a little mismatched to the ones used. this was solved by finding the tap position providing desirable secondary voltage.

9.1.2 Generator Modelling and Simulation

The generators modelled can be considered quite "ideal" and does not take disturbances within the generator into account. The types simulated are supposed to represent inverter interfaced DGs, hence their power output and impact on the network are not considered in any degree of detail. The WTG model is quite sophisticated, yet the Quasi-dynamic simulation will consider steady-state conditions. In practice, the interaction between generator and grid is considered to be very dynamic and, furthermore, the intermittency of delivered power is highly smoothed out in this work. Due to the fact that the WTGs dynamic controller and so on is not in action, the controller info is left out of the paper, as it would be excess information. The static generators are previously introduced and operates in their simplest manner.

9.1.3 Transients and Highly Dynamic Operations Not Considered

The power system can be regarded as a scale where the two masses are never in perfect equilibrium. One of them is always heavier or lighter than the other one, illustrating the balancing that takes place in every instant. This is the balance of production and demand.

This dynamic process, in the regard of this paper, can be illustrated by the fluctuation of both load and production, and hence the power flowing through a line in the DN. This fluctuation is coupled with customer demand, weather (e.g., intermittent renewable sources) and production in the overlying grid, i.e., the HV grid.

9.2 Practical Challenges Present in the Distributed Network

As we know, the grid at higher voltage levels, e.g., HV, is quite "smart" and response times are fast. This is assumed to be strongly connected to the importance of the infrastructure, and the significant strains when lines or components actually fall out. The DN is extensive in size and ranges from urban grids, to rural old networks with aging infrastructure.

9.2.1 Signals Provided for Control Systems

In this paper, the models take the "measurements" as their real value (their real value within the software that is), yet in practice we face numerous challenges when it comes to instrumentation and communication, for instance; such as measurement uncertainty and inaccuracy. This assumption is aimed towards the imagined "smart" DN. The signals provided and used by components in the grid (e.g. DGs, circuit breakers/reclosers, TFs) could be valuable if they were correct. Keep in mind the accuracy and so on will vary from unit to unit. If close to real-time data should be used for operation in almost all of our DN, we are talking a vast number of communication lines, components which must operate under all weather conditions and understand control commands. The term interoperability is vital in this sense, as all components used for a certain task has to "talk the same language" and understand commands. This implies the importance of testing and development of such solutions, if it should be considered feasible to integrate. Keep in mind the integration of such technology must be techno-economically optimal and highly desirable for DSO operation if it should be implemented.

9.2.2 Electrical Challenges in the Presence of Distributed Generators

Many factors have been neglected in this thesis, such as; power electronic loads, unbalanced loads, power quality and changes on the HV and indeed MV side of the system, harmonic distortion, consumer load profiles and so on. Maybe the most significant thing, which is neglected, is the highly dynamic nature of our power system.

The implementation of large quantities of power electronics equipment into the power system is indeed changing the picture of the power system we know. High levels of inertia in the system is favorable in the perspective of frequency (and thereby active power) regulation. As DGs in many cases rely upon an energy input which does not encourage installment of inertial components coupled to the grid (e.g. varying wind speed, solar irradiation), the stability of the DG module relies on power electronics. For instance, say a wind farm without any energy storage locally, is connected to the grid. According to its rated power, it must be able to operate at a range of frequencies and in some cases be able to run in f-control mode. One must admit the fact that these modules may have the capacity to change their power output rapidly with respect to time, and their rate of change must be controlled (e.g. gradient of active power output [p.u./s]). This way, the plant could be seen as a plant with rotating mass and may not interfere with other plants in the same power system. Yet, in cases of large disturbances, it should be well investigated if the module is able to counteract them or the capacity is insufficient. If it is disconnected, it could create cascading oscillations and impacts on the operation of other plants (e.g. hydro) in the network, given that its installed power is quite large.

As the inverters are delivering power by using semiconductor switches which is used for delivering the power of desired quality and characteristics (e.g., leading or lagging current, magnitude) per the control commands; they introduce some harmonics to the network. The current delivered is a

manipulated sine wave, through the gates driven by the controller. This causes the equipment to inject a current not following the typical sine wave shape. The amplitude of the current is not necessarily in harmony with the PCC voltage. Total Harmonic Distortion (THD) is a term of how much percentage of the injected current is distorted.

10 Conclusion & Recommendations

10.1 Concluding Remarks

In this paper the impact of DG implementation in the DN has been assessed, by investigating effects of DGs in general, WTGs in the MV network and PVs in the LV network. The important findings include the fact that DG integration into MV feeders will provoke OLTC control to operate between a higher number of tap position in relation to no - DG scenarios. Furthermore, the differences in voltage profiles between feeders with dissimilar DG penetration have been recorded to, indeed, have relative voltage variations. When OLTC control is acting like normal, a maximum voltage of 1.04 p.u. was recorded, i.e., a voltage rise of 0.02 p.u. along the feeder. The OLTC controls its busbar and does not see that the voltage is almost out of satisfactory limits a long distance from the busbar. The need of revision of voltage control schemes when integrating high penetration of DG on MV feeders is therefore shown.

In terms of plants of several megawatts, the DSO has to consider designated feeders whenever possible. It is found that interconnection of large DG plants directly on MV feeders can raise voltage up to 0.03 p.u. even at 10 km from the interconnection site. The cascading impact is observed to provoke the need of tap changes on NLTCs supplying LV networks, as voltages are pushed out of admissible bounds. This impact will be dynamic and cause problems for the DSO. The significance of proper plant controller tuning is by this illustrated.

The simulations aforementioned show that a penetration of 52.25 % in the LV network is enough to cause over-voltages (1.1 p.u.) in steady-state, and a total voltage variation through the course of a day of some 17 %. Mitigation by $U(S)$ droop curve for controlling the setpoint on the OLTC, when integrated, was commanding 10 tap changes per day, however, it improved the voltage profile at all buses, i.e., the maximum voltage after new control scheme was 1.04 p.u., well within the permissible limit.

Furthermore, for the same penetration ratio (19.25 %), it has been reported that clustering of PVs made the difference between admissible voltages, and voltages breaking regulative laws. Clustering close to the TF facilitated a high PV hosting capacity, yet, clustering at the feeder end caused voltage rises of up to 1.09 p.u. and further penetration is constrained. A penetration ratio of 100 % yielded a maximum voltage in the network of 1.16 p.u.

Constant PF control, due to high R/X ratio, was determined to improve voltage profile by only 0.03 p.u., when a minimum PF of 0.7 cap. was deployed when all PCCs having PV. The maximum reactive power demand seen by the TF increased 115 % in the corresponding case, implying TF overloading considerations must be made by DSOs when applying Q-control of PVs.

10.2 Recommendations for Further Work

The work conducted in this paper strongly encourages further studies on the topic. The literature seems to not be in consensus regarding Q-control of PVs in the LV network, for instance. WT integration is only considered in brief in this research, and thus the cases of different WTG types and their impact on voltage regulation in the DN should be further investigated. The impact DGs have on the DN has a strong connection to the installed capacity and the voltage level of the PCC, which is

illustrated in the results presented. Some key recommendations for further investigations are listed briefly;

- Include a higher amount of details in the LV DN studies of PV impact on voltage. Load – and PV profiles should be included in a more rational manner. The single-phase connection of PVs and loads, and thus the impact on an unbalanced system is of great interest. This could reveal to which degree the TF is in danger of overloading, and investigation of voltage regulation could be studied.
- Penetration ratio has been discussed and is found to be in need of further examination; in light of when critical values are reached in varies types of networks, and the formulation and definition of penetration ratio itself should be developed and tested on a series of representative networks.
- This paper has modelled a LV 0.4 kV TN network, however, the evaluation of a 0.23 kV three-phase network (TT or IT system) would be of great interest. PVs are usually requested to be installed with three-phase interface when single-phase current of power injection exceeds 16 A, but still, it should be investigated if 0.23 kV networks reach voltage violations at an earlier penetration ratio of PVs, due to the increased current in the lines, compare to a 0.4 kV network. It is also recommended to model overhead lines, as those are more common in rural areas.
- Although the DN has to be planned for the highest expected current flow, the integration of more dynamics on the MV side of the MV/LV TF is assumed to increase the credibility of results. Especially the inclusion of an OLTC which actively controls the voltage on the MV feeder, and thus the changing MV voltage will cascade into LV networks connected to it.
- MV feeders with varying degree of DG penetration, which is connected to the same MV busbar, will operate with different voltage profiles, as illustrated. It should be further investigated, how much DG penetration will cause the voltage regulation of MV feeders to be in need of revision, and if independent feeder (or even phase) regulation should be implemented on the MV side of substations.
- With respect to this paper, the external grid should not be modelled as a stiff voltage reference, as this is not in accordance with reality. All dynamic aspects in the power system is hard to include, but the more is included, the more credible results may become. The network should be modelled from the HV and down, through operative OLTCs. Furthermore, regulation equipment (e.g. capacitor banks), network topology and characteristics should be in proven accordance with real networks.
- The OLTC integration on MV/LV TF should be investigated in detail, by testing different regulation schemes. The frequency of tap changes should be sufficient for effective voltage control, yet not cause reduced lifetime of the TF.
- Reactive power support by other state-of-the-art devices (e.g., distributed STATCOM, SVS) should be tried installed on MV lines at critical nodes, in order to investigate if these can improve voltage quality in networks with high penetration of DGs.

References

[1] N. Roy, H. Pota and M. Mahmud, "DG integration issues in unbalanced multi-phase distribution networks," in *Australasian Universities Power Engineering Conference (AUPEC)*, 2016.

[2] IEEE, "1547.2-2008 - IEEE Application Guide for IEEE 1547 (TM), IEEE Standard for Interconnecting Distributed Resources with Electric Power Systems," 2009. [Online]. Available: https://ieeexplore.ieee.org/document/4816078?denied=. [Accessed 2019].

[3] P. N. Vovos, A. E. Kiprakis, A. R. Wallace and G. P. Harrison, "Centralized and Distributed Voltage Control: Impact on Distributed Generation Penetration," *IEEE Transactions on Power Systems,* no. Vol. 22 (1), pp. 476-483, 2007.

[4] V. Danielsen, "Voltage Regulation in the Distributed Network," 2018.

[5] A. N. Azmi, I. N. Dahlberg, M. L. Kolhe and A. G. Imenes, "Impact of increasing penetration of photovoltaic (PV) systems on distribution feeders," in *International Conference on Smart Grid and Clean Energy Technologies*, 2015.

[6] Energi Norge, "Drift og utvikling av kraftnettet - utforming av DSO-rollen," Energi Norge, 2018.

[7] J. O. Tande, "Impact of integrating wind power in the Norwegian power system," SINTEF Energy Research, 2006.

[8] G. Angrisiani, C. Roselli and M. Sasso, "IEA EBC Annex 54 Integration of Micro-Generation and Related Energy Technologies in Buildings," Technische Universitat München, Germany, 2014.

[9] NVE, "Norwegian Water Resources and Energy Directorate," [Online]. Available: nve.no.

[10] Organisation for Economic Co-Operation and Development, "ICT Applications for the Smart Grid: Opportunities and Policy Implications," OECD Digital Economy Papers, No.190, OECD Publishing, 2012.

[11] CIRED, "Smart Grids on the Distribution Level - Hype or Vision?," CIRED, 2013.

[12] EDSO - European Distribution System Operators for Smart Grids, "Smart charging: integratign a large widespread of electric cars in electricity distribution grids," EDSO, 2018.

[13] D. Gantenbein, C. Binding, B. Jansen, A. Mishra and O. Sundstrøm, "EcoGrid EU: An Efficient ICT Approach for a Sustainable Power System," 2012.

[14] T. Ackermann, G. Andersson and L. Söder, "Distributed Generation: a definition," *Electric Power Systems Research,* no. Vol. 57 (3), pp. 195-204, 2001.

[15] D. Aldrich and B. McFetridge, "Distributed Generation Voltage Control Issues and Solutions," IEEE, 2014.

[16] Norwegian Ministry of Petroleum and Energy, "Energy Facts - Norway," 2019. [Online]. Available: https://energifaktanorge.no/en/regulation-of-the-energy-sector/regulering-av-nettvirksomhet/. [Accessed March 2019].

[17] T. Ackermann, K. garner and A. Gardiner, "Wind power generation in weak grids - economic optimisation and power quality simulation," *Renewable Energy,* no. 18(2), pp. 205-221, 1999.

[18] R. Lasseter, "Control of Distributed Resources," *Bulk Power System Dynamics and Control IV, Restructuring ,* pp. 323-329, 1998.

[19] G. Guida, G. Bruno, L. Ortolano, M. Poli, M. Palleschi, G. Miglivacca, D. Moneta, C. Arrigoni, F. Zanellini, G. D. Croce and A. Bridi, "Smart TSO-DSO interaction schemes and ICT solutions for the integration of ancillary services from distributed generation," in *CIGRE*, 2018.

[20] V. Dehalwar, A. Kalam, M. L. Kolhe and A. Zayegh, "Review of IEEE 802.22 and IEC 61850 for real-time communication in Smart Grid," in *Conference on Computing and Network Communications*, 2015.

[21] E. G. G. Celli, M. Loddo and F. Pilo, "Voltage Profile Optimization with Distributed Generation," in *2005 IEEE Russia Power Tech*, 2005.

[22] R. Caldon, M. Coppa, R. Sgarbossa and R. Turri, "A Simplified algorithm for OLTC control in active distribution MV networks," *AEIT Annual Conference 2013,* 2013.

[23] T. Xu and P. C. Taylor, "Voltage Control Techniques for Electrical Distribution Networks Including Distributed Generation," *IFAC Proceedings Volumes,* no. Vol. 41 (2), pp. 11967-11971.

[24] D. Matvoz and M. Maksic, "Comparison of reactive power regulation concepts of distributed generators in the low voltage network," in *2012 IEEE Power and Energy Society General Meeting*, 2012.

[25] M. A. Kashem, A. D. T. Le, M. Negnevitsky and G. Ledwich, "Distributed generation for minimization of power losses in distribution systems," in *IEEE Power Engineering Society General Meeting*, 2006.

[26] W. Lyman, "Controlling Power Flow with Phase Shifting Equipment," *Transactions of the American Institute of Electrical Engineers,* pp. 825-829, 1930.

[27] J. Barr and R. Majumder, "Integration of Distributed Generation in the Volt/VAR Management System for Active Distribution Networks," *IEEE Transactions on Smart Grid,* pp. 576-586, 2015.

[28] A. Indrearne, "Nettilknyttet mikroproduksjon i det norske kraftsystemet," Rasjonell Elektrisk Nettvirksomhet AS (REN), 2014.

[29] G. Andersson, "Modelling and Analysis of Electric Power Systems," 2008. [Online]. Available: https://web.archive.org/web/20170215042633/http:/www.eeh.ee.ethz.ch/uploads/tx_ethstudies/modelling_hs08_script_02.pdf. [Accessed April 2019].

[30] R. Rossi, L. E. B. d. Silva, A. L. O. e. d. Silva, L. S. e. Silva, R. C. Campos and E. M. V. Filho, "Methodology For Mitigation Of Interferences in The Protection System Of Capacitor Banks In Medium And High Voltage," in *IEEE PES Transmission & Distribution Conference and Exhibition - Latin America*, 2018.

[31] M. Lin, R. K. Rayudu and S. Samarasinghe, "A Review of Voltage/var Control".

[32] A. I. O. and O. G. Ibe, "Concepts of Reactive Power Control and Voltage Stability Methods in Power System Network," *IOSR Journal of Computer Engineering,* no. Vol. 11 (2), pp. 15-25, 2013.

[33] M. Juamperez, G. Yang and S. B. Kjær, "Voltage regulation in LV grids by coordinated volt-var control strategies," *Journal of Modern Power Systems and Clean Energy,* pp. 319-328, 2014.

[34] J. Dong, Y. Xue, M. Olama, T. Kuruganti, J. Nutaro and C. Winstead, "Distribution Voltage Control: Current Status and Future Trends," in *2019 9th IEEE International Symposium on Power Electronics for Distributed Generation Systems (PEDG)*, 2018.

[35] I. Afandi, P. Ciufo, A. Agalgaonkar and S. Perea, "A combined MV and LV network voltage regulation strategy for the reduction of voltage unbalance," in *2016 17th International Conference on Harmonics and Quality of Power (ICHQP)*, 2016.

[36] S. Conti and A. Greco, "Innovative Voltage Regulation Method for Distribution Networks with Distributed Generation," in *19th International Conference on Electricity Distribution (CIRED)*, 2007.

[37] V. Calderaro, V. Galdi, F. Lamberti, A. Piccolo and G. Graditi, "Voltage support control of unbalanced distribution systems by reactive power regulation," in *IEEE PES Innovative Smart Grid Technologies, Europe*, 2014.

[38] P. Bousseau, E. Monnot, G. Malarange and O. Gonbeau, "Distributed Generation Contribution to Voltage Control," in *19th International Conference on Electricity Distribution (CIRED)*, 2007.

[39] H. Quan, B. Li, X. Xiu and D. Hui, "Impact analysis for high-penetration distributed photovoltaic generation integrated into grid based od DIgSILENT," in *IEEE Conference on Energy Internet and Energy System Integration (EI2)*, 2017.

[40] I. A. Essackjee and R. T. F. A. King, "The impact of increasing Penetration Level of Small Scale Distributed Generations on voltage in a secondary distribution network," *IEEE International Conference on Emerging Technologies and Innovative Business Practices for the Transformation of Societies (EmergiTech),* 2016.

[41] J. Csatár and A. Dán, "LV Grid Modeling Including Consumption and Distributed PV Generation with Focus on Voltage Profile," in *Periodica Polytechnica Electrical Engineering and Computer Science*.

[42] A. Samadi, R. Eriksson, L. Söder, B. G. Rawn and J. C. Boemer, "Coordinated Active Power-Dependent Voltage Regulation in Distributed Grids With PV Systems," in *IEEE Transactions on Power Delivery (Vol. 29, Iss. 3)*, 2014.

[43] T. Aziz and N. Ketjoy, "Enhancing PV Penetration in LV networks Using Reactive Power Control and On Load Tap Changer With Existing Transformers," *IEEE Access,* pp. 2683-2691, 2017.

[44] K. Rauma, F. Cadoux, N. Hadj-Said, A. Dufournet, C. Baudot and G. Roupioz, "Assessment of the MV/LV on-load tap changer technology as a way to increase LV hosting capacity for photovoltaic power generators," in *CIRED Workshop*, 2016.

[45] K. N. Bangash, M. E. A. Farrag and A. Osman, "Smart Control of on Load Tap Changer depoloyed in Low Voltage Distribution Network," in *2015 4th International Conference on Electric Power and Energy Conversion Systems (EPECS)*, 2015.

[46] M. Nihjuis, G. M and J. F. G. Cobben, "Incorporation of on-load tap changer transformers in low-voltage network planning," in *IEEE PES Innovative Smart Grid Technologies Conference Europe* , 2016.

[47] C. Oerter and N. Neusel-Lange, "IEEE PES General Meeting: Panel Session - Advanced Modelling and Control of Future Low Voltage Networks," 2014. [Online]. Available: https://www.ieee-pes.org/presentations/gm2014/PESGM2014P-002360.pdf. [Accessed April 2019].

[48] European Commision, "Commision Regulation (EU) 2016/631; establishing a network code on requirements for grid connection of generators," 2016.

[49] The Ministry of Oil and Energy, "LOVDATA; Norwegian regulations," [Online]. Available: https://lovdata.no/dokument/SF/forskrift/2004-11-30-1557. [Accessed 2019].

[50] T. V. Cutsem and C. Vournas, Voltage Stability of Electric Power Systems, Springer, 1998.

[51] Reinhausen, "Reinhausen Ecotap Transformer," [Online]. Available: https://www.reinhausen.com/en/desktopdefault.aspx/tabid-1948/2821_read-7910/.

[52] S. Adhikari, Y. Xu, F. Li, H. Li, J. D. Kueck, I. B. Snyder, T. J. Barker and R. Hite, "Utility-Side Voltage and PQ Control with Inverter-based Photovoltaic Systems," *Preprints of the 18th IFAC World Congress,* pp. 6110-6116, 2011.

[53] A. Cabrera-Tobar, E. Bullich-Massagué, M. Aragüés-Penalba and O. Gomis-Bellmunt, "Capability curve analysis of photovoltaic generation systems," *Solar Energy,* 2016.

[54] Sandia National Laboratories, "ESIG Energy - Reactive Power Capability and Interconnection Requirements for PV and Wind Plants," [Online]. Available: https://www.esig.energy/wiki-main-page/reactive-power-capability-and-interconnection-requirements-for-pv-and-wind-plants/. [Accessed April 2019].

[55] N. D. Caliao, "Dynamic modelling and control of fully rated converter wind turbines," *Renewable Energy,* no. Vol. 36 (8), pp. 2287-2297, 2011.

[56] DIgSILENT, "DIgSILENT PowerFactory," [Online]. Available: https://www.digsilent.de/en/powerfactory.html.

[57] DIgSILENT, "Technical Reference Documentation: External Grid," 2018.

[58] DIgSILENT, "PowerFactory Technical Reference: Static Generator," DIgSILENT, 2018.

[59] DIgSILENT, "Powerfactory Technical Reference: General Load," DIgSILENT, 2018.

[60] D. PowerFactory, "Technical Reference Documentation: Tap-Controller," DIgSILENT, 2018.

[61] D. PowerFactory, "Technical Reference: Transformer 3-Phase," DIgSILENT, 2019.

[62] Copper Development Association, "Voltage Disturbances: Standard EN 50160 - Voltage Characteristics in Public Distribution Systems," 2004. [Online]. Available: http://copperalliance.org.uk/uploads/2018/03/542-standard-en-50160-voltage-characteristics-in.pdf. [Accessed 2019].

[63] ENTSO-E, "ENTSO-E Network Code for Requirements for Grid Connection Applicable to all Generators," 2013. [Online]. Available:

https://www.entsoe.eu/fileadmin/user_upload/_library/resources/RfG/130308_Final_Version_NC_RfG.pdf. [Accessed 2019].

[64] Statnett SF, "NVE," 2017. [Online]. Available: http://webfileservice.nve.no/API/PublishedFiles/Download/201500642/2267018. [Accessed 2019].

[65] S. SF, "Statnett SF; Funksjonskrav i Kraftsystemet 2012," [Online]. Available: https://issuu.com/statnett/docs/statnett_fiks_/1?ff&e=2213733/2286337. [Accessed April 2019].

[66] DIgSILENT, "Template Documentation: Fully Rated WTG Template," 2018.

[67] Agder Energi Nett AS, "Agder Energi Nett AS - Technical requirements, Prosumers and DG-operators," 2009. [Online]. Available: https://www.aenett.no/globalassets/dokumenter-importert/vedlegg_3_tekniske_f_23045a.pdf. [Accessed April 2019].

[68] ENERGINET.DK, "Technical Regulation for Electricity-generating Facilities of 11 kW or lower," Energinet.dk, 2008.

[69] P. Vermeyen and P. Lauwers, "Managing Reactive Power in MV Distribution Grids Containing Distributed Generation," in *23rd International Conference on Electricity Distribution*, 2015.

[70] Agder Energi Nett AS, "Agder Energi Nett; Projects," [Online]. Available: https://www.aenett.no/virksomhet/om-ae-nett/prosjekter1/.

[71] K. R. Dosier, "Maintaining long rural feeders with large interconnected distributed generation," in *IEEE Rural Electric Power Conference (REPC)*, 2014.

[72] B. N. Torsæter and H. Kirkeby, "Simuleringsstudie av Spenningskvalitet i Lavspenningsnett med Plusskunder," SINTEF ENergi AS, 2017.

[73] T. Stetz, M. Kraiczy and H. Wang, "IEA PVPS Public report - Outcome of a study conducted for Bayernwerk AG regarding Q-support in the LV network," [Online]. Available: http://iea-pvps.org/fileadmin/dam/public/report/technical/06_-_Stetz_-_PV_as_flexible_resources_-_innovative_reactive_power_management.pdf. [Accessed April 2019].

[74] R. Pedersen, C. Sloth and R. Wisniewski, "Coordination of Electrical Distribution Grid Voltage Control - A Fairness Approach".

[75] M. Kaspirek and J. Jiricka, "Operation of the Distribution Transformer MV/LV with the Voltage Regulation under Load," *IEEEE,* 2014.

[76] Kaspirek, Mezera and Jiricka, "Problems Of Voltage Stabilization In MV And LV Distribution Grids Due To The Operation Of Renewable Energy Sources," in *CIRED, 22nd International Conference On Electricity Distribution*, 2013.

[77] Eisenreich, Cao and Balzer, "Voltage Regulation In Distribution Grids With High Ratio Of Distributed Generation Units," in *CIRED Workshop, Lisbon 29-30 May*, 2012.

[78] Järventausta, Repo, Rautiainen and Partanen, "Smart grid power system control in distributed generation environment," *ScienceDirect,* pp. 277-286, October 2010.

[79] Mouli, Ram, Bauer, Wijekoon, Panosyan and Bärthlein, "Design of a power-electronic-assisted OLTC for grid voltage regulation," *IEEE,* 2015.

[80] Clement-Nyns, Haesen and Driesen, "The Impact of Charging Plug-In Hybrid Electric Vehicles on a Residential Distribution Grid," *IEEE,* Feb 2010.

[81] M. S. Calovic, "Modeling and Analysis of Under-Load Tap-Changing Transformer Control Systems," *IEEE Transaction on Power System Apparatus and Systems,* no. Vol. PAS-103 No. 7, 1984.

Appendices

Appendix A

A.1 - MV Network Results

Base case – 60% Load, 0% DG

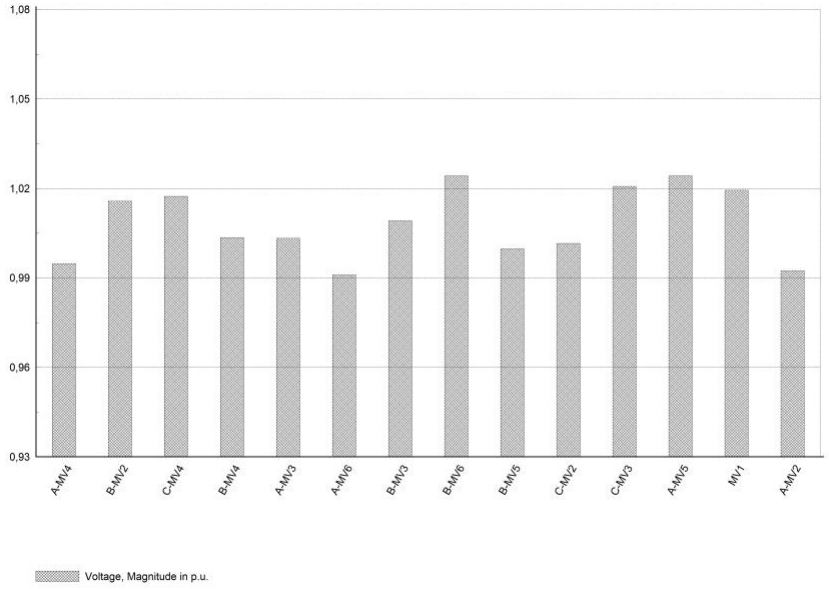

Figure 39: Voltage magnitude in [p.u.] for each bus in Base case. It clearly shows the voltages are within prescribed limits of 0.95 and 1.05 p.u., tap position -3

Operation scenario 2 – 100% Load, 0% DG (HLNP)

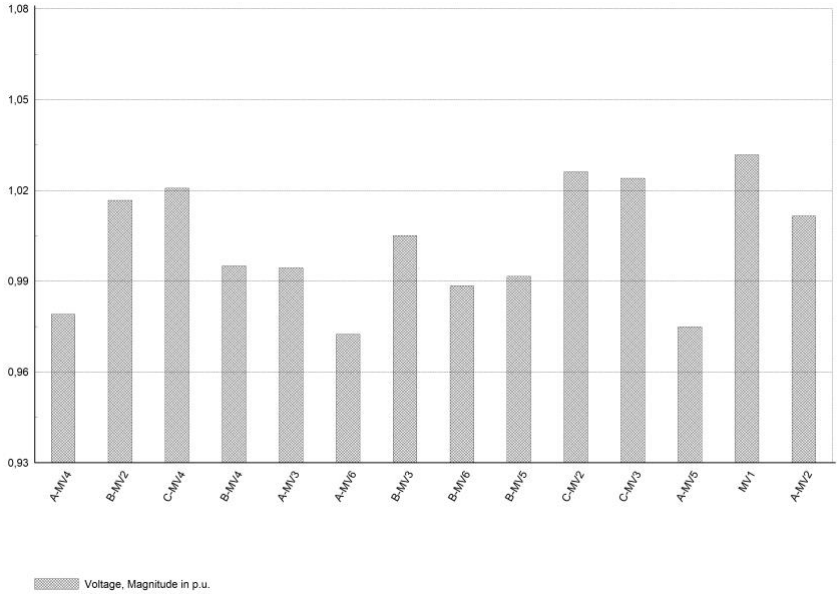

Figure 40: Voltage magnitude in [p.u.] for each bus in operation scenario 2 (HLNP). It clearly shows satisfactory voltages. Tap position -5.

Table 14: Key results from operation case 2 (HLNP), where the wider voltage deviation is clear, with respect to base case.

Parameter	*Value*	*Unit*	*Comment*
U_{max}	1.03	p.u.	ΔU_{max}= 0.06 p.u.
U_{min}	0.97	p.u.	
P_{Load}	34.78	MW	Sum of P, all loads
P_{Loss}	5.22	MW	Network loss (P)
Q_{Load}	12.22	Mvar	Sum of Q, all loads
$\sum Q_{MV1}$	10.80	Mvar	Import to network
$\sum P_{MV1}$	40.00	MW	Import to network

A.2 - MV Network – Transformer, OLTC and LDC Specifications

The network considered is a 22 kV configurated network, without any reactive power compensation devices installed. It is fed through two (2) OLTC transformers which regulates the MV busbar, MV1. The TFs are referred to as *the TF* in many cases, this is ok, because in terms of the simulations performed, they can be view as one TF with the total capacity, indeed.

Table 15: The specifications for the HV/MV TFs connected in parallel (2pcs) between HV and the MV network.

Spec.	*Value*	*Comment*
$U_{nom,HV}$ [kV]	138	HV-side
$U_{nom,LV}$ [kV]	23.1	LV-side
S_{rated} [MVA]	20	Rated power
Vector group	D/Yn1	
f_{rated} [Hz]	60	
u_k [%]	10	Short-circuit voltage
P_{cu} [kW]	96	Copper loss S-C
P_0 [kW]	20	No-load loss
x_{pos} [p.u.]	0.5	HV and LV side (leakage X)
r_{pos} [p.u.]	0.5	HV and LV side (leakage R)
Tap changer range [%]	±8x1.25%	At HV-side.
Tap position	OLTC control	9 available taps.

Table 16: Initial setpoints for the OLTC, which is used throughout simulations if not otherwise stated.

Control setpoint	*Value*
Voltage setpoint [p.u.]	1.00
Lower bound [p.u.]	0.99
Upper bound [p.u.]	1.01
Time constant [s]	0.5

Recall, a test where R and X setpoints for LDC was set to 0.33 and 0.518, respectively, was conducted.

A.3 - MV Network – Bus and Branch Properties (Loads, DG, Cables)

In the case of loads and DGs in the test MV network, the loads are simply selected to represent aggregated loads operating in steady state (a snapshot of the network condition is taken). In the back of your mind, the loads can be seen as *k* distribution TFs, MV/LV, say for instance ca. 200-630 kVA rated. In the case of a 3 MW load, we are talking a number of distribution networks (LV) represented by their TF, to be somewhere between 5 – 15 TFs. Say it's a modern area, so the ratings of the TFs will mostly be in the area around 500-800 kVA and have an underground LV cable layout. Their PF is set to represent some characteristics of the TFs connected to the MV system. *All busbars have a nominal voltage of 22 kV, which is considered 1 p.u. The MV1 busbar follows the voltage setpoint on the OLTC.*

Table 17: The general loads and static generators connected to the MV system. All bus indexes are shown, and the summation of power seen by the MV1 busbar are included.

Bus index	*Load [MW]*	*Load [PF]*	*DG [MVA]*	*DG [PF]*	3_{ϕ} *balanced?*
A-MV2	5	0.95 ind.	-	-	Yes
A-MV3	1.5	0.95 ind.	1,58	1	Yes
A-MV4	5	0.95 ind.	-	-	Yes
A-MV5	3	0.95 ind.	3.16	1	Yes
A-MV6	3	0.95 ind.	3.16	1	Yes
B-MV2	3	0.95 ind.	3.2	1	Yes
B-MV3	1.5	0.95 ind.	1.58	1	Yes
B-MV4	3	0.95 ind.	3.2	1	Yes
B-MV5	3	0.95 ind.	3.16	1	Yes
B-MV6	3	0.95 ind.	3.16	1	Yes
C-MV2	1.9	0.95 ind.	-	-	Yes
C-MV3	4.9	0.98 ind.	-	-	Yes
C-MV4	0.98	0.98 ind.	-	-	Yes
$\sum seen\ at\ MV1$	38.78		22.2		

A.3 cont.

The cables connecting the aggregated loads (busbars) together are presented in the following;

In Table 16, the node index *i* and *j* are used as a term of the line going from bus *i* to bus *j*. All cables are considered buried underground.

Table 18: Node-to-node branch lengths and their cable types in the MV network.

Node i	*Node j*	*Length [km]*	*Cable type index*
MV1	A-MV2	5	Type A
A-MV2	A-MV3	5	Type B
A-MV3	A-MV4	5	Type B
A-MV4	A-MV5	5	Type B
A-MV4	A-MV6	8	Type B
MV1	B-MV2	5	Type A
B-MV2	B-MV3	5	Type A
B-MV3	B-MV4	5	Type A
B-MV4	B-MV5	5	Type A
B-MV4	B-MV6	8	Type B
MV1	C-MV2	2	Type C
C-MV2	C-MV3	1	Type C
C-MV4	0.98	3	Type D

Table 19: Cable type specifications for the MV distribution network. Specifications are noted at their nominal temperature.

Cable type index	*Spec. type*	*r [Ω/km]*	*x [Ω/km]*	*Rated cur. [kA]*
Type A	NA2YSY 1x500rm 18/30kV it (Al)	0.0667	0.1036	0.570
Type B	NA2SY 1x400rm 18/30kV it (Al)	0.0833	0.1099	0.505
Type C	NA2YSY 1x240rm 18/30kV ir (Al)	0.1292	0.1162	0.425
Type D	NA2SY 1x70rm 18/30kV it (Al)	0.4458	0.1413	0.200

Appendix B

B.1 - Wind Farm (Plant) – Network, transformer characteristics

Table 20: MV/LV Transformer specification for Wind farm plant, connecting each WTG to the MV network within the plant. All parameters are kept at default.

Spec.	*Value*	*Comment*
$U_{nom,HV}$ [kV]	20	HV-side
$U_{nom,LV}$ [kV]	0.69	LV-side
S_{rated} [MVA]	2.8	Rated power
Vector group	D/Yn5	
f_{rated} [Hz]	50	
u_k [%]	6	Short-circuit voltage
P_{cu} [kW]	20	Copper loss S-C
P_0 [kW]	10	No-load loss
x_{pos} [p.u.]	0.5	HV and LV side (leakage X)
r_{pos} [p.u.]	0.5	HV and LV side (leakage R)
Tap changer range [%]	2/2,5%	At HV-side.
Tap position	1	(-2, -1, 0, **+1,** +2)

B.2 - General data on the Wind Farm

Table 21: Key characteristics for the Wind Farm (plant) with 6 wind turbines.

Parameter	*Value*	*Additional data*
$U_{nom,MV}$ [kV]	20	20 kV is 1.0 p.u. in this system.
$U_{nom,LV}$ [kV]	0.69	

The tables presented in the following, lists the cables used in between WTGs within the Wind Farm (Type J) and the cable which is installed from the Wind Farm busbar (Busbar WF) to the PCC at the substation (Type K). Note that the Type K cable is later connected halfway down the feeder providing the LV network with power, but this is explicitly described in the section for the LV network.

Table 22: Cable specifications for the two cables installed within the Wind Farm

Cable type index	*Spec. type*	*r* [Ω/km]	*x* [Ω/km]	*Rated cur.* [kA]
Type J	NA2XS(F)2Y 1x150RM it 12/20kV (Al, PVC)	0.211	0.122	0.320
Type K	NA2XS(F)2Y 1x400RM 12/20kV (Al, PVC)	0.102	0.167	0.565

Table 23: Node-to-Node branch specification within the Wind Farm.

Node i	*Node j*	*Length [km]*	*Cable type index*
MV1.1	Busbar WF	2	Type J
MV1.1	MV1.2	0.8	Type J
Busbar WF	MV2.1	3	Type J
MV2.1	MV2.2	1.1	Type J
MV2.2	MV2.3	1.1	Type J
MV2.3	MV2.4	1.5	Type J
Busbar WF	PCC (subst.)	0.2	Type K

B.3 - WTG Power curve (Power vs wind speed) - nominal

Table 24: The nominal active power curve for each WTG in tabulated form.

Wind speed (m/s)	Power output (%)
0	0
1	0
2	0
3	0
3,01	0,5
4	1,5
5	4
6	9
7	15
8	24
9	35
10	50
11	70
12	88
13	96
14	99
15	100
16	100
17	100
18	100
19	100
20	100
21	100
22	100
23	100
24	100
25	100
25,1	0
26	0

B.4 - Active power output of WTG: dynamic scaling curve

The scaling curve consists of relative values, with respect to nominal power output of the WTG. The time resolution is 15 minutes, and it is based on the load profile obtained from the PowerFactory library: “G0/Sommer_Werktag”.

Table 25: Active power output scaling curve, applied on each WTG in the quasi-dynamic simulations performed. It is inderectly representing wind speed.

Time (hh:mm)	Power output (p.u.)
00:00	0,307
00:15	0,2974
00:30	0,287
00:45	0,2758
01:00	0,2641
01:15	0,2533
01:30	0,2438
01:45	0,2354
02:00	0,2292
02:15	0,2255
02:30	0,2234
02:45	0,2221
03:00	0,2217
03:15	0,2209
03:30	0,2213
03:45	0,225
04:00	0,2334
04:15	0,2471
04:30	0,2633
04:45	0,2795
05:00	0,2916
05:15	0,297
05:30	0,2978
05:45	0,2962
06:00	0,2953
06:15	0,2974
06:30	0,3041
06:45	0,3157
07:00	0,3344
07:15	0,3602
07:30	0,3956
07:45	0,4422
08:00	0,5012
08:15	0,5732
08:30	0,6502
08:45	0,7213

09:00	0,7775
09:15	0,8111
09:30	0,8265
09:45	0,8311
10:00	0,8319
10:15	0,8344
10:30	0,8399
10:45	0,8469
11:00	0,8552
11:15	0,8636
11:30	0,8698
11:45	0,8719
12:00	0,8669
12:15	0,8532
12:30	0,8319
12:45	0,8062
13:00	0,7775
13:15	0,7483
13:30	0,7213
13:45	0,6993
14:00	0,6839
14:15	0,678
14:30	0,6801
14:45	0,688
15:00	0,6997
15:15	0,7134
15:30	0,7263
15:45	0,7371
16:00	0,7425
16:15	0,7413
16:30	0,7354
16:45	0,7284
17:00	0,723
17:15	0,7205
17:30	0,7171
17:45	0,708
18:00	0,688
18:15	0,6535
18:30	0,6077
18:45	0,5566
19:00	0,5054
19:15	0,458
19:30	0,4181
19:45	0,3877

20:00	0,3694
20:15	0,3636
20:30	0,3665
20:45	0,3727
21:00	0,3769
21:15	0,3752
21:30	0,3681
21:45	0,359
22:00	0,3498
22:15	0,3428
22:30	0,3378
22:45	0,334
23:00	0,3303
23:15	0,3261
23:30	0,3211
23:45	0,3149

End.

Appendix C

C.1 - LV Distribution Network Characteristics and Properties

The network is supplied by the MV substation busbar in the Wind Farm model, i.e., from a stiff source (SL-bus). A MV cable of 20 km is connected between substation MV busbar (1.0 p.u.) and the primary side of MV/LV Transformer. This is done to replicate an underground MV network. However, no load is connected to the primary side of MV/LV TF unless otherwise is stated. Indeed, the LV network is a TN-C-S system, where three-phase loads operate at 0.4 kV, and single-phase loads operate between phase-neutral, thus a voltage of 0.23 kV. All loads and PVs are considered to be three-phase and balanced. The cable between stiff 20 kV busbar and the MV/LV TF is the following type;

NA2XS(F)2Y 1x400RM 12/20 kV ir. (3x1 single-phase cables laid in a row). The rated current is 0.565 kA. Resistance @90°=0.124 Ohm/km, Capacitance 0.368 uF/km, Reactance 0.102 Ohm/km. (Simulations performed with highest allowable cable temperature).

Table 26: Distribution transformer properties, 3-phase MV/LV, used for supplying LV network from MV grid within the Wind Farm model.

Spec.	*Value*	*Comment*
$U_{nom,HV}$ [kV]	20	HV-side
$U_{nom,LV}$ [kV]	0.4	LV-side
S_{rated} [MVA]	0.63	Rated power
Vector group	D/Yn11	
f_{rated} [Hz]	50	
u_k [%]	6	Short-circuit voltage
P_{cu} [kW]	6.9	Copper loss S-C
P_0 [kW]	1.65	No-load loss
x_{pos} [p.u.]	0.5	HV and LV side (leakage X). Pos. seq.
r_{pos} [p.u.]	0.5	HV and LV side (leakage R). Pos.seq.
Tap changer range [%]	2/2,5%	At HV-side.
OLTC active?	Specified in each case	
Tap position	Specified in each case	Initial neutral position = tap 0.
Fabrication	ASEA	

C.2 - LV Distribution Network – Load & PV system Dynamic Profiles (scaling curves)

For the respective curves plotted (power graph), refer to Section 6.4.

The relative values referred to the nominal rating of each component in LV grid, is listed below (3 pages);

Table 27: Timeseries (time of day, hh:mm) of the scaling profiles implemented on the residential loads and PV systems at all LV buses in the LV network.

Time of day [hh:mm]	House load [relative]	Sunny day PV [relative]	Partly cloudy PV [relative]
00:00	0,2891	0	0
00:15	0,275	0	0
00:30	0,2625	0	0
00:45	0,2517	0	0
01:00	0,2429	0	0
01:15	0,2359	0	0
01:30	0,2304	0	0
01:45	0,2263	0	0
02:00	0,2234	0	0
02:15	0,2213	0	0
02:30	0,2192	0	0
02:45	0,2176	0	0
03:00	0,2159	0	0
03:15	0,2138	0	0
03:30	0,2121	0	0
03:45	0,2101	0	0
04:00	0,208	0	0
04:15	0,2063	0	0
04:30	0,2055	0	0
04:45	0,2059	0	0
05:00	0,208	0	0
05:15	0,213	0	0
05:30	0,22	0	0
05:45	0,23	0	0
06:00	0,2429	0	0
06:15	0,2587	0	0
06:30	0,2804	0,02	0,02
06:45	0,3111	0,05	0,05
07:00	0,3544	0,05	0,05
07:15	0,4114	0,06	0,06
07:30	0,478	0,07	0,07
07:45	0,5483	0,08	0,08
08:00	0,6165	0,08	0,08
08:15	0,6764	0,09	0,09

08:30	0,7234	0,1	0,1
08:45	0,7512	0,1	0,1
09:00	0,7554	0,2	0,2
09:15	0,7325	0,3	0,05
09:30	0,6909	0,3	0,05
09:45	0,641	0,37	0,4
10:00	0,5932	0,4	0,4
10:15	0,5566	0,45	0,45
10:30	0,5333	0,48	0,48
10:45	0,5233	0,55	0,15
11:00	0,5279	0,6	0,6
11:15	0,5458	0,72	0,15
11:30	0,5682	0,76	0,76
11:45	0,48	0,82	0,82
12:00	0,4	0,86	0,86
12:15	0,3	0,9	0,2
12:30	0,3	0,9	0,2
12:45	0,25	0,95	0,4
13:00	0,3	0,98	0,8
13:15	0,15	1	0,6
13:30	0,1	1	0,1
13:45	0,1	1	0,8
14:00	0,3	0,97	0,23
14:15	0,2	0,97	0,7
14:30	0,3	0,95	0,6
14:45	0,35	0,93	0,1
15:00	0,4006	0,9	0,2
15:15	0,4022	0,87	0,2
15:30	0,3	0,84	0,3
15:45	0,3	0,8	0,3
16:00	0,4047	0,75	0,45
16:15	0,4035	0,74	0,47
16:30	0,4027	0,7	0,6
16:45	0,4039	0,65	0,55
17:00	0,65	0,6	0,24
17:15	0,65	0,55	0,3
17:30	0,4359	0,5	0,25
17:45	0,4638	0,45	0,25
18:00	0,5046	0,4	0,2
18:15	0,5591	0,3	0,1
18:30	0,6194	0,28	0,15
18:45	0,6764	0,25	0,2
19:00	0,7205	0,22	0,2
19:15	0,7442	0,15	0,1

19:30	0,7479	0,08	0
19:45	0,7342	0,05	0,05
20:00	0,7051	0,02	0,02
20:15	0,6639	0,02	0,02
20:30	0,6161	0	0
20:45	0,5674	0	0
21:00	0,5241	0	0
21:15	0,4904	0	0
21:30	0,4655	0	0
21:45	0,4455	0	0
22:00	0,4276	0	0
22:15	0,4097	0	0
22:30	0,3914	0	0
22:45	0,3727	0	0
23:00	0,3544	0	0
23:15	0,3369	0	0
23:30	0,3199	0	0
23:45	0,3041	0	0

End.

C.3 - LV Distribution Network; Node-to-node Properties

Table 28: Load and PV rating of each customer (the nominal, which is scaled through the day), and the number of customers in the network

Bus index	*Load [kW/customer]*	*Load [PF]*	*PV [kW/customer]*	*DG [PF]*	3_{ϕ} *balanced?*	*Customers [-]*
LV1	20	0.95 ind.	9.9	1	Yes	5
LV2	20	0.95 ind.	9.9	1	Yes	3
LV3	20	0.95 ind.	9.9	1	Yes	2
LV4	20	0.95 ind.	9.9	1	Yes	5
LV5	20	0.95 ind.	9.9	1	Yes	4
$\sum Seen\ by\ TF$	380		188.1			19

Table 29: Node-to-Node characteristics of the LV network.

Node i	*Node j*	*Length [m]*	*Cable type index*	*Note*
TF:LV side	LV1	5	Type E	Used to simplify power readings (it does also represent a practical element)
LV1	LV2	80	Type F	
LV2	LV3	150	Type G	
LV2	LV4	100	Type H	
LV4	LV5	120	Type I	

Cable specifications follows on the next page.

C.3 cont.

Table 30: Cable specifications of the cables used in the LV network.

Cable type index	*Spec. type*	*r* [Ω/km]	*x* [Ω/km]	*Rated cur.* [kA]
Type E	NAYY 4x240SE 0.6/1kV (Al, PVC)	0.1267	0.0797	0.357
Type F	NAYY 4x150SE 0.6/1kV (Al, PVC)	0.2067	0.0804	0.270
Type G	NAYY-J 3x35/35 0.6/1kV (Al, PVC)	0.8690	0.0851	0.123
Type H	NAYY 4x95SE 0.6/1kV (Al, PVC)	0.3208	0.0819	0.211
Type I	NAYY-J 4x50 0.6/1kV (Al, PVC)	0.6410	0.0848	0.144

C.4 - Load connected to MV side of MV/LV TF in Case E

The load connected has a nominal demand of 5 MW, PF = 0.95 inductive, balanced three-phase. The scaling curve are listed below;

Table 31: MV load scaling curve, when implemented in Case E, at the MV side of the MV/LV TF.

Time of day (hh:mm)	Load scaling (relative)
00:00	0,1891
00:15	0,1907
00:30	0,1868
00:45	0,1821
01:00	0,177
01:15	0,1731
01:30	0,1696
01:45	0,1673
02:00	0,1653
02:15	0,1641
02:30	0,1637
02:45	0,1641
03:00	0,1653
03:15	0,1673
03:30	0,1692
03:45	0,1716
04:00	0,1731
04:15	0,1743
04:30	0,1751
04:45	0,1758
05:00	0,177
05:15	0,1798
05:30	0,1829
05:45	0,1876
06:00	0,193
06:15	0,1993
06:30	0,2059
06:45	0,2118
07:00	0,2165
07:15	0,2196
07:30	0,2208
07:45	0,2212
08:00	0,2204
08:15	0,2196
08:30	0,2184
08:45	0,2173
09:00	0,2165
09:15	0,2165

09:30	0,2177
09:45	0,2216
10:00	0,2282
10:15	0,2392
10:30	0,2521
10:45	0,2661
11:00	0,2794
11:15	0,2907
11:30	0,2997
11:45	0,3064
12:00	0,3111
12:15	0,3134
12:30	0,313
12:45	0,3095
13:00	0,3032
13:15	0,2935
13:30	0,2818
13:45	0,27
14:00	0,2599
14:15	0,2524
14:30	0,2481
14:45	0,2466
15:00	0,2481
15:15	0,2517
15:30	0,2567
15:45	0,261
16:00	0,2638
16:15	0,2634
16:30	0,261
16:45	0,2579
17:00	0,256
17:15	0,2556
17:30	0,256
17:45	0,2552
18:00	0,2521
18:15	0,245
18:30	0,2356
18:45	0,2259
19:00	0,2165
19:15	0,2098
19:30	0,2052
19:45	0,2024
20:00	0,2009
20:15	0,2001

20:30	0,1997
20:45	0,1989
21:00	0,197
21:15	0,193
21:30	0,1884
21:45	0,1841
22:00	0,1809
22:15	0,1805
22:30	0,1813
22:45	0,1833
23:00	0,1852
23:15	0,1864
23:30	0,1872
23:45	0,188

End.